



University of Kentucky
UKnowledge

Theses and Dissertations--Veterinary Science

Veterinary Science

2014

THE ROLES OF ORTHOPAEDIC PATHOLOGY AND GENETIC DETERMINANTS IN EQUINE CERVICAL STENOTIC MYELOPATHY

Jennifer Gail Janes

University of Kentucky, jennifer.janes40@gmail.com

[Right click to open a feedback form in a new tab to let us know how this document benefits you.](#)

Recommended Citation

Janes, Jennifer Gail, "THE ROLES OF ORTHOPAEDIC PATHOLOGY AND GENETIC DETERMINANTS IN EQUINE CERVICAL STENOTIC MYELOPATHY" (2014). *Theses and Dissertations--Veterinary Science*. 16. https://uknowledge.uky.edu/gluck_etds/16

This Doctoral Dissertation is brought to you for free and open access by the Veterinary Science at UKnowledge. It has been accepted for inclusion in Theses and Dissertations--Veterinary Science by an authorized administrator of UKnowledge. For more information, please contact UKnowledge@lsv.uky.edu.

STUDENT AGREEMENT:

I represent that my thesis or dissertation and abstract are my original work. Proper attribution has been given to all outside sources. I understand that I am solely responsible for obtaining any needed copyright permissions. I have obtained needed written permission statement(s) from the owner(s) of each third-party copyrighted matter to be included in my work, allowing electronic distribution (if such use is not permitted by the fair use doctrine) which will be submitted to UKnowledge as Additional File.

I hereby grant to The University of Kentucky and its agents the irrevocable, non-exclusive, and royalty-free license to archive and make accessible my work in whole or in part in all forms of media, now or hereafter known. I agree that the document mentioned above may be made available immediately for worldwide access unless an embargo applies.

I retain all other ownership rights to the copyright of my work. I also retain the right to use in future works (such as articles or books) all or part of my work. I understand that I am free to register the copyright to my work.

REVIEW, APPROVAL AND ACCEPTANCE

The document mentioned above has been reviewed and accepted by the student's advisor, on behalf of the advisory committee, and by the Director of Graduate Studies (DGS), on behalf of the program; we verify that this is the final, approved version of the student's thesis including all changes required by the advisory committee. The undersigned agree to abide by the statements above.

Jennifer Gail Janes, Student

Dr. James N. MacLeod, Major Professor

Dr. Daniel K. Howe, Director of Graduate Studies

THE ROLES OF ORTHOPAEDIC PATHOLOGY AND GENETIC DETERMINANTS IN
EQUINE CERVICAL STENOTIC MYELOPATHY

DISSERTATION

A dissertation submitted in partial fulfillment of the
requirements for the degree of Doctor of Philosophy in the
College of Agriculture, Food, and Environment
at the University of Kentucky

By
Jennifer Gail Janes

Lexington, Kentucky

Director: Dr. James N. MacLeod, Professor of Veterinary Science

Lexington, Kentucky

2014

Copyright © Jennifer Gail Janes 2014

ABSTRACT OF DISSERTATION

THE ROLES OF ORTHOPAEDIC PATHOLOGY AND GENETIC DETERMINANTS IN EQUINE CERVICAL STENOTIC MYELOPATHY

Cervical stenotic myelopathy (CSM) is an important musculoskeletal and neurologic disease of the horse. Clinical disease occurs due to malformations of the vertebrae in the neck causing stenosis of the cervical vertebral canal and subsequent spinal cord compression. The disease is multifactorial in nature, therefore a clearer understanding of the etiology and pathogenesis of CSM will allow for improved management and therapeutic practices. This thesis examines issues of equine CSM diagnosis, skeletal tissue pathology, and inherited genetic determinants utilizing advances in biomedical imaging technologies and equine genomics. Magnetic resonance imaging (MRI) data provided a more complete assessment of the cervical column through image acquisition in multiple planes. First, MRI was compared to standing cervical radiographs for detection of stenosis. Using canal area or the cord canal area ratio, MRI more accurately predicted sites of compression in CSM cases. Secondly, articular process skeletal pathology localized on MRI was found to be more frequent and severe in CSM horses compared to controls. In addition, lesions were generalized throughout the cervical column and not limited to the spinal cord compression sites. A subset of lesions identified on MRI was evaluated using micro-CT and histopathology. Osteochondrosis, osseous cyst-like structures, fibrous tissue replacement of bone, and osteosclerosis were observed. These lesions support likely developmental aberrations of vertebral bone and cartilage maturation with secondary biomechanical influences. Bone cyst-like structures are a novel finding in this disease. Finally, the long-standing question of the contribution of genetic determinants to CSM was investigated using a genome wide association study (GWAS). Multiple significant loci were identified supporting the influence of a complex genetic trait in clinical disease. A simple Mendelian trait controlled by one gene is unlikely given the detection of variants across multiple chromosomes. Major contributions from this research include documentation of articular process bone and cartilage pathology in horses with CSM, support for abnormal cervical vertebrae development being an important contributing factor in the etiology and/or pathogenesis of equine CSM, and evidence that multiple genetic loci contribute to the CSM disease phenotype.

Keywords: Horse, Cervical Stenotic Myelopathy, Wobbler Syndrome,
Vertebrae, Genome Wide Association Study (GWAS)

Jennifer Gail Janes
Student Signature
08/01/2014
Date

THE ROLES OF ORTHOPAEDIC PATHOLOGY AND GENETIC
DETERMINANTS IN EQUINE CERVICAL STENOTIC MYELOPATHY

By

Jennifer Gail Janes

Dr. James N. MacLeod

Director of Dissertation

Dr. Daniel K. Howe

Director of Graduate Studies

08/01/2014

ACKNOWLEDGMENTS

The journey of completing my dissertation work has been fulfilling and rewarding. It would not have been possible without the support and encouragement of my committee, faculty, staff, friends, and family.

I am immensely grateful to my mentor, Dr. James MacLeod. First of all, thank you for taking a chance on me. My education and growth under your guidance has surpassed my expectations. The dedication and commitment shown to his graduate students is beyond compare. Thank you Jamie for being “all in” from start to finish.

My committee was an integral and influential part of my journey through this process. I appreciate all of you for taking time to spend with me. Whenever I had a question all of you responded and were keen to help. Drs. Bailey and Fardo, I appreciate the enthusiasm you both have for genetics and eagerness to share that knowledge. Dr. Williams, your dedication and diligence towards anatomic pathology has had a profound influence on myself. Dr. Reed, the passion and continued interest to further understand CSM are exceptional and inspiring. Dr. Carter, your knowledge of epidemiological issues and enthusiasm for this project has been much appreciated. Finally, thank you to Dr. Rossano for your genuine interest in the work. Thank you to all for pushing me outside my box and impacting my professional development.

I have been lucky to have incredibly supportive lab mates throughout my time at Gluck. Thank you all (past and present). Drs. Mike Mienaltowski and Stephen Coleman you both have been great soundboards whether we chatted about

scientific issues or the Indy 500. Dr. Emma Adam, Dr. Elizabeth Woodward, and Kadie Vanderman thank you for your friendship both in and outside the lab; it definitely carried me through. Lauren Cason, Dr. Rebekah Decker, Ellen Wiegand, and Dr. Parvathy Thampi thank you for all the fun memories. Thank you to Miranda Richardson, I enjoyed working with and mentoring you. Also, thank you to all of the faculty and staff at the Gluck Center who have made this experience fruitful and memorable.

I am immeasurably grateful to the pathologists and staff at the University of Kentucky Veterinary Diagnostic Laboratory. All of you have been amazing in your support of myself completing the dual residency/ PhD program. I couldn't have done it without you. It has been a pleasure to work with Dr. Katie Garrett, Whitney Mathes, Adriel Sitzes, Brent Comer, and Emily Zurkuhlen at Rood and Riddle Equine Hospital.

Last but not least I am grateful to my friends, family and most importantly my parents. You all have stuck by and supported me along my entire educational road; no matter what direction it took me. Thank you for believing in me. I love you all dearly.

TABLE OF CONTENTS

Acknowledgments.....	iii
List of Tables.....	vii
List of Figures.....	viii
Chapter 1: Literature Review of Equine Cervical Stenotic Myelopathy	
Summary.....	1
Introduction and background.....	1
Epidemiology.....	3
Signalment and Etiologic Factors.....	4
Clinical Presentation and Diagnosis.....	6
Disease Categorization.....	11
Treatment and Management.....	12
Cervical Vertebral Anatomy.....	13
CSM Pathology.....	15
Important Knowledge Gaps.....	20
Dissertation Overview and Objectives.....	23
Chapter 2: Comparison of Magnetic Resonance Imaging to Standing Cervical Radiographs for Evaluation of Vertebral Canal Stenosis in Equine Cervical Stenotic Myelopathy	
Summary.....	27
Introduction.....	28
Materials and Methods.....	29
Animals.....	29
Clinical Examination.....	30
MRI Evaluation.....	30
Postmortem Evaluation.....	32
Experimental Group Classification.....	33
Statistical Analysis.....	34
Results.....	35
Identification of False Positive and False Negative Cases.....	35
Anatomic Changes of the Cervical Vertebral Column on MRI.....	38
MRI and Radiographic Assessment for Compression.....	40
Discussion.....	41

Chapter 3: Skeletal Pathology of the Cervical Articular Processes in Equine Cervical Stenotic Myelopathy	
Summary	46
Introduction.....	46
Materials and Methods.....	49
Magnetic Resonance Imaging.....	49
Structural Analyses of Articular Process Lesions.....	51
Histopathologic Assessment of Articular Process Lesions	53
Results	54
MRI Lesion Frequency.....	54
Lesion Severity Analysis.....	55
Microarchitectural Bone Volume Assessment.....	56
Histopathologic Assessments.....	59
Discussion.....	62
Chapter 4: The Role of Inherited Genetic Determinants in Equine Cervical Stenotic Myelopathy	
Summary.....	70
Introduction.....	70
Materials and Methods.....	72
Experimental Samples.....	72
DNA Isolation.....	74
Genotyping.....	74
Quality Control for Data Analysis.....	75
Statistical Analysis	77
Results	79
Correction for Relatedness and Population Structure.....	79
Chestnut Coat Color Association	80
SNP-based Association Analysis.....	81
Haplotype Analysis.....	82
CNV Identification.....	85
Discussion.....	86
Chapter 5: Reflections and Looking Ahead to Future Studies.....	93
Reflections.....	93
Pulling Together our Current Understanding of Equine CSM.....	99
References	105
Vita.....	113

LIST OF TABLES

Table 2.1 Study case categorizations based on different radiographic and histological thresholds and assessments	33
Table 2.2: Comparison of vertebral measurements between control and CSM horses on MRI	39
Table 3.1 Signalment and articular process sites for structural analysis	51
Table 3.2: Trabecular bone volume comparison in articular processes	57
Table 4.1: Summary of the location and genotypes of significant SNPs in the mixed model analysis	82
Table 4.2: Summary of the significant estimated haplotypes identified by the precomputed block of markers	83
Table 4.3: Summary of significant estimated haplotypes identified by the sliding window of 5 markers	84
Table 4.4: Summary of protein coding genes, pseudogenes, and RNA elements in significant loci	85
Table 4.5: Summary of CNVs in the dam that segregates only with CSM progeny	86

LIST OF FIGURES

Figure 1.1: Distribution of the spinocerebellar tracts in the spinal cord.....	6
Figure 1.2: Two adjacent vertebrae in the sagittal plane for intravertebral and intervertebral ratio measurements.....	9
Figure 1.3: Cervical myelogram in the neutral position.....	10
Figure 1.4: Images of cervical vertebral anatomy.....	14
Figure 1.5: Histopathologic sections of the white matter of the spinal cord.....	16
Figure 1.6: Schematic of lesion localization in the spinal cord.....	17
Figure 1.7: Sagittal view of the cervical vertebral column demonstrating vertebral body subluxation	18
Figure 1.8: Normal and gross pathology of articular processes associated with cervical stenotic myelopathy	19
Figure 2.1: Anatomical measurements of the vertebral canal and spinal cord using proton density weighted MR images	32
Figure 2.2: Scatter plot of the MSD ratios from radiographs and canal area measurements from MRI of horses with compressive lesions at C4-5.....	36
Figure 2.3: Scatter plot of the MSD ratios from radiographs and canal area measurements from MRI of horses with compressive lesions at the fourth, sixth, and seventh cervical vertebrae.....	37
Figure 2.4: Scatter plot of the MSD ratios from radiographs and cord canal area ratio (CCAR) from MRI of horses with compressive lesions at the fourth, fifth, sixth, and seventh cervical vertebrae.....	38
Figure 2.5: Transverse MR images showing the absence and presence of spinal cord compression.....	40
Figure 3.1: Summary of the superficial and deep lesion criteria and corresponding severity grading scale	50
Figure 3.2: Number of samples in each grade category analyzed histologically	54
Figure 3.3: Articular process lesion frequency distribution.....	55
Figure 3.4: Articular process lesion severity distribution.....	56
Figure 3.5: Micro-CT and MRI of a deep lesion within the articular process	58
Figure 3.6: Micro-CT and MRI of a superficial lesion within the articular process....	58

Figure 3.7: Osteochondrosis manifesta (grade 3) image series	59
Figure 3.8: Osteochondritis dissecans lesion (grade 3) image series	60
Figure 3.9: Image series of the cyst like structures in deep articular process lesions of CSM horses	61
Figure 3.10: Histopathology photomicrographs of the deep lesions in the mixed category	62
Figure 4.1: Summary of the phenotyping and signalment parameters for CSM horses in the study.....	73
Figure 4.2: Pedigree of a family included in CNV and SNP analysis.....	74
Figure 4.3: Summary of the samples genotyped on each array.....	75
Figure 4.4: Scatter plot of 1 st and 2 nd principal components.....	77
Figure 4.5: Q-Q plots before and after methods for structure correction	79
Figure 4.6: Manhattan plot for chestnut coat color association analysis.....	80
Figure 4.7: Manhattan plot for mixed model analysis with additive effects.....	81
Figure 4.8: Manhattan plot of haplotypes using blocks defined by the precomputed block method.....	83
Figure 4.9: Manhattan plot of haplotypes using blocks defined by a sliding window of 5 markers.....	84
Figure 4.10: Venn diagram of unique and common CNVs between the dam and the database	86
Figure 5.1: Risk factors for cervical stenotic myelopathy (CSM)	100
Figure 5.2: Vertebral gross and histopathologic changes associated with CSM	101
Figure 5.3: Skeletal growth and maturation timeline in the context of variables and pathology associated with CSM.....	103

Chapter 1

Literature Review Of Equine Cervical Stenotic Myelopathy

Summary

Cervical stenotic myelopathy (CSM) is a disease that affects both the neurological and musculoskeletal systems of horses. A diagnosis of CSM often carries a guarded to poor prognosis, making this a serious problem in regards to the health of the horse. A further understanding of the etiology and pathogenesis is needed for improved management and therapeutic practices. This chapter will focus on what is known about the disease in regards to epidemiology, clinical signs, and diagnosis, as well as associated vertebral and spinal cord pathology. Following the review will be a discussion of the long-standing questions regarding the pathogenesis of this disease. At the conclusion of the chapter is an overview of the dissertation.

Introduction and Background

Cervical stenotic myelopathy is a neurologic disease characterized by malformations of the cervical vertebrae that lead to narrowing of the cervical spinal canal and subsequent compression of the spinal cord. This cord compression manifests as clinical proprioceptive neurologic deficits. Compressive myelopathy has been reported in horses, large breed dogs, and humans (Mayhew et al., 1978; Dimock and Errington, 1939; Bland, 1987; da Costa et al., 2006). Specifically in the horse, CSM is thought to be a multifactorial disease with high planes of nutrition,

increased growth rates, alterations in zinc and copper concentrations, and genetic determinants involved in disease development (Nout and Reed, 2003). Although all these factors are known or suspected to play a role, the exact etiology and/or pathogenesis that lead to clinical disease are still somewhat unclear. Over time, CSM has been associated with a variety of terms, each aiming to accurately describe the disease. These include cervical vertebral malformation (CVM), cervical vertebral compressive myelopathy (CVCM), cervical vertebral instability, cervical static stenosis (CSS), Wobblers Syndrome, and cervical stenotic myelopathy (CSM). For unity, the term cervical stenotic myelopathy, abbreviated CSM, will be used throughout the thesis.

The first reports in the literature of CSM are sporadic. Early theories suggested the neurologic incoordination observed in affected horses was the result of a previous traumatic event (Dimock, 1950). Colloquial terms for CSM included, “jinxed back” and “weak loin” in reference to the horse’s appearance (Dimock and Errington, 1939). In the first comprehensive publication regarding CSM, the disease was described as an “equine disease characterized by a bilateral incoordination of the hind limbs...affected are called “wobblers”.” This work identified weaning as a common time for the onset of clinical signs and breed depositions for the Thoroughbred and Saddlebred. The most pertinent clinical sign was hind limb ataxia with occasional fore limb involvement (Dimock and Errington, 1939). Pathologic changes noted in this survey included abnormal stenosis of the cervical canal, arthritis, cervical nerve compression, and degenerative changes of the spinal cord on histology.

Epidemiology

The epidemiology of CSM has been investigated, allowing perspective on the incidence and prevalence of this disease. A retrospective study examined the types of neurologic diseases seen at the University of Kentucky Veterinary Diagnostic Laboratory over a nearly 3-year period from 2000 to 2002. A total of 4,559 equine necropsies were performed during this time. Of the total cases, 397 (8.7%) were determined to be of neurological origin after gross and histopathologic evaluation. Neurological cases were further categorized by etiology as follows: infectious/inflammatory, neoplastic, congenital, degenerative, traumatic and developmental. A total of 158 (39.7%) of the neurologic cases were categorized as having a developmental etiology. CSM was the only disease in the developmental category; therefore, almost 40% of all neurological cases seen in this time period were a due to CSM (Williams, 2003). Although cases were limited to the central Kentucky area, these data support CSM as a significant neurologic disease of the horse.

In addition to the previously described epidemiologic survey, two other groups have made efforts to examine the incidence and prevalence of CSM cases in the horse population. Incidence assesses the number of new cases over a given time period, whereas prevalence measures cases at a defined point in time. One approach examined clinical records from multiple Thoroughbred breeding farms in Europe and the US over a 6-year period. The overall disease incidence was

determined to be 1.3% (Oswald et al., 2010). Previous to this report, an estimated of 2% was published (Rooney, 1969).

Signalment and Etiologic Factors

Multiple publications have contributed to a strong knowledge base regarding the signalment of CSM horses, specifically gender, breed, and age. A well-documented gender bias of male over females is established in the literature. Gender ratios of affected males to females range from 3:1-23:1 (Dimock, 1950; Steel et al., 1959; Falco et al., 1976; Levine et al., 2007; Levine et al., 2008; Levine et al., 2010). A retrospective study examining possible breed associations with CSM found Thoroughbreds, Warmbloods, and Tennessee Walking Horses more likely to develop the disease as compared to other breeds (Levine et al., 2007; Levine et al., 2008; Levine et al., 2010). In regards to age, historically CSM has been thought of as a disease of young horses often falling under the categorization of developmental bone diseases. Various studies have identified the mean ages of CSM horses as less than 2 years (Dimock and Errington, 1939; Mayhew, 1978; Levine et al., 2008; Levine et al., 2010). Recent retrospective studies have identified CSM developing in older horses. That being said, odds ratios still indicate that younger horses between 6 months and 7 years of age are more likely to develop the disease (Levine et al., 2007; Levine et al., 2008).

CSM is a multifactorial disease with environmental and possibly heritable components (Mayhew, 1978; Falco et al., 1976; Mayhew et al., 1993). As previously stated, high planes of nutrition, increased growth rates, alterations in zinc and

copper concentrations, and possibly genetic determinants play a role in disease development. The relationship between nutrition and skeletal growth and maturation is established in multiple species (Kronfeld et al., 1990). It has been noted that often horses with CSM are larger than age matched pasture mates. Commonly the disparity in size can be attributed to changes in feed to promote growth and maturation for performance, competition, or commercial reasons. An additional report suggested horses with a heavier head and longer neck could result in predisposition to CSM (Rooney, 1969).

The role of genetic determinants in the development of CSM is a long-standing question. Initial support for a genetic influence came from a pedigree analysis that suggested a possible recessive transmission in the Thoroughbred (Dimock, 1950). In contrast, a later pedigree study examined the disease in British Thoroughbreds and did not find evidence for genetic influences (Falco et al., 1976). A breeding study crossed dams (n=12) and sires (n=2), with a confirmed clinical diagnosis of CSM, and followed the progeny for approximately one year (Wagner et al., 1985). Crossing a CSM horse with a CSM horse did not produce the disease in the offspring during their first year of life. Interestingly though, the foals did have evidence of other developmental orthopaedic diseases such as osteochondrosis, contracted tendons, and physitis, indicating aberrations in cartilage and bone maturation. Finally, there is strong anecdotal evidence in families across breeds for possible heritability. Therefore, the exact role of genetic determinants in the development of CSM is still unresolved.

Clinical Presentation and Diagnosis

CSM horses present with neurologic proprioceptive deficits due to cervical spinal cord compression. Most commonly, the hind limb ataxia is more pronounced than the fore limb ataxia. Typically, the ataxia is symmetrical in nature with regard to right and left sides of the horse. Situations in which the ataxia is asymmetrical can result from alterations in the size or spatial positioning of the articular processes which causes compression of the lateral spinal cord and nerve roots (Moore et al., 1992). The anatomic arrangement of nerve tracts in the spinal cord explains the distribution of the ataxia. The dorsal spinocerebellar tracts that control proprioception in the hind limbs are located more superficially than the proprioceptive tracts for the forelimbs (de la Hunta, 1983) (Figure 1.1). Therefore when compression occurs, the dorsal spinocerebellar tracts are the first nerves affected leading to development of higher grade of ataxia in the hindlimbs than the fore limbs.

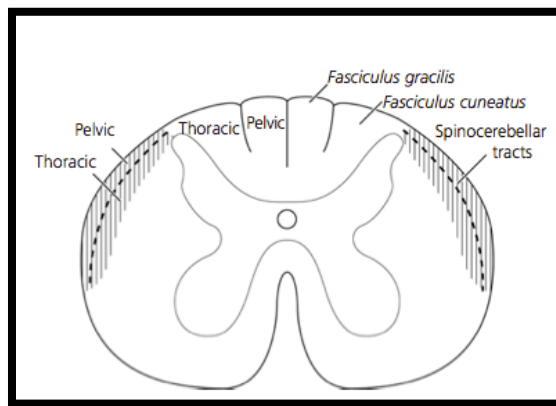


Figure 1.1: Distribution of the spinocerebellar tracts in the spinal cord. The spinocerebellar tracts are located on the lateral aspect of the spinal cord. The tracts for the pelvic limbs are superficial to the thoracic limbs. (Nout and Reed, 2003).

Diagnosis of this disease is focused on a thorough neurologic examination as well as radiographic imaging studies of the cervical column. Neurologic deficits are graded on a scale of 0-5, with 0 being normal and 5 indicating recumbency (Mayhew, 1978). As mentioned previously, CSM horses often present with a bilateral symmetrical hind limb ataxia, with the forelimbs less severely affected. Identification of this type of ataxia helps to differentiate CSM from other equine neurologic diseases such as viral encephalitis (Equine herpesvirus-1, Eastern Equine encephalitis, Western equine encephalitis, Venezuelan equine encephalitis, West Nile Virus, and rabies), protozoal disease (Equine protozoal myeloencephalitis), trauma, or bacterial causes of encephalomyelitis. Deficits of the cranial nerves are typically absent with cervical stenotic myelopathy. In addition to the distribution of the ataxia, evaluation of the cerebral spinal fluid (CSF) can help to rule in or rule out infectious etiologies of neurologic disease.

Findings from multiple investigators have established thresholds for identification of vertebral canal stenosis on both standing cervical radiographs and myelograms. Initially, detection of vertebral stenosis was done with semi-quantitative methods (Mayhew et al., 1993). A radiographic score was assigned based on assessment of the following parameters: stenosis of the vertebral canal, caudal extension of the dorsal lamina, angular fixation, enlarged vertebral physes, delayed bone ossification, and degenerative joint disease. This method was evaluated in a survey of 132 Thoroughbred foals and found to accurately predict disease in horses up to one year of age. A quantitative method evaluating the absolute minimal sagittal diameter of the vertebral canal on standing cervical

radiographs was found to have a high sensitivity and specificity for disease diagnosis (Mayhew, 1978). Subsequent to this work, radiographic intravertebral thresholds or minimal sagittal diameter (MSD) ratios for identification of stenosis for specific vertebral sites were introduced (Moore et al., 1994). The ratio addresses variability associated with radiographic magnification and animal size (Hudson and Mayhew, 2005). The vertebral canal height divided by the height of the vertebral body determines the intravertebral ratio (Figure 1.2). Established intravertebral thresholds for each vertebrae are as follows: C2-3, C3-4, C4-5 < 0.50; C5-6 < 0.52; C6-7 < 0.56. Therefore, a radiographic ratio less than the established value indicate presumptive stenosis at a vertebral site. The sensitivity and specificity of this method was greater than 89% at each vertebral site. While the MSD ratio evaluates the intravertebral measurements, a method has recently been developed to assess stenosis between vertebrae (Hahn et al., 2008). Using the smallest diameter between the dorsal lamina and vertebral body of two adjacent vertebrae and dividing it by the height of the vertebral body gives the intervertebral minimal sagittal diameter ratio (Figure 1.2). A cut off value of <0.485 is suggested for identification of stenosis.

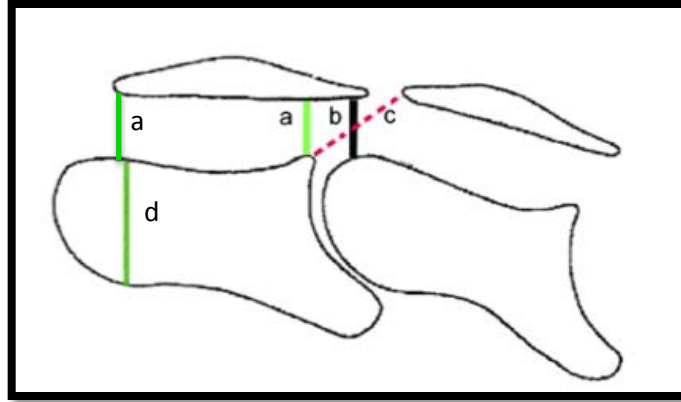


Figure 1.2: Two adjacent vertebrae in the sagittal plane for intravertebral and intervertebral ratio measurements. The intravertebral ratio is composed of the vertebral canal height at the cranial or caudal end of the vertebrae (line “a”) divided by vertebral body height (line “d”). Vertebral canal height (lines “b” or “c”), using the smaller of the two, divided by vertebral body height (line “d”) gives the intervertebral ratio (Adapted from Hahn et al., 2007).

In addition to standing cervical radiographs, other diagnostic imaging techniques are available. Cervical myelography is considered the best antemortem clinical diagnostic for identification of vertebral canal stenosis in the horse. (Rantanen et al., 1981; Papageorges et al., 1987) In contrast to the non-invasive nature of cervical plain films, myelography requires anesthesia for injection of a radio-opaque dye into the subarachnoid space for delineation of the cervical spinal cord on radiographic images. The neck is then manipulated into a variety of positions (neutral, flexed, and extended). In each of these positions, radiographs are evaluated for attenuation of the dorsal and/or ventral dye column, suggesting compression of the spinal cord at a particular vertebral site(s) (Figure 1.3).

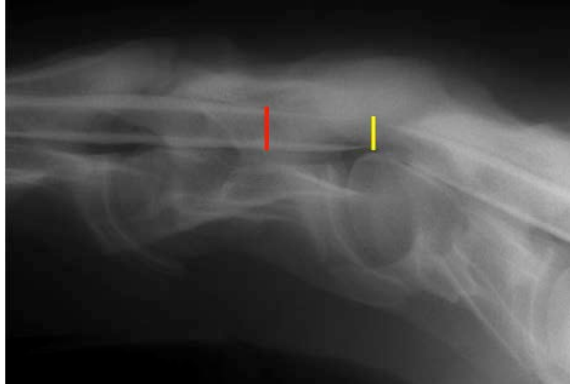


Figure 1.3: Cervical myelogram in the neutral position. The red line is located at a point with normal presence of the dorsal and ventral dye column (no compression). At the yellow line, however, there is attenuation and loss of the dorsal and ventral dye column suggestive of cord compression.

Decision criteria for confident detection of spinal cord compression on myelography have been put forth in the literature (Van Biervliet et al., 2004; Mayhew et al., 1978; Nyland et al., 1980; Nixon et al., 1982; Papageorges et al., 1987; Neuwirth et al., 1992). Such criteria include a dorsal myelographic column of $<2\text{mm}$ at a vertebral site or narrowing of the dorsal and/or ventral dye columns by $> 50\%$ as compared to the cranial vertebral site. Each have a varied ability to confidently identify spinal cord compression associated with vertebral canal stenosis. van Biervliet and co-authors found a 20% reduction in the dural diameter in the flexed position at C6-7 to be highly sensitive and specific for cord compression due to CSM (van Biervliet et al., 2004). Therefore, when evaluating the cervical column for vertebral canal stenosis anatomical site, position (normal, flexed, extended), and threshold criteria should be taken into consideration.

Disease Categorization

Based on myelographic assessment, compression can be classified as dynamic or static. Dynamic compression occurs when attenuation of the dye column happens only with the neck in the flexed or extended position. Often, dynamic compression is seen in the mid cervical region, which encompasses the third to the fifth vertebrae. On the other hand, if dye column attenuation is observed regardless of neck position, then compression is categorized as static. Typically this type of compression is seen in the caudal cervical column from the fifth to the seventh vertebrae (Mayhew, 1999).

Consideration of the presence of specific gross pathologic lesions in the context of signalment lead to a classification system of Type 1 and Type 2 cervical vertebral malformation (CVM) (Mayhew, 1999). Features of type 1 CVM include the following: age of onset from weaning until 2 years, static or dynamic stenosis, pathologic changes of the articular processes such as osteochondrosis, kyphosis or subluxation due to vertebral body malalignment, vertebral body physitis, and caudal extension of the dorsal lamina into the intervertebral space. The lesions and presentation of Type 1 CVM suggest a developmental aberration leading to the described vertebral malformations. In contrast, Type 2 CVM typically affects older horses. Vertebral lesions include osteoarthritic and degenerative changes of the articular processes. Osteophytes and thickening of the articular soft tissues is observed along with synovial cysts. Further descriptions of the vertebral changes mentioned here is in the CSM pathology section of this chapter.

Treatment and Management

Several management and treatment options are available after a diagnosis of CSM has been made. Selecting an appropriate option is dependent on the age of the horse, number of sites of compression, chronicity of clinical signs, and financial resources. Medical management of the disease includes reducing inflammation from the repeated compression of the spinal cord. Routine anti-inflammatory medications including non-steroidal anti-inflammatory drugs (NSAIDs), such as flunixin meglumine, and corticosteroids are used in moderate to severe cases (Nout et al., 2003).

Another focus of medical management is slowing the growth rate in young horses, via a restricted diet to allow for bone remodeling (Donawick et al., 1989; Donawick et al., 1993; Kronfeld et al., 1990). The impact of protein and energy restriction in young horses with either suspected or confirmed neurologic and/or radiographic deficits consistent with CSM has been investigated (Donawick et al., 1989). In addition to diet restriction, reduced exercised was also included. The diet comprised 65-75% of the recommended energy and protein content, supplementation of copper and zinc at 2 times and 3.5 times the recommended NRC level respectively, and access to hay. Conclusions from this study were that, although the horses became quite thin, the dietary restrictions slowed growth rates to allow remodeling of the vertebrae for sufficient space to negate spinal cord compression. Since this study, other “paced” nutritional plans have been developed which reduce energy and protein intake without the dramatic weight loss (S. Reed,

personal communication). Use of the “paced” diet and exercise restriction is most effective in horses under one year of age when maximal growth is occurring.

In situations where nutritional management is not sufficient, surgical options are available, specifically cervical vertebral interbody fusion or dorsal laminectomy. The surgery aims to prevent further spinal cord damage by stabilizing the intervertebral joint and relieving cord compression. A retrospective survey over a 9-year period found that 77% of CSM who underwent surgery had some level of neurologic improvement. Forty-three percent of horses returned to some sort of athletic function (Moore et al., 1993). It was also reported in this study that the number of compression sites did not have an effect on the post surgical outcome.

Cervical Vertebral Anatomy

Before describing the pathologic vertebral changes that have been associated with equine CSM, a brief review of normal vertebral anatomy will be summarized. Seven vertebrae make up the cervical column. Vertebrae are considered irregular bones due to their shape. Other bone categories are long, flat, sesamoid, and short. The vertebral spinal canal is the space occupied by the spinal cord. Vertebral arches (pedicles) border the spinal canal on either side. The dorsal lamina forms the roof of the canal and the vertebral body comprises the floor of the canal. Articular processes are located on the dorsal aspect of the vertebrae (Figure 1.4).

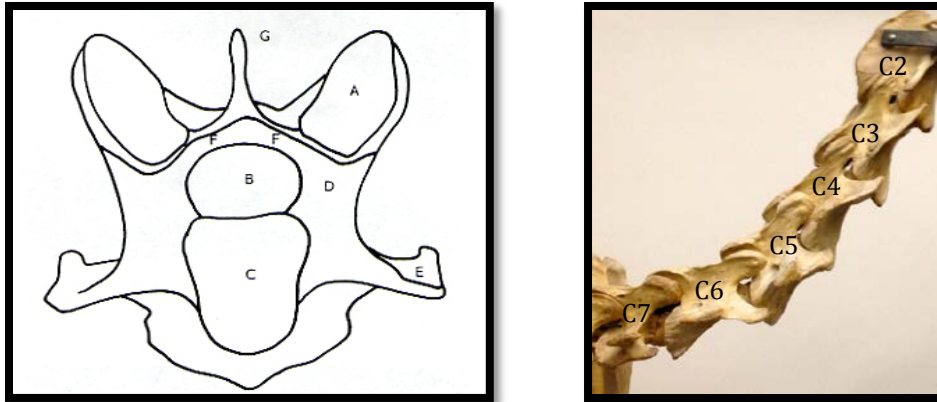


Figure 1.4: Images of cervical vertebral anatomy. The image on the left is a schematic of a single cervical vertebra in the transverse plane. A- articular process; B- vertebral canal; C- vertebral body; D- vertebral arch; E- transverse process; F- dorsal lamina; G- spinous process (Whitwell and Dyson, 1987). On the right, is a photograph of the cervical column from C2-C7 in the sagittal plane.

There is a natural narrowing of the vertebral canal in the mid cervical region. Epiphyseal plates are located at the cranial and caudal aspect of each vertebral body. The cranial physis typically closes around 2 years of age in a ventral to dorsal direction. In contrast, the caudal physis remains open until 4-5 years of age and closes in a dorsal to ventral direction (Whitwell and Dyson, 1987). Cervical spinal nerves exit the vertebral canal through the intervertebral foramen. The second through the seventh cervical vertebrae have articular processes located on the dorsal aspect. The first cervical vertebra, commonly known as the atlas, does not have articular processes. The second vertebra, called the axis, only has 2 articular processes, left and right, located on the caudal aspect of the vertebrae. Whereas cervical vertebrae 3 through 7 have articular processes located on the left and right side in both the cranial and caudal positions. The articular processes articulate with the same structure of the adjacent vertebrae in the cranial or caudal direction

forming synovial joints. The articular process joints function to connect the individual vertebrae together forming the cervical vertebral column. Other anatomic structures that stabilize the column include the following: the ligamentum flavum, which connects dorsal laminae of adjacent vertebrae, fibrous disc material between each vertebral body, and a complex arrangement of skeletal muscle attachments.

CSM Pathology

Spinal Cord

There are characteristic histopathologic lesions that indicate compressive injury to the spinal cord and are visualized in CSM cases. In the white matter, Wallerian degeneration with the varying degrees of demyelination, presence of gitter cells, dilated myelin sheaths, and spheroids (swollen axons) are consistent with spinal cord compression (Figure 1.5). In chronic cases, perivascular fibrosis, motor neuron loss, astrocytosis, and microglial scars are observed. (Summers et al., 1995).

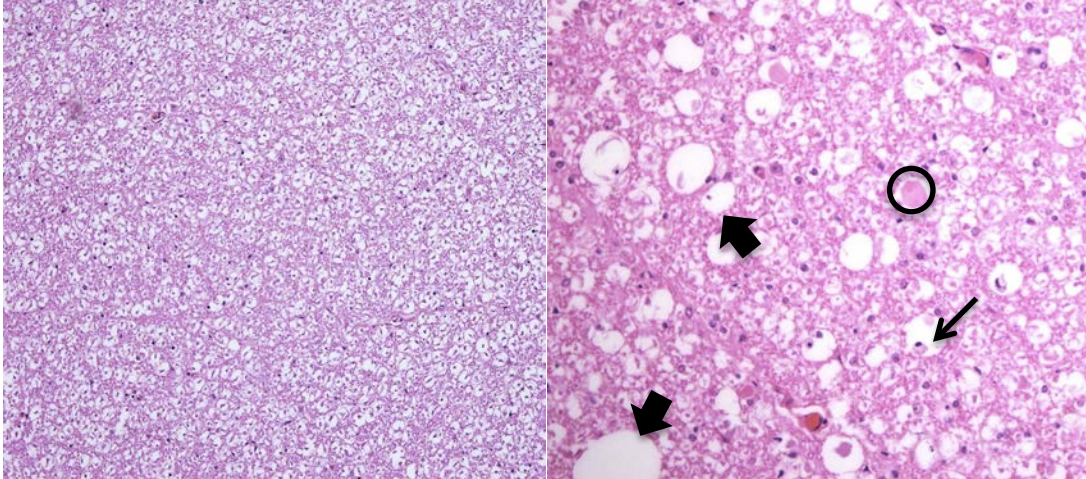


Figure 1.5: Histopathologic sections of the white matter of the spinal cord. The image on the left is normal white matter at 2X magnification. The spinal cord on the right is from a CSM horse at 10X magnification. Dilated myelin sheaths (thick arrows), gitter cells (thin arrows), and spheroids (circle) are consistent with compressive spinal cord injury seen in CSM.

Distribution of the lesions within the funiculi of the white matter aids in lesion localization. Pathologic changes are visualized in the dorsal, lateral, and superficial funiculi at the compression site. The dorsal and superficial lateral funiculi, which contain the ascending nerve tracts, are affected cranial to the site of compression, whereas the descending nerve tracts in the ventral and the deep portion of the lateral funiculi are affected caudal to the site of compression (Figure 1.6).

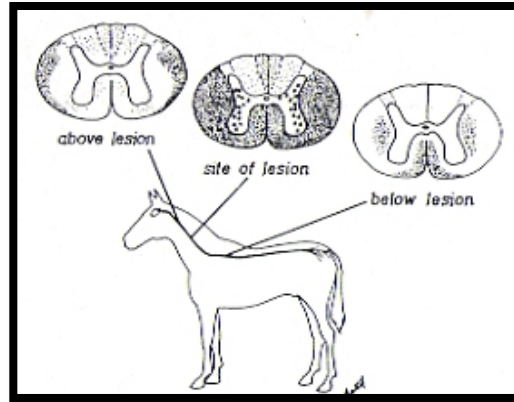


Figure 1.6: Schematic of lesion localization in the spinal cord. Black dots indicate distribution of Wallerian degeneration (Mayhew, 1978).

Vertebral Body

The vertebral body can contribute to compression in several ways. Narrowing of the vertebral canal can occur from dorsal deviation of the vertebral body due to subluxation (Figure 1.7). Also, flaring of the caudal epiphysis results in a focal decrease in canal height. Histopathological changes in the vertebral body include increased bone known as osteosclerosis, mainly in the metaphysis, which leads to distortion of epiphyseal plates. Chondronecrosis, osteonecrosis and retained cartilage cores have been reported in the vertebral body as well (Mayhew et al., 1978).

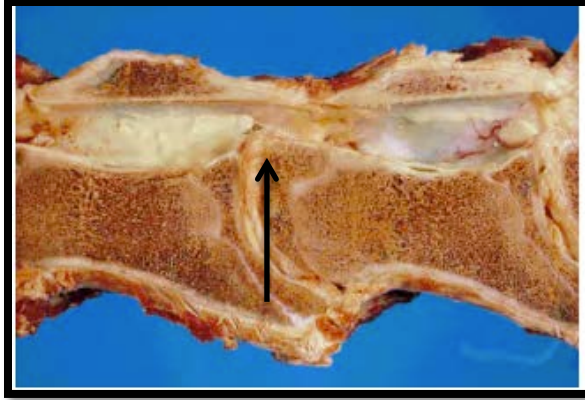


Figure 1.7: Sagittal view of the cervical vertebral column demonstrating vertebral body subluxation. There is upward deviation of the vertebral body into the canal space (arrow). The spinal cord has been removed (Mayhew, 1999).

Articular Processes

The role of the articular processes in vertebral canal stenosis has been the focus of multiple investigations. A variety of lesions have been reported including degenerative joint disease, subchondral osteosclerosis, osteochondrosis, synovial cysts, and thickening of the joint capsule. Similar to the vertebral bodies, osteonecrosis, chondronecrosis, retained cartilage cores have been observed on histopathology (Mayhew et al., 1978; Trostle et al., 1993; Stewart et al., 1991; Fisher et al., 1981). Examples of gross articular process pathology are described in figure 1.8.

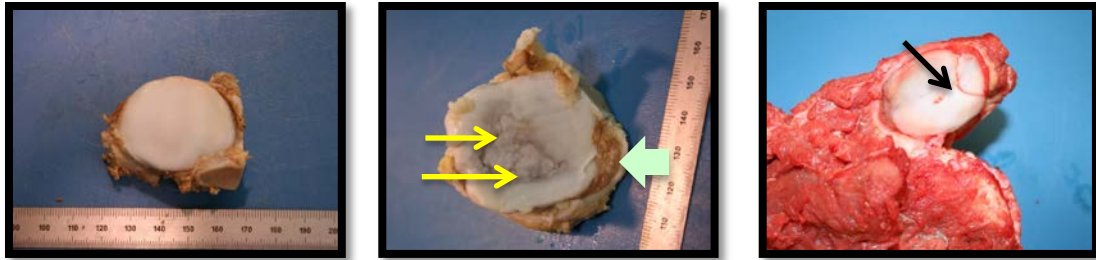


Figure 1.8: Normal and gross pathology of the articular processes associated with cervical stenotic myelopathy. The left picture is an articular process (formalin fixed) from a control horse. The articular surface is smooth, and white with an oval shape. The middle image (formalin fixed tissue) demonstrates degenerative or arthritic changes including cartilage loss, dull and grey discoloration, and fibrillation (yellow arrows). Also, the synovium is moderately thickened (thick arrow). The right image (unfixed tissue) is an articular process with osteochondrosis. This lesion is characterized by invaginations of the cartilage (black arrow).

Osteochondrosis is a developmental orthopaedic disease associated with a failure of normal endochondral ossification in cartilage and bone maturation. Articular process osteochondrosis in the context of CSM has been investigated as well. It was found that although the frequency of articular process osteochondrosis did not differ between CSM and controls, the severity of osteochondrosis did. However both the frequency and severity of osteochondrosis in the appendicular skeleton was greater in CSM horses (Stewart et al., 1991).

Alterations in the size and spatial orientation of the articular processes impact the space available in the vertebral canal. Recently, the anatomy of the articular process joint with relationship to the spinal cord in clinically normal horses was evaluated with CT. The articular process joints were distended with contrast media and the anatomy evaluated. Distention caused dorsolateral

extension of the articular process joint into the vertebral canal. The authors concluded that in the absence of pathologic changes distention of the articular process joint was not sufficient to cause compression. However, it was speculated that in the presence of pathologic changes in regards to size or spatial orientation, joint space effusion could lead to compression (Claridge et al., 2010). Finally, earlier work identified that malformations of the articular process joints caused lateral compression of the spinal cord and peripheral nerve roots exiting the intervertebral foramen (Moore et al., 1992).

Dorsal Lamina and Ligamentum Flavum

Changes to the dorsal lamina and ligamentum flavum have been described primarily in the caudal cervical column, often observed as static cervical stenosis. On gross examination, both the dorsal lamina and ligamentum flavum can be thickened in CSM horses. The most common histopathologic change in the dorsal lamina is osteosclerosis with retained cartilage also observed (Mayhew et al., 1978; Powers et al., 1986). Fibrocartilage is observed at the insertion of the ligamentum flavum at the dorsal lamina. Proliferation of fibrovascular tissue is also seen scattered in the ligamentum flavum (Powers et al., 1986).

Important Knowledge Gaps

So far, this review has focused on what is known about CSM in regards to epidemiology, signalment, diagnosis, treatment options, and pathology. Important remaining questions include the exact etiology/pathogenesis that leads to the development of CSM in the horse. Environmental factors are well documented. CSM

is established as a multifactorial disease but the interplay of the factors, which leads to clinical disease, is still unknown.

Two main theories have been developed to model CSM pathogenesis. The first theory centers developmental abnormalities that lead to vertebral malformations. Osteochondrosis, a developmental orthopaedic disease, has been shown to occur with increased severity in CSM horses (Stewart et al., 1991). Pathologic findings also support suppression of normal bone and cartilage turnover and maturation (Mayhew, 1978). There is potential that these developmental issues could begin *in utero* (Mayhew, 1999). The second theory proposes that CSM occurs due to abnormal stresses on the cervical column leading to vertebral malformation. Since the cervical vertebrae are still remodeling and developing up to approximately 5 years of age, they are more susceptible to biomechanical forces on the neck. Thickening of the soft tissues, osteosclerosis of the dorsal lamina, and osteoarthritis are supportive of the biomechanical model (Powers et al, 1986; Trostle et al., 1993). Further investigation of the pathology associated with this disease could help provide clarity to disease mechanisms for the clinical manifestation of CSM.

A related major knowledge gap is the role of genetic determinants as an etiologic factor in disease susceptibility and/or development. Pedigree analyses and anecdotal reports support a role of genetic determinants in CSM (Dimock, 1950; Errington, 1938). On the other hand, a prospective breeding study minimizes the likelihood of CSM being inherited as a single gene trait (Wagner et al., 1985).

Powerful new scientific resources have been developed in recent years through whole genome sequencing and related advances in the field of genomics that provide new approaches to investigate potential genetic determinants of CSM. In a large collaborative project that started in late 2006, the first horse genome was sequenced to 6.8x coverage and assembled into the reference equine genome (Wade et al., 2009). In addition to determining the primary nucleotide sequence of the equine genome and specific chromosomal loci for functional elements such as protein coding genes, this work led to the identification and characterization of millions of genetic polymorphisms distributed throughout the equine genome. This large number of polymorphic markers enables the potential for equine linkage analyses, which can investigate co-segregation of genetic markers with hereditary traits in families. Co-segregation studies can provide data to assess mode of inheritance, identify genome regions or loci of importance, and help identify potential candidate genes for a trait of interest. This family-based analysis is called genome wide linkage study (GWLS).

Equine breeders, however, avoid matings that might produce hereditary diseases. As a result, it is often difficult to assemble kindreds to study disease traits using GWLS approaches. Furthermore, incomplete penetrance and complex genetics will limit the effectiveness of family studies. Fortunately, the large number of genetic markers allows an alternative approach based on distribution of genes and the traits in closed breeding populations. Basically, individuals within a closed breeding population will, on average, have the same chance of possessing any of the genetic markers. However, if the population is divided into two groups based on a

distinguishing characteristic, for example, whether or not they exhibit black-pigmented hair, then any genetic markers that co-distribute with the trait will signal that the trait is genetic and that a gene controlling that trait has a locus close to that genetic marker. This approach is called a genome wide association study (GWAS). GWAS can be very effective at uncovering individual genes regulating a trait based on an unambiguous phenotype with a simple pattern of Mendelian inheritance. The *Extension* locus alleles that regulate coat color are an example (McCue et al., 2012). GWAS can also be applied, however, for investigating more complex genetic diseases where the possibility exists of multiple variants that individually have a small impact but collectively influence the phenotype of interest. Nucleotide sequence variants distributed across the genome include single nucleotide polymorphisms (SNPs), copy number variants (CNVs), microsatellites, and insertion/deletion polymorphisms (INDELS) (Shafer and Hawkins, 1998). SNPs are variations in a single base whereas CNVs range in size from a couple of hundred bases to several megabases in length. With the availability of these new genomic technologies and reagents in the horse, reexamination of the role of genetic determinants in CSM is justified.

Dissertation Overview and Objectives

CSM is one of the most common neurologic diseases in the horse. Depending on the severity of clinical signs, euthanasia is often elected for humane and safety reasons. Further investigation of remaining questions regarding the interaction of etiologic factors and pathogenesis could help improve diagnostic, management, and

treatment options of this important disease. The work presented in this thesis re-investigates the etiology and pathogenesis of equine CSM using contemporary imaging and genomic techniques.

Chapter 2: Comparison Of Standing Cervical Radiographs And Magnetic Resonance Imaging For Evaluation Of Vertebral Canal Stenosis In Equine Cervical Stenotic Myelopathy

The aim of the work described in Chapter 2 was to determine if magnetic resonance imaging (MRI) allows for more accurate identification of cervical canal stenosis as compared to lateral radiographs in CSM horses. The sensitivity and specificity of lateral cervical radiographs to evaluate horses suspected of cervical stenotic myelopathy (CSM) are limited by the assessment being restricted to the sagittal plane. The ability of MRI to acquire images in multiple planes addresses this issue. Radiographic cervical canal height measurements categorized by standard minimal sagittal diameter (MSD) intravertebral and intervertebral ratios produced several false positive and false negative canal stenosis determinations as defined by spinal cord histopathology. Postmortem MRI measurements of canal area and cord canal area ratio more accurately predicted sites of cord compression in CSM cases. No differences in spinal cord measurements were observed when comparing CSM to control horses, but each of the vertebral canal parameters achieved significance at multiple sites. Results from this study support vertebral canal area and cord canal area ratio as better parameters to predict the location of cervical canal stenosis compared to only the sagittal plane of canal height. Therefore in the future, development of MRI or computed tomography (CT) equipment capable of evaluating the cervical column of adult horses will substantially enhance evaluation

of CSM patients. This chapter has been published in Equine Veterinary Journal (Janes et al., 2013).

Chapter 3: Skeletal Pathology Of The Cervical Articular Processes In Equine Cervical Stenotic Myelopathy

Experiments reported in chapter 3, focus on the characterization and evaluation of articular process skeletal pathology associated with CSM. First, identified articular process pathology was assessed both quantitatively in regards to the number and location of lesions, and qualitatively in regards to severity. Subsets of lesions were then structurally evaluated using micro-CT and routine histopathology methods. It was found that lesions identified on MRI occurred at an increased frequency and severity in CSM horses compared to controls. Also, pathology was observed both at and away from the site of compression, supporting a generalized problem of bone and cartilage maturation in the cervical column of horses with CSM. Histologically, lesions included osteochondrosis, osseous cyst-like structures, fibrous replacement of trabecular bone and the bone marrow, and osteosclerosis. These lesions support a disease model with developmental skeletal pathology as a primary issue with likely secondary biomechanical influences on the articular processes leading to malformations.

Chapter 4: The Role Of Inherited Genetic Determinants In Equine Cervical Stenotic Myelopathy

Chapter 4 re-examines the question of whether inherited genetic determinants contribute in a substantial way to the susceptibility, etiology, and/or pathogenesis of CSM. The experiments utilized equine genomic reagents and protocols developed over the last several years. Carefully phenotyped CSM horses

were compared to population data using the Equine SNP50 and Equine SNP 70 Bead Chips for a genome wide association study (GWAS). In addition, a copy number variant (CNV) assessment for identification of possible unique CNVs within a family with increased disease prevalence was performed. Results of the GWAS identified multiple significant loci composed of individual SNPs and haplotypes localized to several chromosomes. Results of this study support a genetic role in the development of CSM, but given that interesting regions were identified across the genome, it is unlikely one or only a few major genes control the CSM phenotype. Genetic contributions are likely more complex in nature with multiple loci involved versus a simple Mendelian trait. This is consistent with the understanding that clinical disease due to CSM is multifactorial in nature resulting from both genetic and environmental variables.

Chapter 5: Reflections And Future Directions

The emphasis of this chapter will be a reflection on how experiments in this thesis have contributed to reducing and/or refining the existing knowledge gaps in our understanding of equine CSM. In addition, possible future studies based on the results of this dissertation research are discussed.

Chapter 2

Comparison Of Magnetic Resonance Imaging To Standing Cervical Radiographs For Evaluation Of Vertebral Canal Stenosis In Equine Cervical Stenotic Myelopathy.

Summary

Experiments in this chapter aimed to determine if magnetic resonance imaging (MRI) allows for the more accurate identification of cervical spinal canal stenosis as compared to lateral cervical radiographs in CSM horses. In addition, a morphometric assessment of the vertebral canal was performed. Nineteen Thoroughbred horses with CSM were compared to nine control Thoroughbreds. Antemortem, the subjects had neurologic examinations and standing cervical radiographs with sagittal ratios calculated from C3-C7. Intact cervical column MRI scans and histologic examinations of the spinal cord were performed postmortem. Morphometric parameters were measured on the vertebral canal, spinal cord, and intervertebral foramen. Radiographic cervical canal height measurements categorized by standard minimal sagittal diameter (MSD) intravertebral and intervertebral ratios produced several false positive and false negative canal stenosis determinations as defined by spinal cord histopathology. Postmortem MRI measurements of canal area and cord canal area ratio more accurately predicted sites of cord compression in CSM cases. Development of MRI or computed tomography (CT) equipment capable of evaluating the cervical column of adult horses will substantially enhance evaluation of CSM patients.

Introduction

Cervical stenotic myelopathy (CSM, Wobbler Syndrome) is the result of malformations of the cervical vertebrae, which cause stenosis of the vertebral canal and compression of the spinal cord. Compressive myelopathy has been reported in multiple species including horses, dogs, and humans (Mayhew, 1978; Dimock and Errington, 1939; Bland, 1987; da Costa et al., 2006). CSM typically affects young horses with an increased incidence in certain breeds, including Thoroughbreds, Tennessee Walking Horses, Quarter Horses, and Warmbloods (Levine et al., 2008). There is a well-documented gender ratio of males over females with reports ranging from 3:1 up to 23:1 (Dimock, 1950; Falco et al., 1976). CSM is a multi-factorial disease with genetics, high planes of nutrition, alterations in copper and zinc ratios, rapid growth rates, and trauma thought to potentially play a role in the etiology and pathogenesis.

Several groups of researchers have made important contributions to antemortem diagnostic criteria of equine CSM using standing cervical lateral radiographs and myelography (Mayhew et al., 1993; Moore et al., 1994; Hahn et al., 2008; van Biervliet et al., 2004). Thresholds have been established using anatomical measurements converted to intravertebral and intervertebral ratios to identify presumptive areas of canal stenosis both at the intervertebral joint and within vertebrae. With myelography, spinal cord compression can be visualized due to attenuation of the dorsal and/or ventral contrast medium columns and interpreted using published criteria for contrast medium column measurements. Compression from the lateral aspect can also occur due to altered articular process shape, size,

and spatial positioning. While both methods are important diagnostic aides, the levels of false positives and false negatives remain problematic (Papageorges et al., 1987). A factor contributing to this problem is the limitation of assessment to the sagittal plane with lateral images. Changes in vertebral canal structure that might lead to spinal cord compression are not restricted to reductions in the dimension of dorsal-ventral height. Dorsal ventral radiographic views can be obtained as well, but these views capture the articular processes and not the vertebral canal. Therefore, a more complete view of the cervical column should improve diagnostic assessment. The ability of magnetic resonance imaging (MRI) to evaluate a structure of interest in multiple planes, as well as provide images of both soft tissues and osseous structures *in situ* has the potential to overcome major limitations of lateral radiographs when assessing equine patients for CSM. Given these characteristics, this study was designed to test the hypothesis that MR imaging provides a more rigorous assessment of the cervical vertebral canal as compared to standing cervical radiographs in the horse. The objectives were to: 1) Compare the ability of standing cervical radiographs and MRI to identify vertebral canal stenosis in horses with CSM, and 2) Evaluate anatomic parameters of the vertebral canal, spinal cord, and intervertebral foramen between control and CSM horses on MRI.

Materials and Methods

Animals

Horses utilized in the study were identified based on clinical history, neurological assessment, cervical radiographs, and postmortem examination.

Nineteen Thoroughbred horses with CSM (17 males, 2 female, age range 6-50 months with a mean of 18.1 months) were compared to nine control Thoroughbred horses (6 males, 3 females, age range 9-67 months with a mean of 12.4 months). Case and control horses were identified in collaboration with local veterinary practitioners.

Clinical Examination

A neurologic examination was performed on each horse. A grading scale of 0-5, where 0 indicated no neurologic deficits and 5 indicated recumbency, was used to classify the severity of clinical signs in the forelimbs and hind limbs (Mayhew, 1978). Standing lateral cervical radiography was obtained on all horses. Radiographic images were measured and evaluated by a single blinded assessor. Standard minimal sagittal diameter (MSD) intravertebral ratios (C2-C5 <0.50; C6 <0.52; C7 <0.56) (Moore et al., 1994) and intervertebral ratios (C2-C7 <0.485) (Hahn et al., 2008) were calculated from C2-C7 using Dicom Viewer software (eFilm Workstation, Merge eMed, Chicago, Illinois). After antemortem clinical examination and radiographs, owner-elected euthanasia was performed with an overdose of a barbiturate following AVMA guidelines. Control horses had normal neurological function, but were euthanized for other health-related reasons.

MRI Evaluation

Within 4 hours of euthanasia, the cervical spinal column was disarticulated in the area of T3 to T5. Loss of cerebral spinal fluid was prevented by placing putty in the vertebral canal at the disarticulation site. MR imaging was performed using a 1.5 Tesla magnet with a flexible surface receiver coil and spinal coil. The cervical

column was imaged in cranial (C2-5) and caudal (C4-C7) sections. Sagittal, transverse, and dorsal plane images using multiple sequences were acquired for each section. The cervical column was evaluated in the neutral position.

Morphometric measurements were made by two independent assessors at the mid-point of intervertebral joints for all parameters using an open source DICOM viewer program (Osirix, Geneva, Switzerland) (Rosset et al., 2004). Measurements were as follows: spinal cord height, spinal cord width, spinal cord circumference, spinal cord area, vertebral canal height, vertebral canal width, vertebral canal circumference, vertebral canal area, left intervertebral foramen height, right intervertebral foramen height, and a ratio of the measured spinal cord area to vertebral canal area (Figure 2.1).

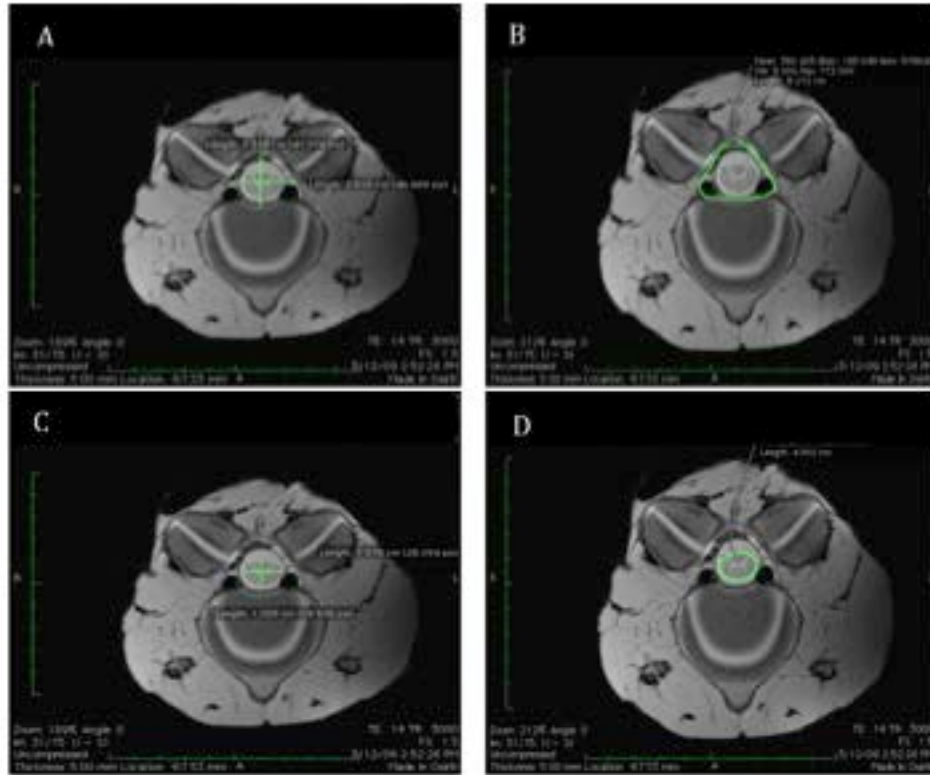


Figure 2.1. Anatomical measurements of the vertebral canal and spinal cord using proton density weighted MR images. Transverse plane images demonstrate spinal cord and vertebral canal measurements at the midpoint of the cervical vertebral articulation. A. Height and width measurements of the vertebral canal. B. Vertebral canal area and circumference. C. Spinal cord height and width measurements. D. Spinal cord area and circumference

Postmortem Evaluation

Postmortem examinations were performed by two assessors. The spinal cord was removed from the vertebral column during disarticulation of intact vertebrae. Intervertebral sites on the spinal cord were identified and marked during disarticulation. The spinal cord was placed in 10% neutral buffered formalin for fixation and processed routinely for histopathologic examination. Two to four tissue sections were evaluated at each intervertebral site from C1-C2 to C6-C7. Cervical stenotic myelopathy was confirmed by identifying compressive lesions

microscopically at specific intervertebral sites based on the characteristic changes of Wallerian degeneration with presence of gutter cells, dilated myelin sheaths, spheroids (swollen axons), and fibrosis in appropriate dorsal, lateral, and ventral funiculi within the white matter (Summers et al., 1995). Postmortem and histopathologic examinations were also used to rule out other infectious, inflammatory, or degenerative neurologic diseases of the spinal cord.

Experimental Group Classification:

Antemortem criteria for CSM horses included: 1) hind limb ataxia and proprioceptive deficits, and 2) narrowing of the cervical canal on radiographs based on intravertebral (C3-5 <0.50; C6 < 0.52; C7 <0.56) or intervertebral (<0.485) minimal sagittal ratios. Histopathologic evidence of spinal cord compression on postmortem examination was the definitive parameter used for a CSM diagnosis and for specific site localization of disease (Table 2.1). Inclusion criteria for control horses were an absence of neurologic deficits on the clinical examination and an absence of compressive lesions on histologic examination of the spinal cord.

Site	Standard MSD thresholds for intravertebral sites, and intervertebral sites at 0.485 (radiographs)		Intra and intervertebral thresholds at 0.485 (radiographs)		Histopathological evidence of spinal cord compression (postmortem)	
	Controls	CSM	Controls	CSM	Controls	CSM
C2-3	1	6	0	5	0	1
C3-4	3	16	1	12	0	13
C4-5	2	11	1	4	0	7
C5-6	1	16	0	10	0	11
C6-7	5	15	3	5	0	6

Table 2.1. Study case categorizations based on different radiographic and histological thresholds and assessments. Control (n=9) and CSM (n=19) horses were classified at each individual intervertebral site. Some CSM horses were narrowed at multiple sites accounting for variation in numbers in the CSM category.

Statistical Analysis

Vertebral canal measurements at sites of spinal cord compression as identified by histopathology in CSM horses were compared to control horses at the same cervical position. Therefore, the total number of CSM samples analyzed at each vertebral site was different (Table 2.1). Data measurements from all nine controls were used at each vertebral site. Using the Anderson-Darling test, morphometric parameter data were normally distributed. Data for morphometric parameters were analyzed using a mixed statistical model that accounted for variables of vertebral site, age, and gender using the PROC MIXED procedure in SAS (SAS, Cary, NC). PROC LOGISTIC was used to determine if intravertebral and intervertebral radiographic ratios, MRI canal area, and cord canal area ratios (CCAR) could localize sites of histopathologic lesions on a vertebral site-by-site comparison. To determine whether canal area and CCAR could predict a lesion regardless of vertebral site, a generalized estimating equation accounting for repeated measures was constructed with the additional variables of age, gender, site, and set.

Evaluation of the two MRI image assessors for concordance was done by calculating an intraclass correlation coefficient for each morphometric parameter. Coefficients, using a scale range of 0.00 to 1.00, were classified as follows: excellent (>0.75), good (0.4-0.75), and poor (<0.4) (Shokuri and Edge 1996). The intraclass correlation analysis was performed using the software program MedCalc for Windows, version 12.5 (MedCalc Software, Ostend, Belgium). Significance was defined at $p < 0.05$.

Results

Identification of False Positive and False Negative Cases

Based on the established radiographic MSD ratio and intervertebral thresholds with reference to histopathologic assessment of spinal cord compression, a subset of control and CSM horses were categorized as false positives or false negatives (Table 2.1). Misclassifications based on MSD ratios were observed at each vertebral site and are illustrated in figure 2.2 at the level of C4-5. Two control horses were classified as having vertebral canal narrowing at C4-5, while three of the CSM horses had vertebral canal ratios above thresholds used to indicate a likelihood of stenosis. In contrast, using canal area determined from the MRI images, control and CSM horses segregated more distinctly (Figure 2.2).

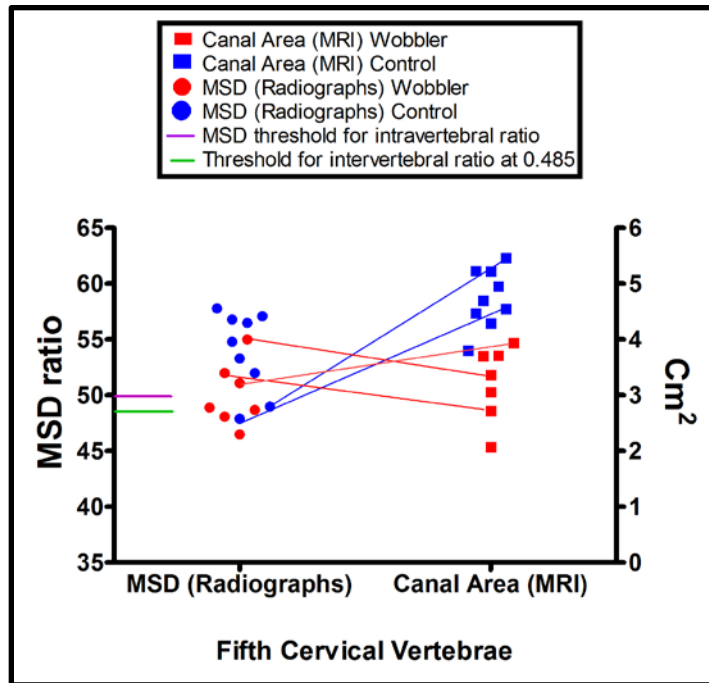


Figure 2.2: Scatter plot of the MSD ratios from radiographs and canal area measurements from MRI of horses with compressive lesions at C4-5. The left ordinate is for the sagittal radiographic ratios with positions of the established thresholds indicated. The right ordinate is for the MRI canal area data. Two control horses (blue circles) have MSD ratios indicative of spinal cord compression, which was not present on postmortem histology. Three CSM horses (red circles) fall above the radiographic thresholds, even though spinal cord compression was confirmed by postmortem histology. Canal area values for two false positive control and three false negative CSM horses (blue and red diagonal lines respectively) cluster within the appropriate groups.

Similar partitioning of CSM and control groups based on canal area and CCAR was observed at the other cervical vertebral sites (Figures 2.3 and 2.4).

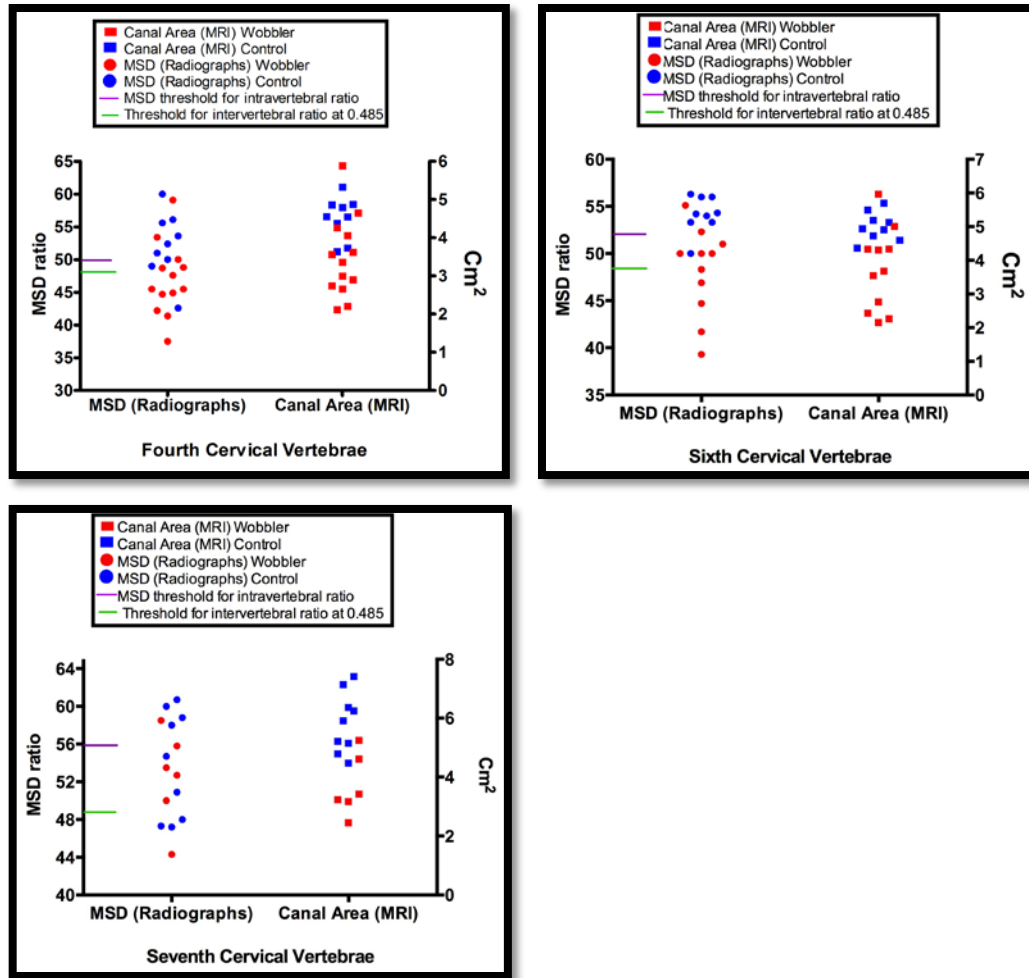


Figure 2.3: Scatter plot of the MSD ratios from radiographs and canal area measurements from MRI of horses with compressive lesions at the fourth, sixth, and seventh cervical vertebrae.

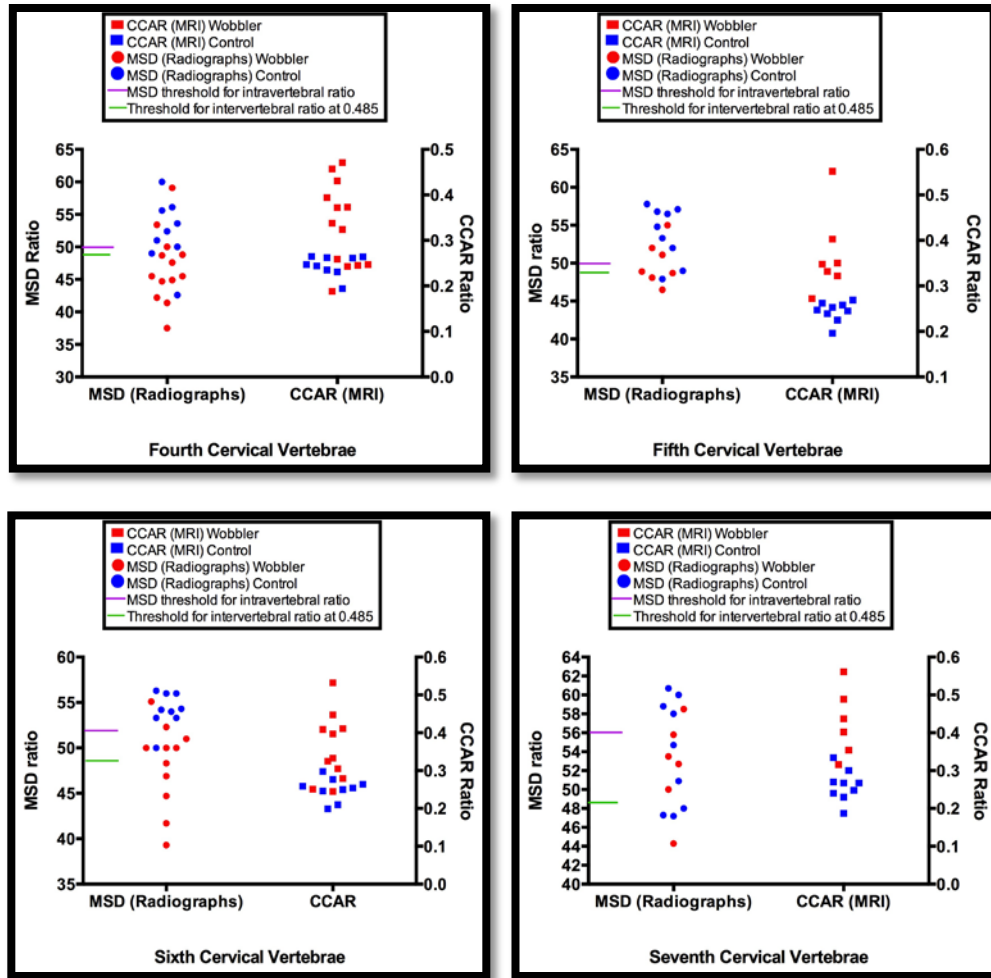


Figure 2.4: Scatter plot of the MSD ratios from radiographs and cord canal area ratio (CCAR) from MRI of horses with compressive lesions at the fourth, fifth, sixth, and seventh cervical vertebrae.

Anatomic Changes of the Cervical Vertebral Column on MRI

While no significant differences in spinal cord measurements on MRI were observed, each of the vertebral canal parameters achieved significance at multiple sites when comparing CSM to control horses (Table 2.2).

Site	Number	Canal Height (cm)	Canal Width (cm)	Canal Circ. (cm)	Canal Area (cm ²)
C2-3	Control (n=9)	2.63±0.52	2.17±0.20	8.85±1.29	5.65±1.31
	CSM (n=1)	2.56	4.432	10.096	7.419
C3-4	Control (n=9)	2.18 ± 0.30	2.44±0.41	8.00±0.94	4.62±0.97
	CSM (n=13)	1.92±0.28**†	2.12±0.43**	6.94±.96	3.49±0.95**†
C4-5	Control (n=9)	2.14±0.28	2.59±0.35	8.10±0.98	4.70±0.90
	CSM (n=7)	1.75±0.28**	2.26±0.41**	6.75±0.74**	3.21±0.66**
C5-6	Control (n=9)	2.18±0.26	2.76±0.27	8.60±0.56	5.07±0.58
	CSM (n=11)	1.80±0.35**	2.51±0.59*	7.22±1.38**	3.73±1.19**†
C6-7	Control (n=9)	2.37±0.41	3.14±0.53	9.77±0.114	6.40±1.33
	CSM (n=6)	1.85±0.46**	2.69±0.55**	8.20±1.48**†	4.38±1.52**

Site	Number	L IV Foramen Height (cm)	R IV Foramen Height (cm)	Cord Area/ Canal Area Ratio
C2-3	Control (n=9)	0.76±0.15	0.78±0.17	0.21±0.07
	CSM (n=1)	1.136	1.262	0.148
C3-4	Control (n=9)	0.88±0.17	0.88±0.17	0.28±0.07
	CSM (n=13)	0.66±0.23**	0.73±0.17**	0.33±0.08**†
C4-5	Control (n=9)	0.91±0.14	0.95±0.17	0.25±0.05
	CSM (n=7)	0.72±0.24**†	0.74±0.30*	0.37±0.08**†
C5-6	Control (n=9)	1.05±0.11	0.98±0.17	0.26±0.03
	CSM (n=11)	0.75±0.21**	0.80±0.23**	0.36±0.09**†
C6-7	Control (n=9)	1.18±0.18	1.20±0.23	0.25±0.05
	CSM (n=6)	0.73±0.30**	0.80±0.30**†	0.38±0.10**†

Table 2.2: Comparison of vertebral measurements between control and CSM horses on MRI. Data are presented as the means and standard deviations. CSM disease status was based on postmortem histopathologic evaluation of the spinal cord. *p<0.05; **p<0.01, however site C2-3 had only one CSM horse and could not be statistically evaluated. † indicates significant interaction of age; Circ.=circumference; L IV= Left Intervertebral; R IV= Right Intervertebral

The ratio of spinal cord area to vertebral canal area was larger in the CSM group, consistent with a decreased space within the vertebral canal for the spinal cord to occupy. The intraclass correlation coefficient evaluating assessors ranged from 0.70 to 0.89, indicating good to excellent concordance for the morphometric parameter assessment.

MRI and Radiographic Assessment for Compression

CSM horses frequently demonstrated circumferential attenuation of cerebral spinal fluid on transverse images suggestive of compression (Figure 2.5).

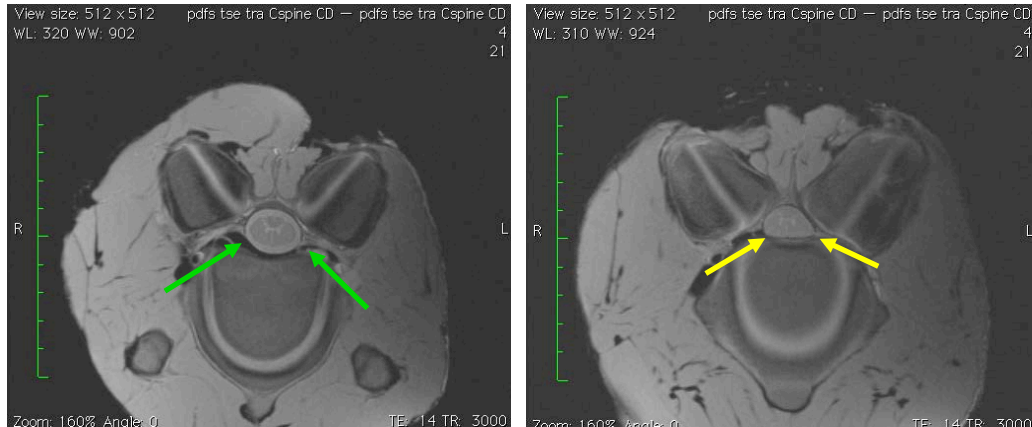


Figure 2.5: Transverse MR images showing the absence and presence of spinal cord compression. The image on the left is at the level of C4-5. The spinal cord is round with circumferential cerebral spinal fluid (CSF) (green arrows). From the same horse, the image on the right is at the level of C5-6 and demonstrates a narrowed canal area with ventral compression of the spinal cord, attenuated CSF, and encroachment of the articular process joints (yellow arrows). Compression of the spinal cord at C5-6 was confirmed on histologic examination.

Canal area and CCAR measured on MRI were evaluated for the ability to predict compressive lesions in a site-by-site comparison. All vertebral sites achieved statistical significance with canal area and CCAR ($p < 0.05$) as the predictor of a compressive lesion at a particular vertebral site. In contrast, for the radiographic parameters, lesion site significance ($p < 0.05$) was limited to C3-4 and C5-6 for both intravertebral and intervertebral ratios. The MRI canal area parameter ($p < 0.05$) was able to predict compressive lesions across the entire sample set regardless of vertebral site. CCAR was also significant for predicting compressive lesions.

Discussion

The primary objective of this study was to compare standing cervical radiographs to MRI for the evaluation of cervical vertebral canal stenosis in horses. MRI allows examination of both soft tissue and skeletal structures *in situ* in multiple planes, which addresses the current limitation of only evaluating the sagittal plane when using standing radiography. The ability to assess the cervical column in a transverse plane allows for the application of additional anatomic parameters and a more rigorous evaluation of the variability in cervical vertebral structure, which can cause stenosis in diseased cases. The results indicate that MRI is superior as an imaging tool for the identification of vertebral canal narrowing in horses with CSM when compared to standing cervical radiographs. This finding is consistent with the results of a study that examined the use of MRI to assess canine cervical vertebral pathology. Comparison of myelography and MRI techniques in Doberman Pinchers found that MRI had a higher degree of accuracy for identifying the site and severity of spinal cord compression (da Costa et al., 2006). In the current study, spinal cord compression of CSM horses frequently demonstrated circumferential attenuation of cerebral spinal fluid on transverse images (Figure 2.5). Significant differences were seen in anatomical measurements of the vertebral canal (Table 2.2), but not the spinal cord itself. This finding is consistent with a pathogenesis that starts with skeletal malformations resulting in compression of the cervical spinal cord (Stewart et al., 1991; Mayhew, 1978).

Interestingly, multiple control horses had at least one area with radiographic measurements suggestive of cervical spinal canal narrowing on standing lateral

views, yet no neurological deficits on clinical examination or histopathologic evidence of spinal cord compression. Figure 2.2 is a graphic comparison of the corresponding canal areas and standard MSD intravertebral ratios for all horses in the study with compressive lesions at C4-5 and the controls. Using either the standard MSD or 0.485 thresholds for cervical radiography at intravertebral and intervertebral sites, two controls fall below these lines and are false positives given their absence of compressive lesions on histology. In addition, three horses with cord compression confirmed by histology have values above these thresholds, making them false negatives on radiographs. Canal area measurements obtained from MR images at the same sites, however, segregate more accurately. As a two-dimensional transverse measurement, canal area accounts for variability not only in canal height but other directions as well. Sagittal plane views on lateral cervical radiographs are limited to assessment of canal height in the dorsal-ventral direction only. Variation in vertebral canal shape may provide adequate room for the spinal cord despite a low canal height. This is a possible explanation for the subset of horses with a suggestion of compression on lateral radiographs, yet an absence of clinical or pathologic lesions consistent with CSM. While some ambiguity remains, as represented by an overlap of canal area and CCAR measurements between CSM and control horses at various vertebral sites (Figures 2.3 and 2.4), the results of this dataset indicate an improvement over lateral cervical radiographs.

Neck position is an additional opportunity for improving the accuracy of diagnostic imaging. Myelograms have been used to demonstrate how cord compression can be accentuated in flexion or extension in some cases (Nixon et al.,

1982). This has led to a description of lesions as dynamic if flexion or extension accentuates the compression, or static if compression is evident regardless of neck position. Dynamic lesions might also explain the apparent paradox of cord canal area ratios being less than one at sites of compression in CSM horses. While the mean values are significantly higher than the controls, measurements ranging from 0.33 – 0.38 cm² still suggest adequate space for the spinal cord within the vertebral canal. However, if the compression is position-dependent, then the true severity of the stenosis may not be reflected in the CCAR with the neck in a neutral position. There are also varying degrees in the severity of stenosis, and therefore the average CCAR for the sample set does not reflect the gradient of stenosis observed in individual cases.

Intervertebral foramen heights varied at different vertebral sites, but were consistently smaller in CSM horses. This finding supports previous work in which CSM horses were examined by computed tomography (CT) with lateral compression of cervical spinal nerve roots due to malformations in the articular processes (Moore et al., 1992). In this study as well, altered position of the articular processes impacted intervertebral foramen height. Identification of significant differences between CSM and control groups in regards to intervertebral foramen heights is largely dependent on the spatial positioning and size of the articular processes.

As discussed above, the determination of canal area is a more accurate assessment of canal size, but the ability to predict compressive lesions is the important diagnostic issue. In contrast to intervertebral and intravertebral sagittal ratios, canal area and CCAR were able to predict histopathologic compressive

lesions regardless of vertebral site. Overall, vertebral canal area was smaller at sites of compression identified by histologic examination as compared to the controls. In the exceptions, where CSM canal areas segregated with canal area of controls, it is felt this is largely due to the limitations of only the neutral position being evaluated in this study. Therefore, in the future, canal area and CCAR could be developed as morphometric parameters for antemortem assessment of Wobbler Syndrome in the horse.

Age was found to have an influence on several morphometric parameters in this study (Table 2.2). The growth plates of the vertebral endplates in the cervical column do not close until 4-5 years of age. Horses included in the sample set were up to 5.5 years of age; therefore, there is continued maturation of the vertebrae as the result of normal growth patterns in the horse. These findings reflect the young age of onset often seen in the development of CSM.

The current study was performed with a sample set of 19 CSM horses and 9 controls, yet was still able to detect significant differences between the two groups of horses. Examination of more horses in future studies will provide additional power for the establishment of threshold MRI criteria to predict the presence or absence of stenosis, as is currently defined for the assessment of standing cervical radiographs with the intravertebral and intervertebral minimal sagittal diameter ratios. With an increased sample size, a receiver operating characteristic (ROC) curve could be constructed for assessment of diagnostic accuracy and determination of the sensitivity and specificity of the canal area parameter. Given the significance of canal area and CCAR to identify specific sites of compression on postmortem MRI,

it is felt these parameters could possibly provide an increased sensitivity and specificity for identifying canal stenosis antemortem. This could have a strong impact on site selection for cases undergoing review for surgical treatment. Further investigation of the vertebral canal area and CCAR is necessary in regards to the influence of position and establishment of intervertebral site-specific thresholds. However, breed differences are likely to be important (Mitchell et al., 2012). All horses evaluated in the current sample set, both cases and controls, were Thoroughbreds with an age range of 6 months to 5.5 years. Absence of breed variation likely contributed to the finding that canal area could accurately predicted lesion site, in contrast to the earlier study. For this reason, CCAR or another ratio parameter may prove to better accommodate breed and age variations than the absolute measure of vertebral canal area.

Technology is continuing to advance in regards to both MRI and CT units. Although the size of most adult equine patients currently precludes antemortem assessment of the complete cervical column by MRI, large bore CT scanners may permit imaging of the entire equine cervical vertebral column. It is feasible that transverse plane vertebral column measurements could be obtained in this fashion for clinical cases. The ability to image the cervical vertebral column in the transverse plane and multiple neck positions will substantially enhance clinical evaluation of CSM horses.

Chapter 3

Skeletal Pathology Of The Cervical Articular Processes In Equine Cervical Stenotic Myelopathy

Summary

Skeletal lesions in the articular processes of cervical vertebrae C2 – C7 were compared between horses with cervical stenotic myelopathy (CSM n=19) and controls (n=9). Lesions identified by magnetic resonance imaging (MRI) occurred with an increased frequency and severity in CSM horses and were not limited to the site of compression. Pathology involved both the articular cartilage and trabecular bone, including osteochondrosis, osseous cyst-like structures, fibrous tissue replacement of trabecular bone, and osteosclerosis. The identification of osseous cyst-like structures is a novel finding. These lesions and their generalized distribution indicate that developmental abnormalities of the cervical spine are primary changes associated with equine CSM.

Introduction

Equine CSM is a multifactorial disease of the musculoskeletal system that presents clinically with proprioceptive neurologic deficits that are worse in the pelvic limbs. The disease is characterized by malformations of one or more cervical vertebrae that lead to stenosis of the spinal canal, cord compression, and damage to nerve tracts. Proposed etiologic factors include high planes of nutrition, accelerated growth rates, altered ratios of copper and zinc, and inherited genetic determinants. While much is known regarding signalment and clinical diagnosis, the exact pathogenesis of CSM remains unclear and likely reflects more than one path to a similar clinical presentation. Over the years, two theories have been proposed

based on multiple studies. The developmental theory proposes an underlying disorder of bone and cartilage tissue morphogenesis and maturation leading to cervical vertebral malformations. The biomechanical theory, in contrast, advances a process whereby abnormal mechanical stresses and forces on the cervical column result in structural vertebral changes leading to canal stenosis.

Efforts put forth by multiple groups have contributed to a knowledge base for aberrations in vertebral development associated with CSM. A comprehensive examination of pathologic lesions (Mayhew et al., 1978) suggested abnormal bone and cartilage maturation manifested as osteosclerosis and osteochondrosis. Interestingly, lesions were also observed in the costochondral junction of the ribs supporting a possible systemic bone and cartilage maturation issue. Further work examined the frequency and severity of osteochondrosis in the articular processes with comparison to the appendicular skeleton (Stewart et al., 1991), finding an increased severity of osteochondritic lesions in both the axial and appendicular skeleton of CSM horses. It has also been suggested that cervical malformations could start as early as *in utero* (Mayhew, 1999).

On the other hand, there is support for a model of pathogenesis whereby abnormal biomechanical forces lead to vertebral malformations and canal stenosis. Maturation of equine vertebrae continues until approximately 5 years of age at which point the vertebral body growth plates close (Whitwell and Dyson, 1987). During this time and even following growth cessation, vertebrae are responsive to biomechanical forces on the neck through Wolff's Law and related variables of

mechanical regulation (Wolff, 1986; Chen et al., 2010). Mechanical variables in the form of strain, oscillation, and vibrations have been demonstrated to impact bone morphology (Judex et al., 2009). Lesions consistent with abnormal forces on the neck include degenerative changes of the articular processes, thickening of the dorsal lamina, and hypertrophy of the ligamentum flavum (Powers et al., 1986; Trostle et al., 1993).

The major knowledge gap(s) in regards to CSM pathogenesis is/are the mechanism(s) by which these lesions develop and progress to clinically significant spinal canal stenosis. The rapid development of imaging technologies allows for examination of the cervical column *in situ* for pathologic lesions associated with CSM. This study focuses on the articular processes, given that changes in their shape, size, and spatial orientation frequently contributes to spinal cord compression (Moore et al., 1992).

Experiments in this chapter aim to assess, both quantitatively and qualitatively, cartilage and bone lesions observed by MRI in the articular processes of CSM horses as compared to controls. A subset of representative lesions is then further characterized with micro-CT and routine histopathology. Achieving a better understanding of the distribution and types of lesions that occur within the articular processes will lead to greater insight into the etiopathogenesis of CSM in the horse.

Materials and Methods

Magnetic Resonance Imaging

Sample Acquisition

Horses identified for these experiments follow the criteria previously outlined in chapter 2 of this thesis. Briefly, CSM horses (n=19) underwent neurologic examinations and standing cervical radiographs. Postmortem, gross and microscopic evaluation of the spinal cord was performed. Presence of a focal compressive lesion was used as the criteria to confirm CSM and specific site localization. All control horses (n=9) had an absence of clinical and postmortem characteristics consistent with neurologic disease. Acquisition of MRI data from the cervical column was performed within 4 hours of euthanasia. T2, PSFD, and STIR images were obtained. Immediately following MRI, each vertebrae was disarticulated intact from the cervical column and placed in 10% neutral buffered formalin for fixation.

Articular Process Lesion Identification, Location Classification, and Severity Scale

Variations from expected MRI signal intensity were identified as perspective lesions and classified as either superficial or deep based on anatomic location. Superficial lesions involved the articular cartilage and/or subchondral bone with possible extension into the trabecular bone. Lesions within an articular process that did not involve the articular cartilage or subchondral bone were defined as deep. Lesions were then assigned a grade of 0-3 based on a scale adapted from previous work (Smith et al., 2012) and described below (Figure 3.1). Lesions were required

to be present on a minimum of 2 of the 3 MRI image studies (PDFS, T2, STIR).

Superficial lesion scoring criteria: Involvement of the articular cartilage and/or the subchondral bone and possible extension into the underlying trabecular bone.

Grade 0: Normal (no pathology detected)

Grade 1: Subtle irregularity of chondro-osseous margin with no involvement of subchondral bone

Grade 2: Irregular chondro-osseous margin with subchondral bone defect of < 0.7cm in either dimension

Grade 3: Irregular chondro-osseous margin with subchondral bone defect of > 0.7cm in either dimension

Deep lesion scoring criteria: Trabecular bone involvement with no involvement of the articular cartilage or subchondral bone.

Grade 0: Normal (no pathology detected)

Grade 1: Generalized mild signal alterations

Grade 2: Generalized moderate signal alteration or focal signal intensity changes < 1 cm in any dimension

Grade 3: Generalized severe signal alterations or focal signal intensity changes > 1 cm in any dimension

Figure 3.1: Summary of the superficial and deep lesion criteria and corresponding severity grading scale.

Statistical Analysis

A generalized linear statistical model was used to determine if there were significant differences in frequency of articular process lesions between CSM and control groups. In this model, lesion count was regressed on group using the Poisson regression (SAS, Cary, NC). For assessment of severity, a generalized linear equation with a multinomial model to account for the grading scale of 0-3 was used. Significance was defined as $p < 0.05$.

Structural Analyses of Articular Process Lesions

Sample Identification

A subset of samples from the above-described dataset was selected for structural analyses. Four CSM horses with deep lesions and four CSM horses with superficial lesions were chosen (Table 3.1). Control horses with an absence of lesions on MRI were identified to match as best as possible for anatomical site, gender, and age of the CSM horses. No horse was repeated within or across groups. Articular process sites varied between groups. All lesions were assessed as a grade 2 or grade 3. Articular processes both at and away from the site of spinal cord compression were included. The table below summarizes the signalment of the groups. Articular processes were removed from the vertebrae for scanning.

Deep Lesions				
	CSM (n=4)		Control (n=4)	
Site	Age	Gender	Age	Gender
Left caudal C5	11 months	Male	17 months	Male
Left cranial C6	6 months	Male	10 months	Male
Right cranial C6	13 months	Male	15 months	Male
Right cranial C7	18 months	Male	23 months	Male

Superficial Lesions				
	CSM (n=4)		Control (n=4)	
Site	Age	Gender	Age	Gender
Left caudal C2	15 months	Male	17 months	Male
Left cranial C4	20 months	Male	22 months	Female
Left caudal C6	10 months	Female	9 months	Female
Left cranial C7	50 months	Female	67 months	Female

Table 3.1: Signalment and articular process sites for structural analysis.

Micro-CT Image Acquisition and Visualization

A custom micro-CT scanner (150/225 Ffi-HR-CT, BIR, Lincolnshire, IL) with a 225kV X-ray source, 5 μ m focal spot, and image intensifier with a 1024 x 1024 pixel digital camera was used. X-ray power settings were 135 KeV and 0.059 mA with a distance of 703 mm from the x-ray source to the image detector (Voor et al., 2008). The source to object distance was 177.5 mm. Scanning was performed in the offset mode with the center of the tube 15 mm lateral to the center of the x-ray beam. The articular process was placed in a radiolucent acrylic holder and scanned using a 360 degree-plus-fan-angle rotation. A total of 107 slices were captured per revolution with each slice representing a thickness of 30 μ m. The final reconstruction resulted in image stacks of 2048 x 2048 pixels. Image stacks contained 30 μ m voxels with a 16 bit gray scale..

Image stacks were imported into VGStudio Max for construction of 3D models of the articular processes (v1.2.1, Volume Graphics, Heidelberg, Germany). Regions of interest were identified based on localization from MRI data demonstrating the lesions. The cranial or caudal most point of the articular margin was identified on MR and used as the starting point for measurements to localize the lesion.

Trabecular Bone Volume Measurement

Images stacks of 200 slice increments were imported into Image J (Abramoff et al., 2004) at 25% of the total image size. Coordinates were acquired for image stack borders for trabecular bone volume measurements in a custom bone volume

analysis program using MATLAB (v7.1, The Mathworks, Natick, MA). Trabecular bone volume was calculated as percentage of total volume.

Statistical Analysis

A generalized linear model was used to determine if there were significant differences in trabecular bone volume of the articular processes identified in CSM horses with deep lesions compared to controls, CSM horses with superficial lesions compared to controls, and then a combination of the deep and superficial groups compared to controls (SAS, Cary, NC). Significance was defined as $p < 0.05$.

Histopathologic Assessment of Articular Process Lesions

Sample Identification

A representative subset of articular process lesions identified on MRI from both CSM and control horses were assessed histologically. All lesions imaged with micro-CT were included in this study. The figure below summarizes the sample numbers and distribution of grades within each group (Figure 3.2). No horses were repeated within a grade or a group, although in some cases independent lesions from the same horse were used across groups.



Figure 3.2: Number of samples in each grade category analyzed histologically. Grades are variable within the mixed group, as often the superficial and deep components would qualify for different grades based on severity. Control horses had a very limited number of deep lesions available for assessment.

Histopathologic Processing and Evaluation

Transverse sections of the region of interest from the articular processes were excised using a scroll saw based on MRI localization and measurements. Sections were decalcified using Decalcifier Rapid S (Labsco), embedded in paraffin, and 5 µm sections processed routinely for hematoxylin and eosin staining. Slides were examined for histopathologic changes.

Results

MRI Lesion Frequency

Lesions identified on MRI studies were evaluated for significant differences in frequency between CSM and control horses. Analyses compared anatomic localization (superficial or deep), compression site or noncompression site, as well as the entire cervical column. Significant differences were identified on frequency comparisons using all lesions at all sites, all superficial lesions, all deep lesions, and

deep lesions at noncompression sites (Figure 3.3). Within the group of CSM horses, there were individuals with compression and others without compression at each vertebral site. Therefore, the corresponding control dataset used for comparison are the same within All Lesion, Superficial Lesion, and Deep Lesion categories.

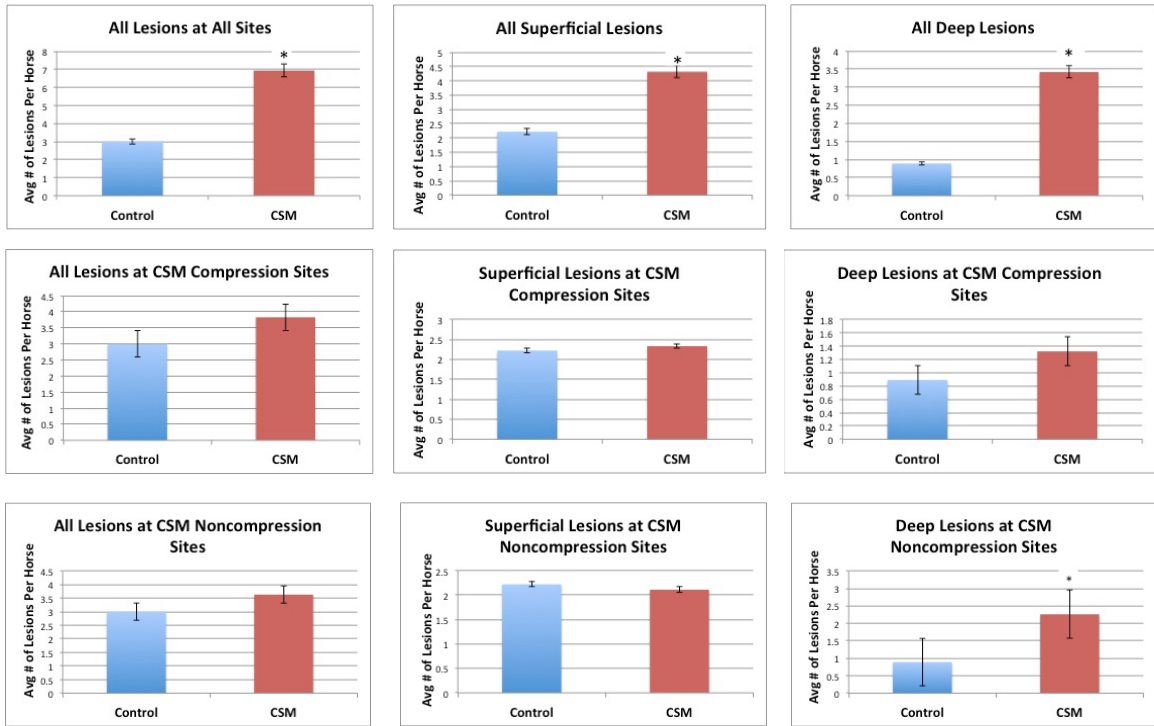


Figure 3.3: Articular process lesion frequency distribution. Compression and noncompression designations refer to anatomical locations of stenosis for the CSM horses, with comparison to the corresponding anatomical sites from control horses. By definition, control horses have no cervical spinal cord compression sites. Data are represented as average number of lesions per horse in each group. * p value <0.01.

Lesion Severity Analysis

In addition to the number of articular process lesions, severity of the lesions was assessed between CSM and control horses. The same categories of anatomic location of the lesion within the articular process as well as location in the cervical

column with respect to compression were analyzed. Significance was observed in all comparisons except for superficial lesions at noncompression sites. Distribution of lesion grade for all comparisons is shown below (Figure 3.4).

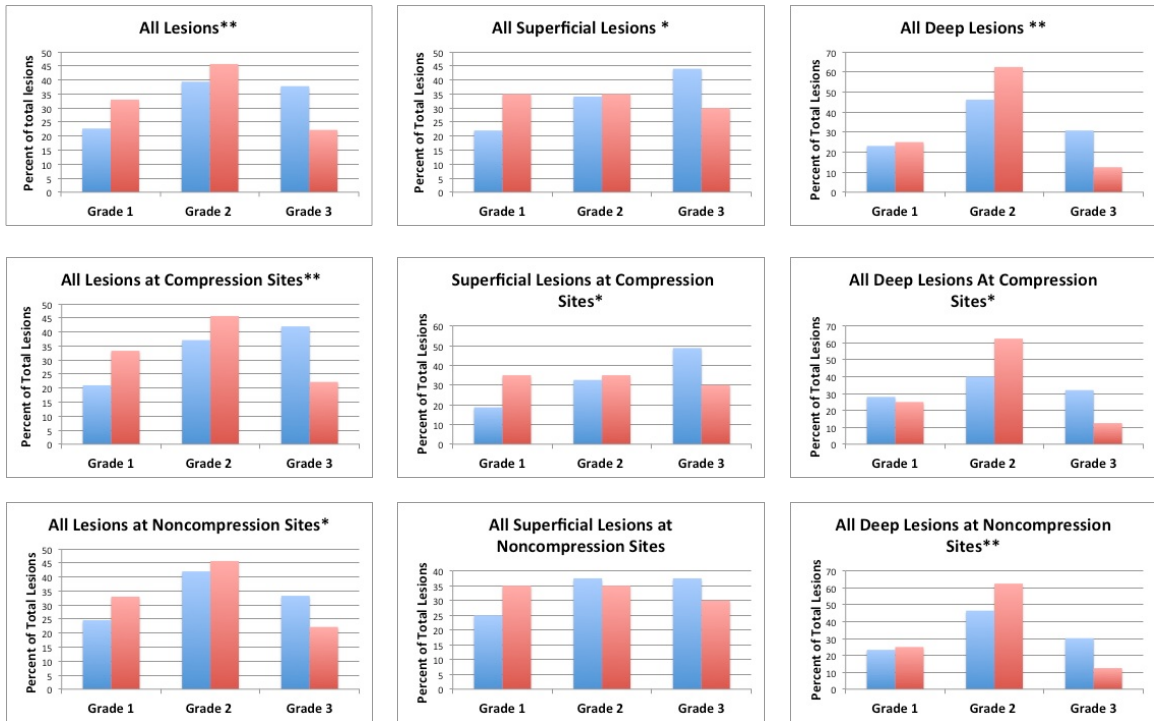


Figure 3.4: Articular process lesion severity distribution. Data are presented as the percent of the total number of lesions for each grading category. Severity distribution patterns were significantly shifted to greater severity in CSM horses in all categories except for superficial lesions at noncompression sites. Blue bars represent the control group and red bars represent the CSM group. * p value < 0.05; ** p value < 0.01

Microarchitectural Bone Volume Assessment

A subset of lesions identified on MRI was imaged using micro-CT for assessment of trabecular bone volume and an evaluation of trabecular bone architecture. No significant differences in trabecular bone volume were found ($p > 0.05$) when comparing the articular processes with superficial lesions to controls,

articular processes with deep lesions to controls, or combination of the two groups (Table 3.2).

Lesion Categorization	Sample Groups		p-value
Deep Lesion	CSM (n=4)	Control (n=4)	
Trabecular Bone Volume	0.3885 ±0.04	0.3431±0.02	0.087
Superficial Lesion	CSM (n=4)	Control (n=4)	
Trabecular Bone Volume	0.3591±0.02	0.3495±0.03	0.500
All Articular Processes	CSM (n=8)	Control (n=8)	
Trabecular Bone Volume	0.3738±0.03	0.3463±0.02	0.059

Table 3.2: Trabecular bone volume comparisons in articular processes. Data are represented as the percentage of total volume occupied by trabecular bone based on micro-CT analyses. Averages and standard deviations for each group are listed. No significant differences between control and CSM horses were identified.

Analyses of deep lesions on micro-CT demonstrated that they were not composed of bone (Figure 3.5). This finding was observed in all 4 articular processes analyzed in the deep lesion group. An absence of bone was also observed for superficial lesions in the four articular processes examined, including when there was extension of the lesion into the subchondral region (Figure 3.6). In contrast, perilesional regions often, but not always, exhibited trabecular thickening consistent with areas of bone sclerosis (Figures 3.5 and 3.6).

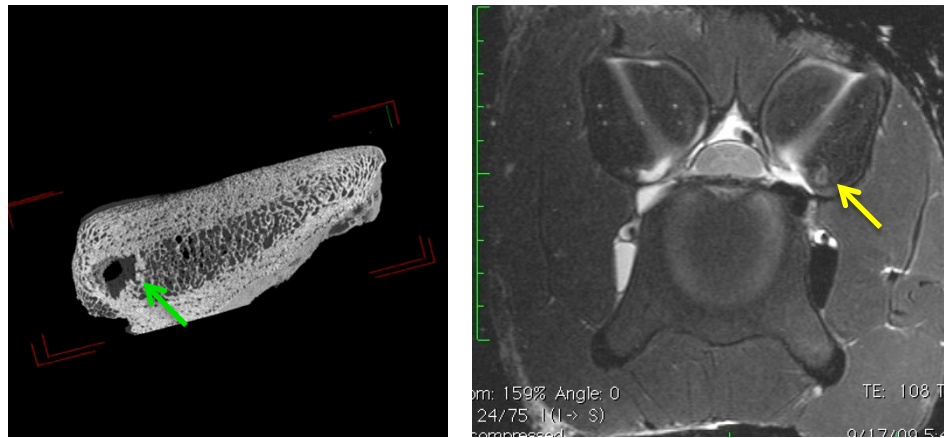


Figure 3.5: Micro-CT and MRI of a deep lesion within the articular process. This is the left cranial articular process from C7 of a CSM horse. The left image is a 3D model generated by micro-CT showing a deep lesion in cross section. A discrete focus with absence of trabecular bone structure is observed (green arrow). On the right, the MR image is localized to the same level as the 3D model. A focal signal increase within the trabecular bone is seen (yellow arrow). The difference in resolution between the imaging modalities accounts for the size discrepancy of the lesion in each of these images.

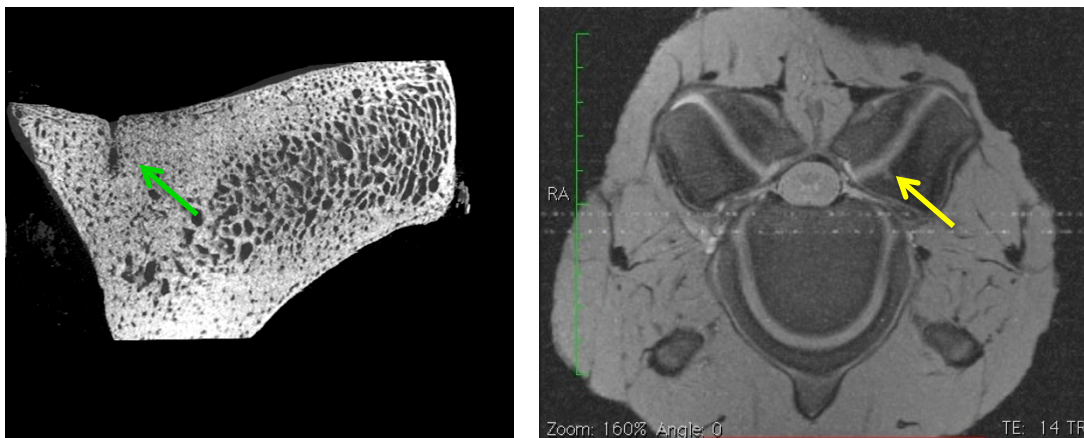


Figure 3.6: Micro-CT and MRI of a superficial lesion within the articular process. This is the left cranial articular process from C4 of a CSM horse with a grade 2 lesion identified on MRI. The left image is a 3D model of the articular process in cross section. At the green arrow is an invagination into the subchondral bone that is not composed of bone. Adjacent to the invagination, the trabecular bone is markedly thickened (sclerosis). On the right is the corresponding localization of the lesion on MRI. There is a focal signal increase that extends from the articular surface into the subchondral bone (yellow arrow). Also, there is an adjacent decrease in signal indicating bone sclerosis consistent with the thickened trabecular bone observed on micro-CT.

Histopathologic Assessments

All superficial lesions identified in CSM and control horses were consistent with varying degrees of osteochondrosis. Both osteochondrosis manifesta (OM) and osteochondritis dissecans (OCD) were observed (Figure 3.7 and 3.8). Since the lesion grading categories were based on size, both OM and OCD were seen in grade 2 and grade 3 categories. Associated with the cartilaginous defects was a moderate to severe thickening and remodeling of the subchondral bone, which extended variably into the trabecular bone of the articular process.

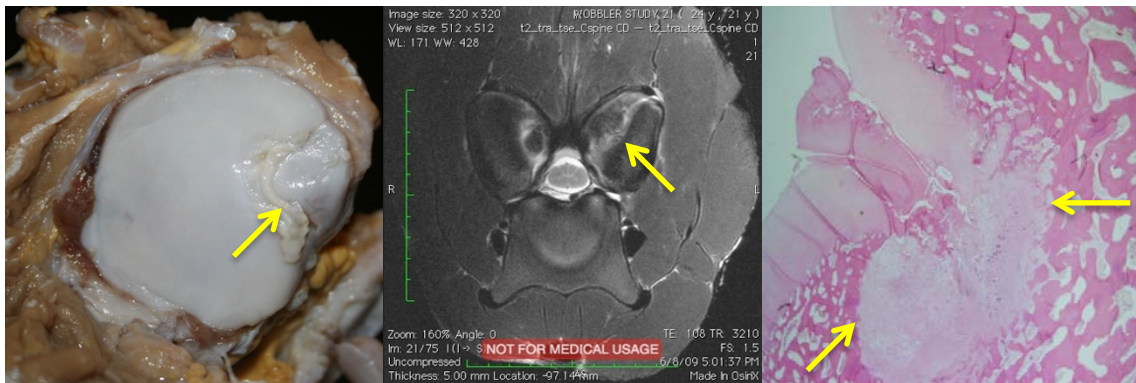


Figure 3.7: Osteochondrosis manifesta lesion (grade 3) image series. On the left is a gross image of the articular defect (arrow) identified on left caudal C6 of a CSM horse. The middle image is the same lesion on MRI. The arrow indicates an irregular chondro-osseous margin with an adjacent increase in signal intensity. On the right, is a photomicrograph of the same lesion at 2X magnification. There is a focal area of cartilage necrosis (arrows) surrounded by thickened subchondral bone.

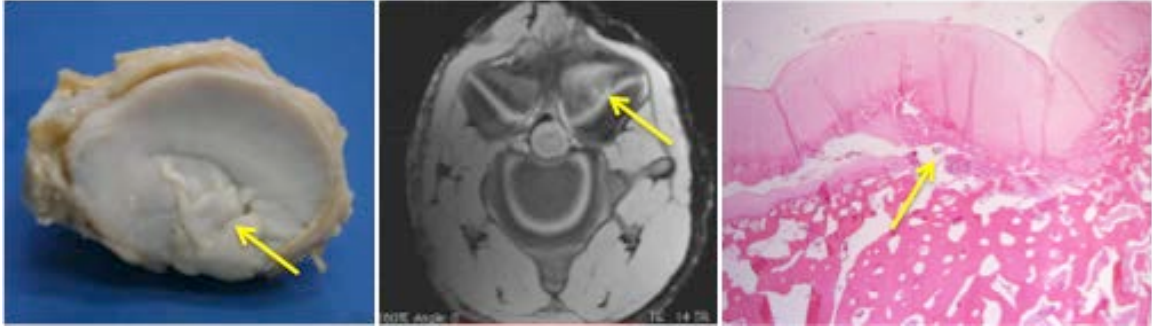


Figure 3.8: Osteochondritis dissecans lesion (grade 3) image series. On the left is a gross image of the articular defect (arrow) identified on the left caudal articular process from C2 of a CSM horse. The middle image is the same lesion on MRI (arrow) composed of a slightly irregular chondro-osseous margin with an increase in signal intensity extending into the bone. On the right is a photomicrograph at 2X magnification. The arrow indicated the separation of the articular cartilage from the bone consistent with OCD.

Deep only lesions in CSM horses were composed of cyst-like structures within the trabecular bone, fibrous tissue replacement of trabecular bone, and retention of variably size foci of cartilaginous matrix deep in the trabeculae (Figure 3.9). Cells lining the lumen of the cyst-like structures were negative for cytokeratin, a marker for epithelium. Cyst-like structures were surrounded by organized fibrous connective tissue. The two deep lesions identified in control horses were both retention of small to moderate amounts of cartilaginous matrix within the trabecular bone. No cyst-like lesions in the articular processes of control horses were observed.

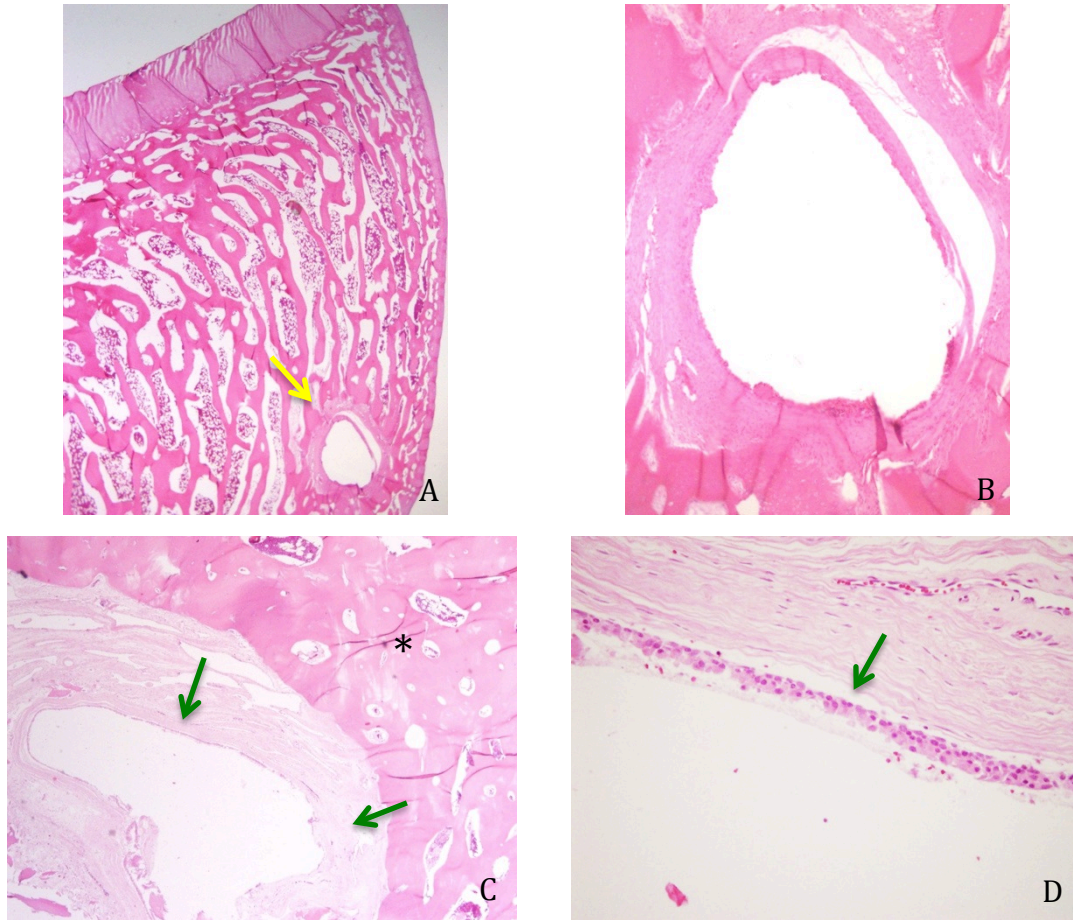


Figure 3.9: Image series of cyst-like structures in deep articular process lesions of CSM horses. Image A shows a cyst-like structure in the trabecular bone at 2X magnification. Higher magnification (10X) of the same structure is seen in figure B. The cyst-like structure is composed of a surrounding fibrous stroma with no discernable epithelial lining. Image C shows a different cyst-like structure (green arrow) at 4X magnification surrounded by trabecular bone sclerosis (asterisk). The cells lining the cyst-like structure are shown at 40X magnification in figure D (green arrow).

Mixed lesions were composed of a variety of pathologies. Consistent with the superficial only lesions, the superficial component of the mixed lesions fell under the spectrum of osteochondrosis. The deep lesions away from the articular surface were composed of areas of fibrous replacement of trabecular bone with active bone

remodeling, cyst-like structures, occupation of the marrow cavity with varying amounts of fibrous connective tissue, and mature venous sinuses within the marrow space (Figure 3.10).

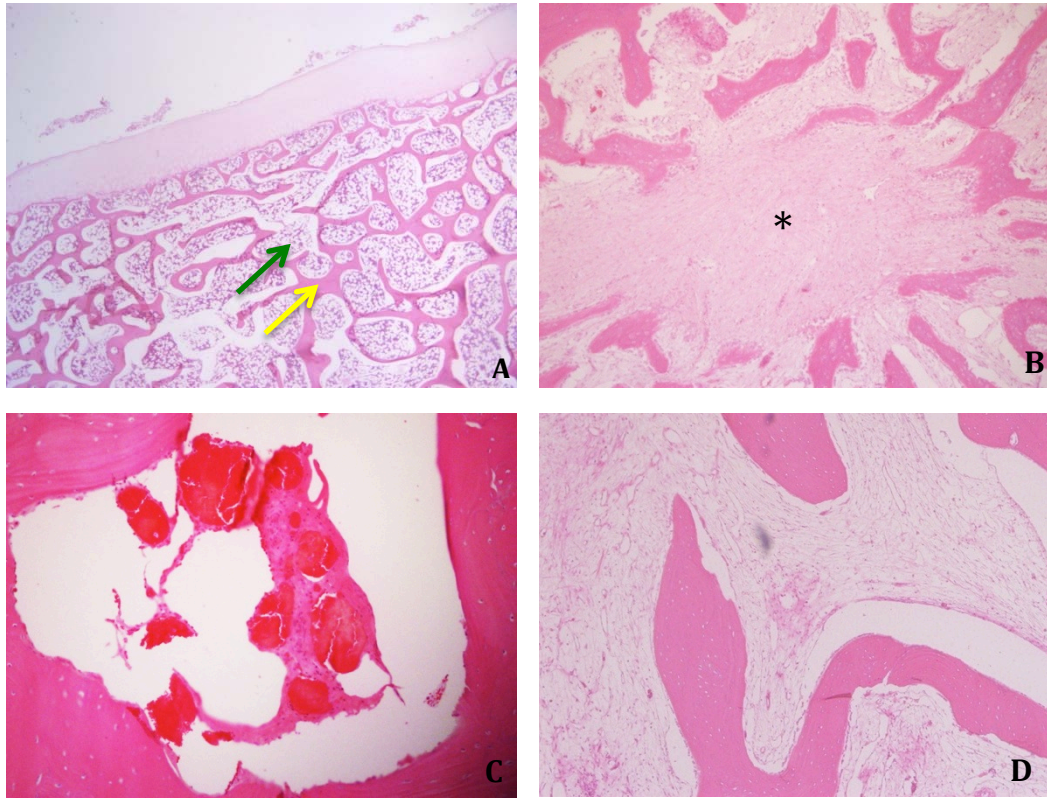


Figure 3.10: Histopathology photomicrographs of the deep lesions in the mixed category. Figure A shows normal trabecular bone (yellow arrow) and marrow space (green arrow) at 2X magnification. Replacement of trabecular bone with dense streams and bundles of fibrous connective tissue (*) is shown in figure B at 10X magnification. On the bottom left in figure C, organized prominent venous sinuses occupy the marrow space with paucity of normal marrow elements at 20X magnification. Loosely organized fibrous connective tissue replacing hematopoietic elements in the marrow space is shown in figure D at 10X magnification.

Discussion

The objective of these experiments was to evaluate and compare the frequency and severity of skeletal lesions in articular processes of cervical vertebrae

identified on MRI between CSM and control horses. A representative subset of these lesions was further characterized using micro-CT and routine histopathology. Lesion frequency, location, and severity analyses examined the cervical column as a whole, at the site of cord compression, and away from the site of compression. While lesions were observed in both control and CSM horses, frequency and severity were significantly increased in the CSM group. Lesion frequency was higher in the CSM horses across the entire cervical column for both superficial and deep lesions, as well as for deep lesions at noncompression sites. In addition, identified lesions had an increased severity in the CSM horses. These data support previous work that concluded pathology in the neck of CSM horses is generalized and not limited to the site of compression (Stewart et al., 1991).

A variety of lesions were observed on histopathology of the articular processes. All superficial lesions identified on MRI that were further evaluated using histopathology fell under the continuum of osteochondrosis (OC). OC is a developmental disease that results from localized failure of endochondral ossification. Recently, efforts to improve nomenclature for OC has resulted in 3 categorizations, osteochondrosis latens, osteochondrosis manifesta, and osteochondritis dissecans (Ytrehus et al., 2007). Osteochondrosis latens is a focal area of cartilage necrosis within the epiphyseal cartilage. When cartilage necrosis extends into the adjacent subchondral bone it is classified as osteochondrosis manifesta. The most severe manifestation, osteochondritis dissecans, occurs when the integrity between the cartilage and bone is lost and a flap or loose body of cartilage is released. Osteochondrosis manifesta lesions were observed in control

and CSM horses whereas OCD was only seen in CSM horses. The presence of OCD in CSM horses is supportive of the increased severity distribution in CSM pathology. On micro-CT, the four OC lesions evaluated had loss of bone structure consistent with the retention of cartilage through failure of endochondral ossification. Osteochondrosis in the cervical column of CSM horses has been reported previously (Stewart et al., 1991; Mayhew, 1978). Findings in this study further substantiate the association of OC with CSM.

Deep lesions on MRI displayed a variety of histopathological changes. An interesting finding was the presence cyst-like structures within the trabecular bone away from the articular surface in the CSM horses. This is the first report of these lesions in the articular processes of CSM horses. On micro-CT, all 4 articular processes with deep lesions were visualized as focal areas with an absence of trabecular bone structure (Figure 3.5). Histopathology confirmed that 3 of the 4 deep lesions analyzed using micro-CT were cyst-like structures composed of an empty lumen surrounded by organized fibrous connective tissue. Classically, bone cysts are characterized as simple, subchondral, or aneurysmal (Carlson and Weisbrode, 2012). Simple cysts are lined by fibrous tissue and contain clear to serosanguinous fluid. Remodeling of the bone adjacent to the cyst can be a feature as well. Cyst-like structures observed in the articular processes fit best with the simple categorization. The exact cause of simple bone cysts is unknown. Suspected causes include vascular malformations, hemorrhage, ischemic necrosis, occlusion of venous drainage, or developmental abnormalities (Carlson and Weisbrode, 2012; Chigira et al., 1983; Khurana JS, 2009).

The identification of these cyst-like structures generates the following question: are these structures related to osteochondrosis in some fashion? As noted earlier, OC is a developmental problem of endochondral ossification impacting bone and cartilage in diarthrodial joints. Subchondral bone cysts adjacent to the articular cartilage have been described with OC. It is unknown at this time if the cyst-like structures in the current study were another manifestation of OC or independent. Their localization was frequently deep in the trabecular bone away from the articular cartilage-subchondral bone interface, which could be a confounder for a direct relationship with OC.

While the identification of the cyst-like structures is novel in the articular processes, there are previous reports of this pathology in other bones of the horse. Osseous cyst-like lesions have been reported in the appendicular joints of horses, specifically the fetlock joint, carpal joint, tarsus joint, navicular bone, and phalanges (Murray et al., 2011; Anastasiou et al., 2003). The presence of these lesions is often associated with trauma, but can also be related to developmental factors. Clinical significance of these lesions in the appendicular joints can be either incidental or pathologic. If the surrounding bone is normal, then cyst-like lesions are usually interpreted as incidental. In cases where adjacent sclerosis is observed, cyst-like lesions are considered pathologic (Powell, 2011; Murray et al., 2011). Using these criteria, both incidental and pathologic cyst-like structures were observed in the CSM horses.

Several other interesting lesions were observed in individual cases. In articular processes from a 6 month old colt with CSM, well-defined, prominent venous sinuses were observed scattered in the marrow space both adjacent to the articular surface near OC lesions and deep in the trabecular bone (Figure 3.10). Hematopoietic elements in these areas were rare. Given the fluid nature of blood, the lesions were visualized as multifocal pinpoint increases in signal intensity on MRI. Their significance is unclear.

Another interesting lesion observed in several cases was varying degrees of fibrous replacement of marrow elements and trabecular bone often surrounded by marked bone remodeling (Figure 3.10). This fibrosis was observed near OC lesions and in the trabecular bone without communication to the articular surface. The remodeling bone was characterized by haphazardly arranged trabeculae lined by osteoblasts (woven bone), and scalloped basophilic cement lines indicative of active bone resorption and replacement. These foci of fibrous connective tissue and collagen surrounded by bone remodeling could represent sites of previous injury that are in the process of stabilization and repair. Foci closer to the articular surface could be a response to adjacent chronic OC lesions. The cause of the fibrous foci deeper in the trabecular bone is unknown, but interesting nonetheless. One possibility is the deeper lesions could be previous cyst-like structures that collapsed and are now in a healing process. Identification of the original cause of these fibrous lesions may help clarify contributing steps in the pathogenesis of CSM.

Previous studies have described trabecular bone sclerosis in the dorsal lamina and vertebral body endplates of vertebrae in CSM horses (Mayhew, 1978; Powers et al., 1986; Trostle et al., 1993). Bone sclerosis can develop due to impaired function of osteoclasts and osteoblasts, as well as metabolic signals that affect normal remodeling and resorption. However, osteosclerosis can also occur as a compensatory response to increased mechanical stress with suppression of bone resorption resulting in an increase of bone mass as described in Wolff's law. When occurring in response to biomechanical forces, areas of osteosclerosis contain normal sized lacunae (Powers et al., 1986; Trotter et al., 1976; Wright et al., 1973; Parfitt, 1977). This was observed for the sclerotic regions of subchondral and trabecular bone in the current study, implicating biomechanical forces as the cause versus an impairment of normal bone turnover from cellular or hormonal mechanisms.

Given previous reports and the observations in the current study of osteosclerosis in the articular processes, the trabecular bone volume of the entire articular process in CSM and control horses was evaluated. Although mean trabecular bone volumes were numerically greater in CSM horses in each category (Table 3.2), the differences were not significant. Combining samples from the superficial and deep lesion groups yielded a p value of 0.051. Given the extent of trabecular bone thickening perceived in the superficial, deep, and mixed lesions during histopathologic examination, it is possible that with an increase in sample size, significant trabecular bone volume differences would be detected. Analyses of

bone volume in lesion areas relative to areas distant from any lesions identified on MRI would also be interesting.

Other comparisons that were not significant included the frequency of superficial lesions regardless of site, frequency of superficial lesions at noncompression sites, and the severity of superficial lesions at noncompression sites. A possible explanation is that all superficial lesions in this study were identified as some form of osteochondrosis. Prevalence of osteochondrosis in the Thoroughbred is estimated at ~25% (Lepeule et al. 2009) and has been documented in the cervical column of horses previously (Stewart et al., 1991 and Mayhew, 1978). The prevalence of osteochondrosis in general and its observation in both control and CSM horses in this study may explain the lack of significance in several of the superficial lesion comparisons.

MRI studies permit cervical column evaluation *in situ* allowing for a more complete identification and assessment of articular process pathology associated with CSM. Consistent with a previous report, pathology was not localized to only compression sites, but observed throughout the cervical column (Stewart et al, 1991). These findings support a generalized issue of bone and cartilage in the cervical column. The focus of this study was pathology of the articular processes. It would be useful to investigate if similar bone and cartilage lesions are observed in other parts of the vertebrae, as well as in the appendicular skeleton.

The new data reported provide further evidence that developmental aberrations of cervical vertebrae morphogenesis is important in the pathogenesis of

equine CSM, manifested as both osteochondrosis and cyst-like-lesions. In contrast, osteosclerosis may reflect a compensatory response in still maturing CSM horses to abnormal biomechanical stresses on the cervical column. Therefore, both developmental and biomechanical mechanisms may lead to the bone and cartilage changes observed in CSM. A model where biomechanical changes are secondary to primary developmental issues seems more likely. The intersection of developmental and biomechanical influences in the growing horse sets the stage for a complex interaction of variables. Future studies focusing on associations of CSM etiologic factors (high planes of nutrition, abnormal growth rates, abnormal copper and zinc levels, inherited genetic determinants) with specific bone and cartilage pathology in cervical vertebrae will help further elucidate the pathogenesis of equine CSM.

Chapter 4

The Role Of Inherited Genetic Determinants In Equine Cervical Stenotic Myelopathy

Summary

Experiments in this chapter tested the hypothesis that inherited genetic determinants contribute to the susceptibility of equine cervical stenotic myelopathy (CSM). Single nucleotide polymorphism (SNP) allele frequencies in the genomic DNA (gDNA) of carefully phenotyped CSM horses (n=59) were compared to population data (n=427) using the Equine SNP50 and Equine SNP70 Bead Chips for a genome wide association study (GWAS). Results of the GWAS identified multiple significant loci, both individual SNPs and haplotypes, across the genome. An additional association analysis was conducted by comparing the inheritance of genomic copy number variants (CNVs) across 8 individuals in a single family with a high incidence of the disease. The data support a genetic contribution to the etiology and/or pathogenesis of CSM, with inheritance likely complex in nature involving multiple gene loci. Results are consistent with the understanding that CSM is influenced by both genetic and environmental variables.

Introduction

Cervical stenotic myelopathy (CSM) results from malformations in the cervical vertebrae, which leads to vertebral canal stenosis and spinal cord compression. The condition is thought to be multifactorial, with both environmental and genetic variables contributing to etiology and pathogenesis. Known environmental factors include accelerated growth rates, high planes of nutrition, and altered copper and zinc concentrations. The importance of heritable

genetic determinants in regards to equine CSM has been studied by several groups, but remains an unresolved and debated issue.

An initial published investigation for the role of genetic determinants came from a multigenerational pedigree analysis looking at 6 Thoroughbred families (Dimock, 1950). Sire lines were examined and concluded that 43% of CSM progeny in the pedigrees traced to one of the three Thoroughbred foundation sire lines. A possible recessive inheritance, but not simple autosomal recessive was suggested from this work. Additional support for a possible recessive mode of inheritance came from a German investigator (Weischer, 1944; Weischer, 1946), based on observations. Previous to this, it was suggested that particular mares produced multiple affected offspring (Errington, 1938). Finally, there are numerous anecdotal reports predominately within Thoroughbred horses, but other breeds as well, of particular sires or dams that seem to produce an increased number of CSM progeny.

There are also published papers to the contrary, where investigators reached a conclusion that genetic determinants have a limited role in the development of CSM. Pedigrees of British Thoroughbreds with CSM were examined in comparison to controls (Falco et al., 1976). It was noted there was no increase in disease incidence in closed inbreeding populations, arguing against a simple recessive mode of inheritance. Additional smaller studies found no support for inheritance as well (Steel et al., 1959; Jones et al., 1954; Schultz et al., 1965). Wagner and colleagues (Wagner et al., 1985) conducted a prospective breeding study crossing dams and sires each with a confirmed diagnosis of CSM. Progeny were closely monitored with

serial neurologic examinations and radiographs for the onset of neurological deficits up to one year of age. None of the foals developed CSM during this study period. However, an increased incidence of other developmental orthopaedic diseases were noted such as physitis, contracted tendons, and osteochondrosis. This study effectively ruled out a simple mode of inheritance for CSM, but it is still possible CSM might be one clinical manifestation of a complex hereditary disease.

The current study was designed to test the hypothesis that inherited genetic determinants contribute to the susceptibility or pathogenesis of CSM. Identification of possible associations between single nucleotide polymorphisms (SNPs), haplotypes, and copy number variants (CNVs) with the CSM phenotype was carried out using both population- and family-based approaches.

Materials and Methods

Experimental Samples

SNP Association Sample Selection:

A total of 59 Thoroughbred horses with CSM were identified for study. Study subjects were limited to Thoroughbreds to eliminate breed as a variable and reduce confounding genetic heterogeneity unrelated to CSM. Two different phenotyping levels were used for identification of CSM cases (Figure 4.1). Fully phenotyped horses underwent antemortem and postmortem examinations as was previously outlined in chapter 2 of this thesis. A second classification level of CSM cases was a clinical diagnosis cohort. These horses were identified based on neurologic examination and standing cervical radiographs that strongly supported a clinical

diagnosis of CSM. Also, a subset of horses in this group had a myelogram and/or surgical intervention. For all CSM study subjects, clinical diagnosis needed to be made by 5 years of age. The control group was composed of 6 fully phenotyped horses that had no clinical neurological deficits and no evidence of spinal cord pathology on postmortem, as well as archived SNP data from 427 general population Thoroughbreds genotyped for reasons unrelated to CSM.

Fully Phenotyped:	Clinical neurologic examination, standing cervical radiographs, postmortem confirmation of cervical spinal cord compression
Clinical Diagnosis:	Clinical neurologic examination, standing cervical radiographs, myelogram and surgery in subset of cases
Breed Examined:	Thoroughbred only
Age Parameter:	Clinical CSM diagnosis made at 5 years of age or younger
Gender of Cases:	53 males; 6 females

Figure 4.1: Summary of the phenotypic assessment and signalment parameters for CSM horses in the study.

CNV Association Sample Selection

A Thoroughbred family with an increased incidence of CSM was identified for CNV analysis (Figure 4.2). This family was also included in the SNP analysis. All CSM horses within the family were phenotyped at the clinical diagnosis level. Absence of the CSM phenotype in the other progeny labeled as ‘control’ was inferred based on productive athletic careers in racing and personal correspondence. Two progeny, one CSM and one control have the same sire. This sire was also analyzed.

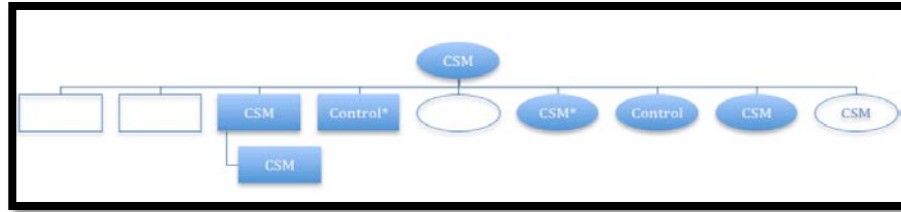


Figure 4.2: Pedigree of family included in CNV and SNP analysis. The solid blue fill indicates the horse was included for analysis. The phenotype status for known progeny is listed as CSM or control. Open shapes with no CSM or control categorization indicate the specific phenotype for that horse is unknown. * indicates the same sire for both progeny. This sire is included for analysis as well.

DNA Isolation

Whole blood samples were collected in ethylenediaminetetraacetic acid (EDTA) tubes from CSM horses, the 6 fully phenotyped controls, and the family samples. Genomic DNA (gDNA) was extracted using the Genra Puregene Blood kit and protocol from Qiagen (Germantown, MD). Spectrophotometric analysis (Maniatis, 2012) was used to quantify gDNA and assess purity. Samples were diluted to $100\text{ng}/\mu\text{l} \pm 10\text{ng}/\mu\text{l}$ for genotyping submission.

Genotyping

SNP Genotyping Arrays

For SNP genotyping, both the Equine SNP50K Bead Chip (Illumina), composed of 54,602 SNPs, and the Equine SNP70K Bead Chip (Illumina), which contains 65,157 SNPs, platforms were used. Polymorphisms are distributed across the autosomes and X and Y chromosomes, but these chips contain only two Y chromosome SNPs. Between the two platforms 45,703 markers are shared. Samples were sent to Geneseek (Omaha, NE) for genotyping. A summary of the phenotype classification and array used is given below (Figure 4.3).

Equine SNP 50K		Equine SNP 70K	
Cases (23)		Cases (36)	
Fully Phenotyped	16	Fully Phenotyped	0
Clinical Diagnosis	7	Clinical Diagnosis	36
Control (25)		Control (408)	
Fully Phenotyped	6	Fully Phenotyped	0
General Population	18	General Population	408

Figure 4.3: Summary of the samples genotyped on each array. The number of samples and phenotype classification is provided.

CNV Array

Genomic DNA samples from the family samples (Figure 4.2) were run on a custom designed exome tiling array (Doan et al., 2012). The array consists of 418,576 unique oligonucleotides distributed across all autosomes and the X chromosome (Agilent Technologies Inc.). Oligonucleotides range from 45-60bp in length. Preparation of gDNA samples for comparative genomic hybridization was performed according to a published protocol (Doan et al., 2012). Arrays were scanned on an Agilent High Resolution Microarray Scanner 62505C (Agilent Technologies Inc.). Feature extraction 10.5 software (Agilent Technologies, Inc.) was used to extract data.

Quality Control for Data Analysis

SNP Array Quality Control

Genotype data from both 50K and 70K arrays were merged for data analysis. Quality control and association analyses were performed using the SNP Variation Suite (SVS) version 7 software (Golden Helix Inc.). SNPs were excluded based on genotyping rate < 0.90, minor allele frequency < 0.01, and Hardy Weinberg

equilibrium p value < 0.001 thresholds. After these filters, 33,729 SNPs were left for analysis. Samples were also checked for gender discrepancy. Nine samples from the general population data were excluded for indeterminate gender assignment based on data provided.

Identification of Cryptic Relatedness and Population Structure

For identification of cryptic relatedness, a genomic best linear unbiased predictor (gBLUP) relationship matrix was constructed (vanRaden, 2008). The kinship matrix was based on genotypes and corrected for gender. This matrix functions to control for relatedness between samples that can lead to spurious associations. Population structure, another variable that can lead to spurious association, was addressed using principal component analysis (PCA). The first principal component was determined to be the best correction for structure and was used as a covariate in the association study (Figure 4.4). Inclusion of the first principal component in the mixed model produced the lowest Bayesian Information Criterion (BIC) value (Segura et al., 2012).

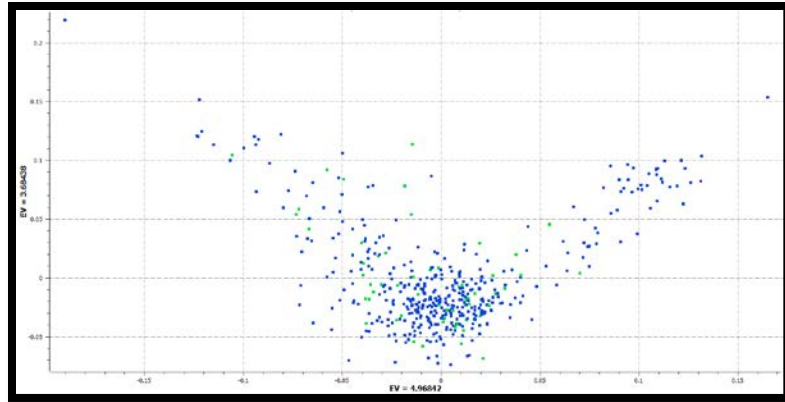


Figure 4.4: Scatter plot of 1st and 2nd principal components. The overlay of case and control samples supports minimal population structure in the data set. Control horses are blue diamonds. CSM horses are green diamonds.

CNV Array Quality Control

All arrays passed quality control checks using the feature extraction software for uniform signals in spots, background noise, and signal intensity achieving “good” or “excellent” assessments.

Statistical Analysis

Mixed Model Analysis for SNP GWAS

A mixed model analysis approach for additive effects was used for the SNP genome wide association analysis. This approach allows for the incorporation of fixed and random effects while correcting for relatedness. The multi-locus mixed model (MLMM) option was selected in SVS given the likelihood of CSM being controlled by a complex of multiple variants (Segura et al., 2012). The kinship matrix was included in the model along with the first principal component and

gender as covariates. A p value of < 0.05 after the Bonferroni correction was determined to be significant.

Haplotype Analysis

A case control association analysis was also performed evaluating haplotypes. This analysis was performed in SVS using precomputed haplotype blocks. The precomputed block method defines haplotype block boundaries using a confidence interval algorithm for identifying linkage disequilibrium (Gabriel et al., 2002). This method identified 4,790 variably sized blocks. A second method defined haplotype blocks based on a sliding window of 5 markers moving along all SNPs regardless of the degree of linkage disequilibrium. It defined 33,697 haplotype blocks. The Chi squared statistic with both the Bonferroni correction and 10,000 full scan permutations for multiple testing correction were computed. A p value of < 0.05 after either the Bonferroni correction or 10,000 maximum permutations was identified as significant. The Bonferroni correction is calculated by dividing the number of samples by the total number of tests. In this case, each SNP represents an individual test. Haplotype frequencies were computed using EM estimation (Dempster et al., 1977; Excoffier and Slaton, 1995).

Copy Number Variant Identification

Copy number variants from the dam in the family pedigree (Figure 4.2) were called in Agilent Genomics Workbench 5. The aberration detection method 2 (ADM-2) algorithm identified CNVs in respect to a reference sample. The reference sample was a male Thoroughbred defined as a control based on absence of neurologic signs and lesions consistent with CSM on clinical and postmortem examination. The list of

CNVs detected in the dam was compared to the equine (various breeds) CNV database at Texas A&M for identification of aberrations unique to the mare. These dam-specific CNVs were then analyzed for segregation to her progeny and level of association with the CSM phenotype.

Results

Correction for Relatedness and Population Structure:

In order to account for possible spurious associations due to cryptic relatedness among samples or possible population structure, gBLUP and PCA were used respectively. Q-Q plots were constructed to evaluate the effectiveness of these two methods (Figure 4.5). In the plot on the left there is a gradual deviation of SNPs from the line indicating genomic inflation that could lead to false positives. The plot on the right is the data after correction, where SNPs follow the line until the distinct upward deviation at the lowest P values. These methods appeared to have sufficiently corrected for relatedness and structure in the data set.

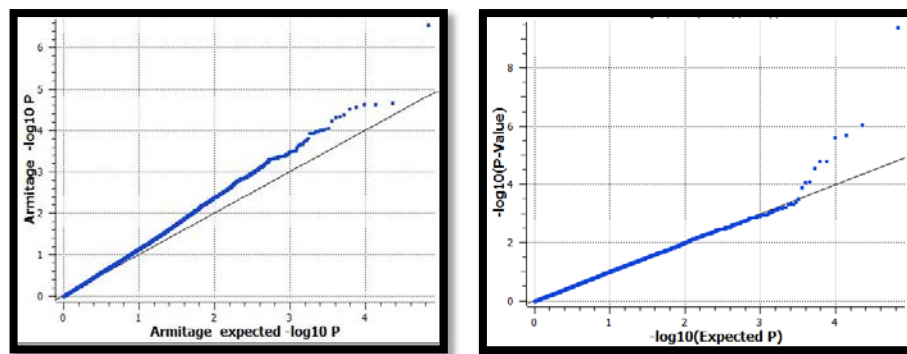


Figure 4.5: Q-Q plots before and after methods for structure correction. Each blue box represents an individual SNP. The plot on the left is the data without correction and a gradual deviation from the line is observed consistent with inflation. The plot on the right is after the use of gBLUP and PCA and the inflation has resolved.

Chestnut Coat Color Association

Coat color information based on individual registration records from the Thoroughbred breed organization was acquired for each horse. This information was used to run a chestnut coat color association analysis as a positive control for the data set. The association identified a significant association on ECA 3 in the region of the MC1R gene, which is known to control the chestnut coat color phenotype (Figure 4.6).

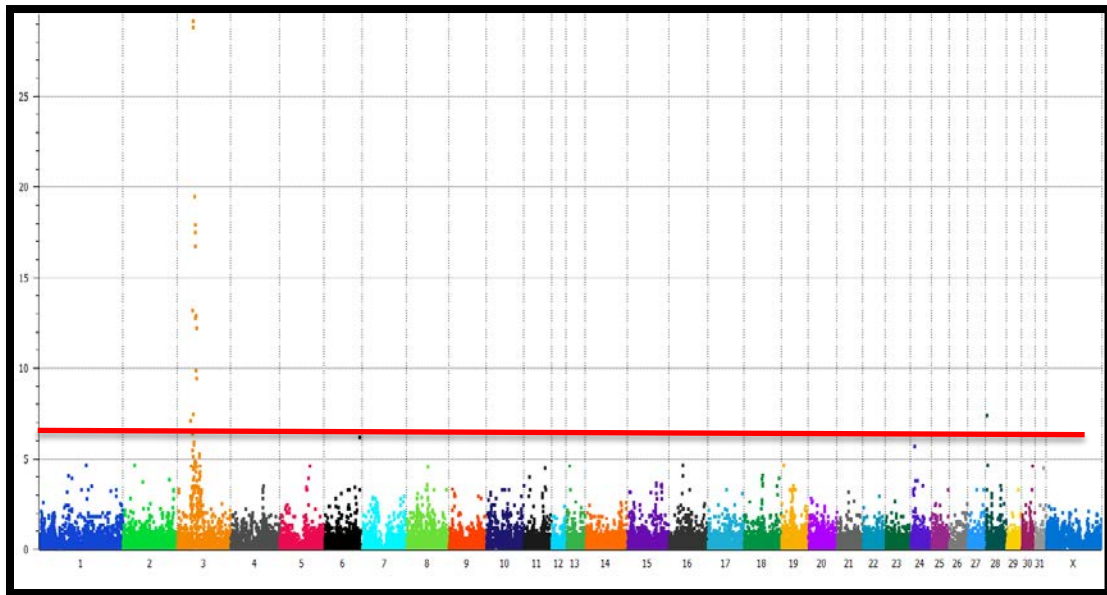


Figure 4.6: Manhattan plot for chestnut coat color association analysis. Each colored box represents an individual SNP. The negative log of the p value is displayed on the y-axis scale. Position along the x-axis indicate the individual equine chromosomes. The red line defines significance based on the Bonferroni correction for multiple testing. A strong peak of SNPs in linkage disequilibrium is observed on ECA 3 in the region of the MC1R gene known to control for the chestnut coat color phenotype.

SNP-based Association Analysis

Results of the SNP mixed model analysis with additive effects identified two SNPs with association to the CSM disease phenotype. Significance was assigned based on $p < 0.05$ after the Bonferroni correction. SNPs are located on ECA 12 and ECA X (Figure 4.7).

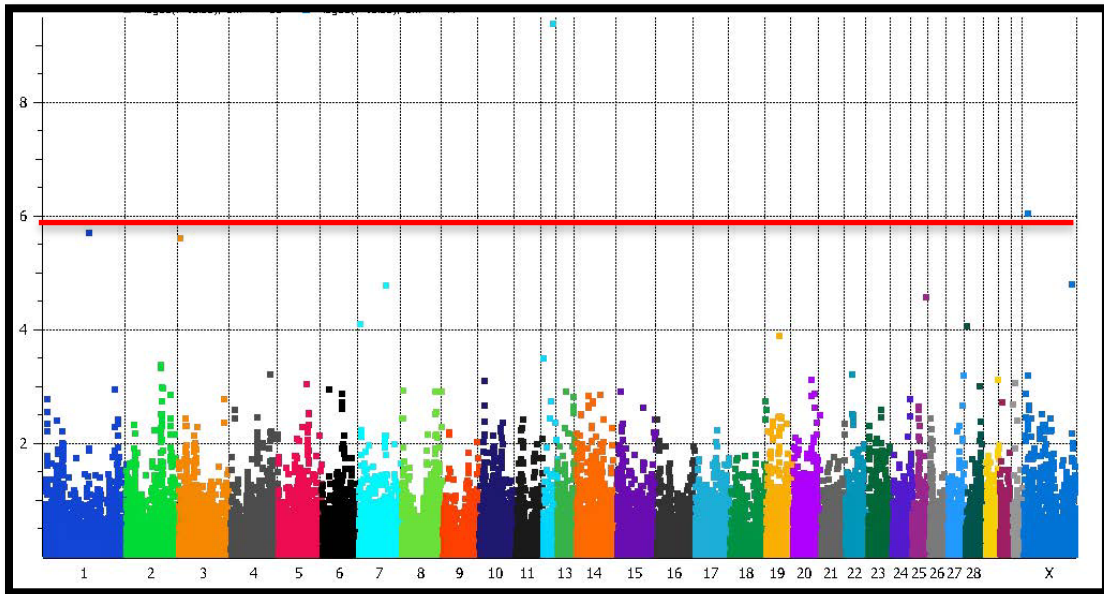


Figure 4.7: Manhattan plot for mixed model analysis with additive effects. The red line indicates significance based on the Bonferroni correction for multiple testing. SNPs on ECA 12 and ECA X are positioned above the significance threshold.

The allele frequencies and distribution of genotypes of the significant SNPs identified in the mixed model analysis between the case and control groups are summarized in the table below.

SNP ID	Location (Chr.bp)	P value	Genotype	Cases n=59	Controls n=424
BIEC2_193603*	12.22368861	4.17e-10	AA	32 (54.2%)	340 (80.2%)
			AG	24 (40.7%)	72 (17.0%)
			GG	3 (5.1%)	3 (0.71%)
BIEC2_1109022	X.8192913	7.07 e-7	AA	40 (68.0%)	351 (83.0%)
			AC	4 (6.7%)	50 (11.9%)
			CC	15 (25.4%)	23 (5.0%)

Table 4.1: Summary of the location and genotypes of significant SNPs in the mixed model analysis. *Control group had 9 samples for which the genotypes of BIEC2_193603 were not called. Chr = chromosome; bp = base pair.

Haplotype Analysis

Significant haplotypes were identified using both the precomputed block and sliding window of 5 makers. In one or both approaches, significant haplotypes were identified that included the two individual significant SNPs on ECA 12 and ECA X. The location of significant haplotypes using both methods is depicted below (Figure 4.8 and 4.9). Estimated haplotype frequencies were also calculated (Table 4.2 and 4.3). Significant haplotypes varied between 5.9%-28.81% in the CSM group; whereas the haplotype frequency in the control group was below 11.1%. The degree of linkage disequilibrium (LD) varied in the regions covered by the significant haplotypes.

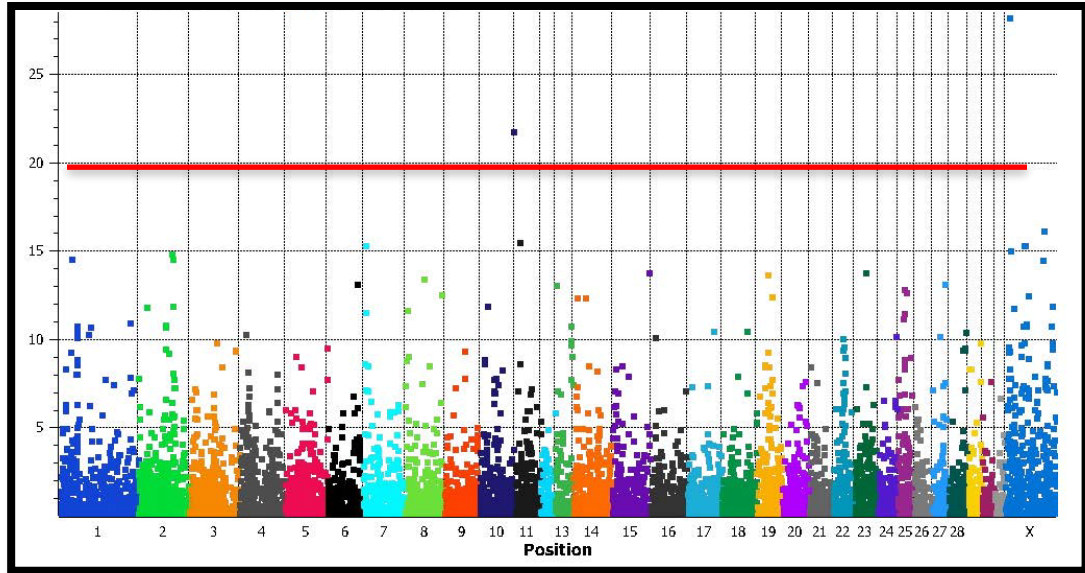


Figure 4.8: Manhattan plot of haplotypes using blocks defined by the precomputed block method. The red line indicates significance after applying the Bonferroni correction. The y-axis is the Chi squared statistic. Each individual box presents the first SNP in each haplotype. Significant haplotypes are located on ECA 10 and ECA X.

Chr	Basepair	Haplotype	Overall Freq	CSM Freq	Control Freq	Bonf p value	Perm. p value
ECA X*	7,959,875-8,192,913	AGAAC	13.23%	28.80%	11.07%	0.001	0.055
ECA 10	80,425,724-80,478,372	GAGA	13.71%	6.14%	0.72%	0.038	0.235

Table 4.2: Summary of the significant estimated haplotypes identified by the precomputed block of markers. *Indicates haplotype contains significant SNP from individual SNP analysis. Freq.= frequency; Bonf.= Bonferroni; Perm.= permutation

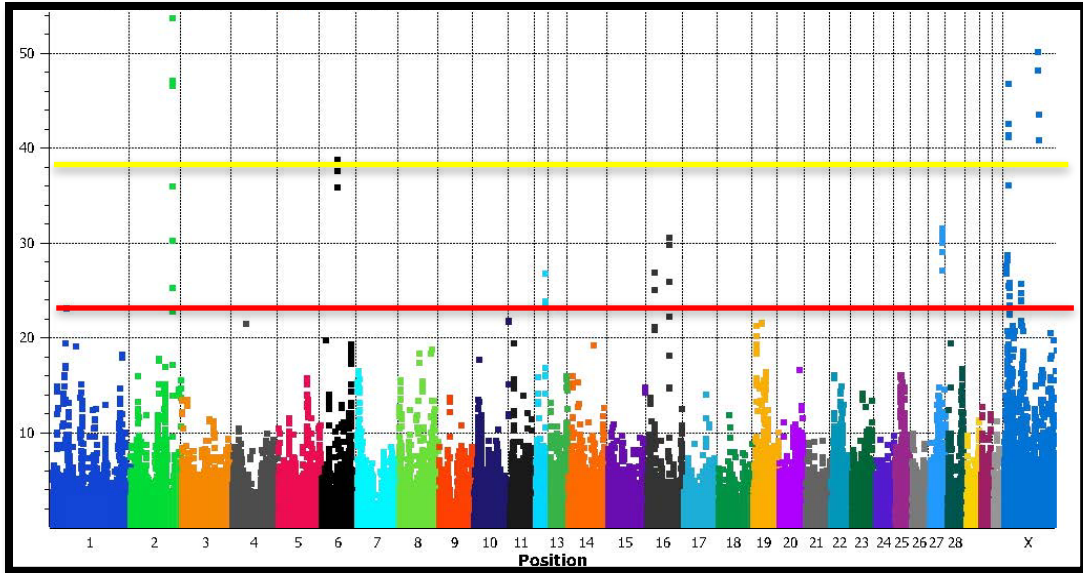


Figure 4.9: Manhattan plot of haplotypes using blocks defined by a sliding window of 5 markers. The yellow line indicates significance of $p < 0.05$ after applying the 10,000 maximum permutations of the data. The red line indicates significance after applying the Bonferroni correction. The y-axis is the Chi squared statistic. Each individual box presents the first SNP in each haplotype. Significant haplotypes are located on ECA 2,6,12,16,27, X.

Chr	Basepair	Haplotype	Overall Freq	CSM Freq	Control Freq	Bonf p value	Perm. p value
ECA 2	98,861,186-98,960,646	AGCGG	2.51%	12.39%	1.13%	4.46e-8	0.002
ECA X	5,790,320-5,983,253	AAAAG	1.46%	6.90%	0.71%	0.029	0.360
ECA X*	7,963,553-8,196,534	GAACA	13.3%	28.81%	11.10%	0.016	0.299
ECA X	9,204,707-9,322,958	CAGGA	3.20%	13.12%	1.81%	1.34e-5	0.023
ECA X	11,478,740-11,558,592	AGAGC	2.36%	11.02%	1.06%	1.48e-6	0.008
ECA X	80,036,076-81,737,962	AAAAA	3.83%	15.79%	2.13%	2.73e-7	0.004
ECA 6	37,546,839-38,002,001	GGGAA	1.57%	8.65%	0.64%	9.91e-5	0.044
ECA 27	30,165,151-30,499,043	GCCAG	1.04%	5.91%	0.36%	0.004	0.170
ECA 16	17,568,806-17,754,789	GAAGG	1.22%	6.32%	0.51%	0.042	0.418
ECA 16	52,363,165-52,401,989	GGACG	3.80%	12.65%	2.60%	0.006	0.212
ECA 12*	22,162,774-22,688,422	AGGGG	1.50%	6.63%	0.74%	0.043	0.421

Table 4.3: Summary of the significant estimated haplotypes identified by the sliding window of 5 markers. *Indicates haplotype contains significant SNP from individual SNP analysis. Freq.= frequency; Bonf.= Bonferroni; Perm.= permutation

One megabase windows on either side of significant regions were used to curate lists of protein coding genes, pseudogenes, and other elements (Table 4.4). Ensembl.org was used to identify these elements.

Gene Summary				
Chr	Basepair	Protein Coding	Pseudogenes	Types of RNA
ECA 2	98,861,186-98,960,646	2	4	2
ECA X	5,790,320-5,983,253	10	7	0
ECA X*	7,963,553-8,196,534	9	0	2
ECA X	9,204,707-9,322,958	16	1	3
ECA X	11,478,740-11,558,592	22	8	1
ECA X	80,036,076-81,737,962	59	17	3
ECA 6	37,546,839-38,002,001	35	9	0
ECA 27	30,165,151-30,499,043	2	1	2
ECA 16	17,568,806-17,754,789	9	3	0
ECA 16	52,363,165-52,401,989	12	9	3
ECA 12*	22,162,774-22,688,422	73	22	12
ECA 10	80,425-724-80,478,372	12	3	0

Table 4.4: Summary of protein coding genes, pseudogenes, and RNA elements in significant loci. The window used for identifying these elements extends 1 MB on either side of the stopping points of the basepair column. * indicates this region contains a significant SNP from the individual SNP analysis.

CNV Identification

A total of 276 CNVs were called in gDNA from the dam of the previously described family pedigree (Figure 4.2). When compared to the equine CNV database, this mare had 207 unique aberrations (Figure 4.10). Unique is defined as CNVs identified in the mare only and not present in the database. Sixty-nine CNVs were identical between the mare and common CNVs in the database. Finally, 4,987 CNVs in the database were not identified in the mare. Three CNVs were found to segregate with the CSM disease phenotype (Table 4.5). Of these 3, an amplification on ECA 9 has not been described previously as a locus for CNV polymorphism.

Whereas the other two, both of which suggest heterozygous deletions on ECA 7, were located at loci already listed in the equine CNV database.

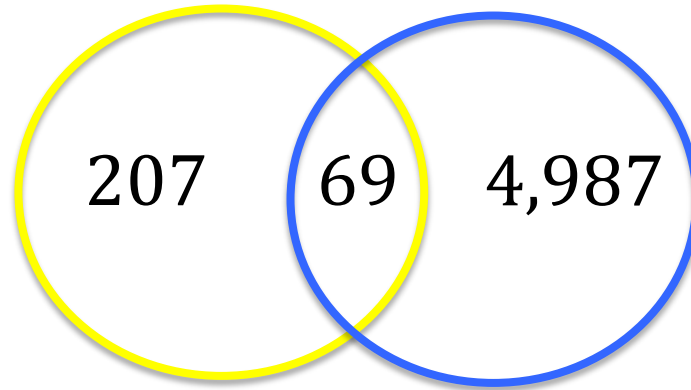


Figure 4.10: Venn diagram of unique common CNVs between the dam and the database. The yellow circle represented CNVs called in the dam. The blue circle represents CNVs from the database.

Chromosome	Start base pair	Stop base pair	Direction
ECA 7	34,644,877	34,682,871	Deletion
ECA 7	52,736,448	52,736,967	Deletion
ECA 9	31,306,365	31,306,958	Amplification

Table 4.5: Summary of CNVs in the dam that segregates only with CSM progeny. Two deletions on ECA 7 and one amplification on ECA 9 were identified in all CSM horses in this family.

Discussion

The focus of these experiments was to re-examine the long-standing question regarding the role of genetic determinants in the etiology and/or pathogenesis of CSM using genome-wide assessments of polymorphic DNA markers. This was accomplished by performing GWAS analyses to evaluate SNP and haplotype associations between horses with CSM and the general Thoroughbred population. Results of this analysis identified multiple significant loci associations distributed across the genome supporting a genetic contribution in some fashion to the etiology

and/or pathogenesis of CSM. Significant SNPs identified on ECA 12 and X were also included in significant haplotypes. In addition, significant loci were identified on ECA 2, 6, 10, 16, and 27.

An important consideration is what can be determined from the data in regards to the possible inheritance pattern. The GWAS for the CSM disease phenotype, assessing both individual SNPs and haplotypes, identified significant loci across multiple chromosomes. This finding is not consistent with a simple mode of inheritance, but instead, suggests a more complex genetic trait. These data are supportive of earlier pedigree and breeding studies (Dimock, 1950; Errington, 1938; Weischer, 1944; Wagner et al., 1987) that also concluded a simple mode of inheritance was unlikely. The multiple associations with CSM is in contrast to the single strong focal peak observed for chestnut coat color, composed of numerous SNPs on ECA 3 in the region of the MC1R gene known to regulate the chestnut phenotype with a recessive mode of inheritance (Marklund et al., 1996).

For complex traits, often there are multiple genomic loci and variants involved that individually have a small effect, but in combination can reach a threshold affecting the phenotype (McCarthy et al., 2008). Complex diseases in the human literature include Crohn's disease and type 2 diabetes (Bao et al., 2013; Tsianos et al., 2012), where multiple genetic loci in combination with environmental factors lead to manifestation of clinical disease. CSM is most likely a similar situation. Established environmental factors that contribute to CSM include high planes of nutrition and increased growth rates. The model predicts environmental

factors and inherited genetic variants interacting in potentially complex ways to produce the CSM disease phenotype.

SNPs and haplotypes significantly increased in CSM over controls are candidate susceptibility or risk loci. Conversely, polymorphic markers found to be significantly increased in control horses may be close to genes that influence protective mechanism. Regions on ECA 12 and ECA X are particularly interesting given they were significant on the analysis of both individual SNPs and haplotypes. One megabase genomic intervals on either side of significant SNPs and haplotypes were examined for possible genes of interest (Table 4.4). Genes identified in these regions were associated with a variety of ontologies. One specific gene of interest, neuronal membrane glycoprotein gene (GPM6B) located on ECA X, has been shown to regulate osteoblast function and bone formation (Drabek et al., 2011). GPM6B controls cytoskeleton formation and matrix vesicle release for mineralization. Osteosclerosis, increased bone density due to the presence of excessive mineralization, is a pathologic lesion associated with CSM (Mayhew, 1978; Powers et al., 1986; Chapter 3). Therefore, GPM6B could be a gene of interest for future studies.

Identification of regions of interest on the X chromosome is potentially interesting given the prominent gender bias of male over females in this disease. Since males are hemizygous for the X chromosome, they will express an X-linked disease whether it is dominant or recessive. It is unlikely that CSM is completely explained by an X linked inheritance, but the potential contribution of the X

chromosome and the documented male over female bias is interesting. A role for the X chromosome is also intriguing given anecdotal evidence of “unaffected” dams producing CSM offspring.

The CNV experiment looked for association of specific copy number variants with the CSM disease phenotype. The family studied is unusual given the increased number of affected horses, since the overall prevalence of CSM in the Thoroughbred population is estimated at 2% (Oswald et al., 2002). It is possible this mare could have additional or even unique *de novo* mutations contributing to the high incidence of disease observed. In a preliminary analysis of the CNV data, the index mare contains 207 unique CNVs relative to an equine CNV database (Figure 4.10). This database is comprised of data from a multiple horse breeds (Scott Dindot and Cole McQueen- personal communication), therefore variation unique to the Thoroughbred is likely included in this group of CNVs. Three of the mare’s CNVs were inherited only by the foals that developed CSM (Table 4.7). Current annotation of these loci is limited to genes encoding uncharacterized proteins.

Several studies have identified the occurrence of osteochondrosis (OC) in cervical vertebrae of horses affected by CSM (Mayhew et al, 1978; Stewart et al, 1991; Chapter 3). OC is another multifactorial musculoskeletal disease where the role of genetic determinants has been examined in various horse breeds (Distl, 2013 ; Corbin et al., 2011, Wittwer et al., 2007; Dierks et al., 2010; Felicetti et al., 2009; Lampe et al., 2009). Multiple loci have been identified across the genome with significant association to the OC phenotype. Given that many pathological

lesions in the articular joints of cervical vertebrae of CSM horses are OC, the previously published SNPs from the GWAS studies of equine OC were compared to loci found in the current CSM analysis. No concordance between regions of interest of the two diseases was found.

Given limitations in the number of CSM samples evaluated, an important point to consider in the current dataset is statistical power. While sufficient horses were analyzed to detect a trait regulated by a single gene with a recessive mode of inheritance, as clearly demonstrated with chestnut coat color, the assembled sample set may not be sufficient to resolve complex genetic determinants for CSM. When investigating complex genetic traits in genome wide studies, a larger sample size is required for sufficient power to identify variants that individually have a smaller effect. In this study, a larger general population data set was used for the control group in an effort to more confidently establish SNP frequencies in the Thoroughbred for comparison to the CSM samples. Also, it is important to note that the general population Thoroughbreds used for controls were genotyped for reasons unrelated to CSM. As such, we cannot be sure that all of these horses were free of neurological deficits. Any horses with CSM in the control population sample set would also diminish statistical power.

Analysis in this study combined SNPs from two commercial Illumina platforms, the 50K and 70K equine chips. Therefore, it is possible there may be a chip bias. The PCA plot demonstrated decent overlay of the 50K and 70K horses indicating bias might be less of an issue. That being said, some of the significant

haplotypes in the sliding window analysis were heavily represented on one chip versus the other making them less convincing compared to other identified loci. Haplotypes identified in the sliding window analysis distributed on samples from both chips include ECA 6, 27, and X. giving these regions support and priority for further validation and investigation.

In addition to sample size contributing to lack of power, a smaller number of SNPs was evaluated since only those common to both chips were used. One method to address this issue would be imputation. Imputation gives the probability of a SNP at an ungenotyped location based on the LD of the variants surrounding it. An imputation mechanism for the 50K and 70K Equine Bead Chips has been put forth in the literature (McCoy et al., 2013). This method would allow for evaluation of all horses in the sample set at approximately ~65,000 SNPs before filtering versus the ~33,000 SNPS analyzed currently. Increasing the number of SNPs evaluated allows for denser coverage of the genome and would facilitate locating significant variants that contribute to CSM.

Additional studies will enable further refinement of loci identified in this work. First, a new and independent population of CSM and control horses is needed for validation of these regions. Another issue that may be critically important is refinement of phenotyping parameters. In other words, CSM could represent a common clinical syndrome that results from more than one pathogenic mechanism. The anatomical structures of the vertebrae that can participate in canal stenosis are variable (i.e. articular processes, vertebral body subluxation, epiphyseal flaring, or

extension of the dorsal lamina). As such, it may be better to assess each type of vertebral malformations independently by assembling CSM sample sets based on specific vertebral malformations. Attempts to define phenotypic subcategories with the current sample set did not improve GWAS resolution, likely because this subgrouping further reduced the number of CSM cases available for comparison.

This is the first study to investigate the role of inherited genetic determinants in equine CSM using a genome-wide analysis of gDNA polymorphisms. Data support the contribution of genetic determinants to the development of disease. Control of the CSM phenotype by one major gene is improbable, as multiple significant loci were identified across the genome. Therefore, it is likely instead that CSM is a complex genetic trait with the phenotype influenced by multiple genes and several environmental variables. Subsequent studies validating loci and investigating the role of these variants and any other contributing factors is warranted. Also, the interaction of genetic and environmental variables is an additional investigative point for consideration in future efforts to elucidate the etiology and pathogenesis of CSM.

Chapter 5

Reflections and Looking Ahead to Future Studies

Reflections

Research efforts in this dissertation thesis were aimed at examining important questions related to the etiology and pathogenesis of equine CSM. The specific objectives were: 1) compare the ability of MRI and standing cervical radiographs to detect and localize cervical vertebral canal stenosis in CSM horses, 2) evaluate the frequency and severity of skeletal lesions identified by MRI in the articular processes of cervical vertebrae in CSM horses, 3) characterize the lesions in articular processes of CSM horses on structural and histological levels, and 4) investigate the role of inherited genetic determinants in CSM.

CSM remains a major problem in various equine breeds including Thoroughbreds, Warmbloods, and Tennessee Walking Horses to name a few. Since CSM often results in substantial neurologic deficits, it has a significant impact on the welfare of the horse. Justification for the re-examination of CSM etiology and pathogenesis in the context of my PhD dissertation are three-fold. First, these issues are of fundamental importance for efforts to improve the diagnosis, management, and/or treatment of this disease. In other words, research on these issues has the potential to have a near-term, real-world impact. Second, technological advances in equine science have been achieved in recent years in areas related to diagnostic imaging and genomics. Working with these technologies provided a valuable educational opportunity for me and increased the potential that the research would yield results with a positive impact for horses. Finally, this dissertation research

focus has allowed me the opportunity to advance my interests in anatomic pathology and the equine musculoskeletal system while achieving the primary educational goal of PhD level training in experimental biology. The project has provided direct synergy of my educational priorities to continue to develop as a veterinarian pursuing clinical diagnostic and discovery science interests.

In chapter 2, the hypothesis was tested that MRI is superior to standing cervical radiographs for identification and localization of canal stenosis. It was felt MRI could potentially improve the specificity and sensitivity of stenosis diagnostic assessment given the ability to obtain multiple views of the cervical column as compared to standing cervical radiography. The morphometric assessment of the vertebral column on MRI identified canal area and the cord to canal area ratio as useful metrics for determination of compression. Indeed, when compared to standing cervical ratios, both canal area and CCAR on MRI demonstrated an improvement in spinal cord compression localization. The data supported the hypothesis originally put forth. There are limitations of this study that need to be addressed in further studies. First, canal area and CCAR need to be evaluated in both the extended and flexed neck position. Our study was limited to the neutral position. On myelography, it has been demonstrated that there are cases where cord compression is only visualized in the extended or flexed position. Secondly, additional horses need to be evaluated to enable the establishment of thresholds for stenosis in a clinical setting. With increased numbers and statistical power, a Receiver Operating Characteristic (ROC) curve could be constructed to determine sensitivity and specificity and identification of possible cutoffs for each vertebral

site. The establishment of thresholds for canal area and CCAR would allow for application in the diagnostic setting as technology continues to evolve to accommodate imaging of the equine cervical column antemortem.

Experiments reported in chapter 3 use this same MRI primary dataset to evaluate bone and cartilage pathology in the articular processes of CSM horses. The study quantified an increased number and severity of lesions relative to controls, followed by histological and microstructural assessments of pathological changes in the lesions. The findings support a generalized bone and cartilage developmental issue of the cervical column, in which pathology is not limited to only the site of compression in horses with CSM. A subset of lesions evaluated structurally and/or histologically found osteochondrosis, osseous cyst-like structures, fibrous tissue replacement of trabecular bone and bone marrow, and osteosclerosis. The data are consistent with primary skeletal developmental issues, associated with secondary biomechanical stresses on the vertebral column leading to CSM pathology in the articular processes. It is important to note that growth plates in equine vertebrae do not close until 4-5 years of age, so CSM normally develops and becomes clinically apparent while horses are still very much in a phase of growth and maturation. Prior to growth cessation, the vertebrae are likely more responsive to the abnormal biomechanical forces.

Analyses of the pathological lesions have provided important new information about equine CSM. Most notably, these include pathologic lesions identified regardless of compression site and descriptions of novel osseous cyst-like

lesions present in the articular processes. Further studies are needed to determine if similar pathology is observed in other parts of the vertebrae and appendicular skeleton. If this occurs, it would further support a generalized defect in bone and cartilage morphogenesis and/or maturation.

The long-standing question that probably generates the most interest among equine veterinarians and horse owners is the extent to which inherited genetic determinants are an important variable in the etiology, pathogenesis, and/or susceptibility of horses to this disease. It really is an important issue to re-investigate, given that the entire equine genome has now been sequenced and related genomic DNA analytical reagents are now available. The hypothesis tested was that there are inherited genetic determinants that contribute to the susceptibility of CSM in the horse. A genome wide association study (GWAS) using single nucleotide polymorphisms (SNPs) and haplotypes was performed. Multiple significant loci associating with the CSM phenotype were identified across the genome supporting the role of genetic determinants in clinical disease. Control of CSM by a single gene consistent with a simple Mendelian trait is unlikely given the results of this study. Instead, the identification of multiple loci supports a complex trait. Complex traits are influenced by multiple genes and the phenotype does not follow simple Mendelian patterns of inheritance. Many complex traits are also regulated by environmental variables. Findings from the current work are generally consistent with earlier research from other groups, indicating that equine CSM is a multi-factorial disease. Importantly, these data can also serve as a starting point for continued investigation of genetic determinants associated with CSM. Validation of

the identified loci using a new and independent sample set is needed as studies move forward. An important point to keep in mind for experimental design of subsequent analyses is sample phenotyping. There are different anatomical ways to achieve cord compression that should be considered for subgrouping of samples for testing. Different combinations of genotypes could control the various anatomic phenotypes. Comparison of genotypes across the types of compression would identify if there were genetic heterogeneity associated with CSM as well.

Experiments in this dissertation provide support for the role of genetic determinants in CSM. The next logical step is fine mapping of validated regions with either a high density SNP array or targeted genome sequencing for further refinement. This would allow for identification of strong candidate genes. Another approach is the use of whole genome sequencing of a family with multiple affected individuals, such as the family described in chapter 4. The cost of whole genome sequencing has fallen in recent years making it potentially feasible for studies with smaller sample sets. It would allow for identification of multiple variants in protein coding genes and regulatory elements. There are logistical considerations that would need to be considered with whole genome sequencing such as cost, number of animals, and mechanisms to confidently identify variants associated with the disease phenotype. However, if possible it could be a powerful tool for further refinement of the role of genetic determinants in CSM.

Although establishment of equine CSM as a multi-factorial disease makes issues related to etiology, pathogenesis, and susceptibility more complex, it also

identifies important strategies for research going forward. One example would be to search for epigenomic factors. Epigenetics is the field of science that focuses on changes in gene expression without alterations in the DNA nucleotide sequence. Multiple studies have confirmed alterations in environmental factors, specifically nutrition, can lead to epigenetic modifications affecting disease susceptibility (Wolff et al., 1998; Waterland et al., 2003). Also, it has also been demonstrated that epigenetic signatures can be inherited (Jirtle and Skinner, 2007). By investigating the interaction between environmental and genetic variables in equine CSM, it could provide valuable new insights about this disease.

Given the evidence that developmental issues of bone and cartilage morphogenesis and/or maturation have an important role in CSM pathogenesis, investigation of the cervical column during gestation and the early postnatal period will almost certainly be of value. There have been reports of subclinical stages of osteochondrosis in late gestation (Olstad et al., 2011). It is possible that predisposition for vertebral malformation could begin *in utero*. Identification of critical time points of cervical vertebral development would be useful for establishing windows when the vertebrae are susceptible to influences leading to malformations.

The obvious clinical relevance of continuing to address factors implicated in the etiology and pathogenesis of CSM is improved diagnosis, management, treatment, and even possibly prevention of the disease. Work in this dissertation supports a role of genetic determinants as an etiologic factor in equine CSM. Future

studies need to confirm the identity of important loci and specifically define contributing genetic factors. This will enable genetic risk scores for application to management practices and breeding decisions to be developed. Likewise, further understanding of the cervical vertebral column development could identify critical time points for optimal implementation of disease modifying management practices.

Pulling Together our Current Understanding of Equine CSM

Organizing published literature and the work from this thesis, it is possible to summarize factors that confer an increased or decreased risk of developing CSM (Figure 5.1) and pathological changes observed with the disease (Figure 5.2).

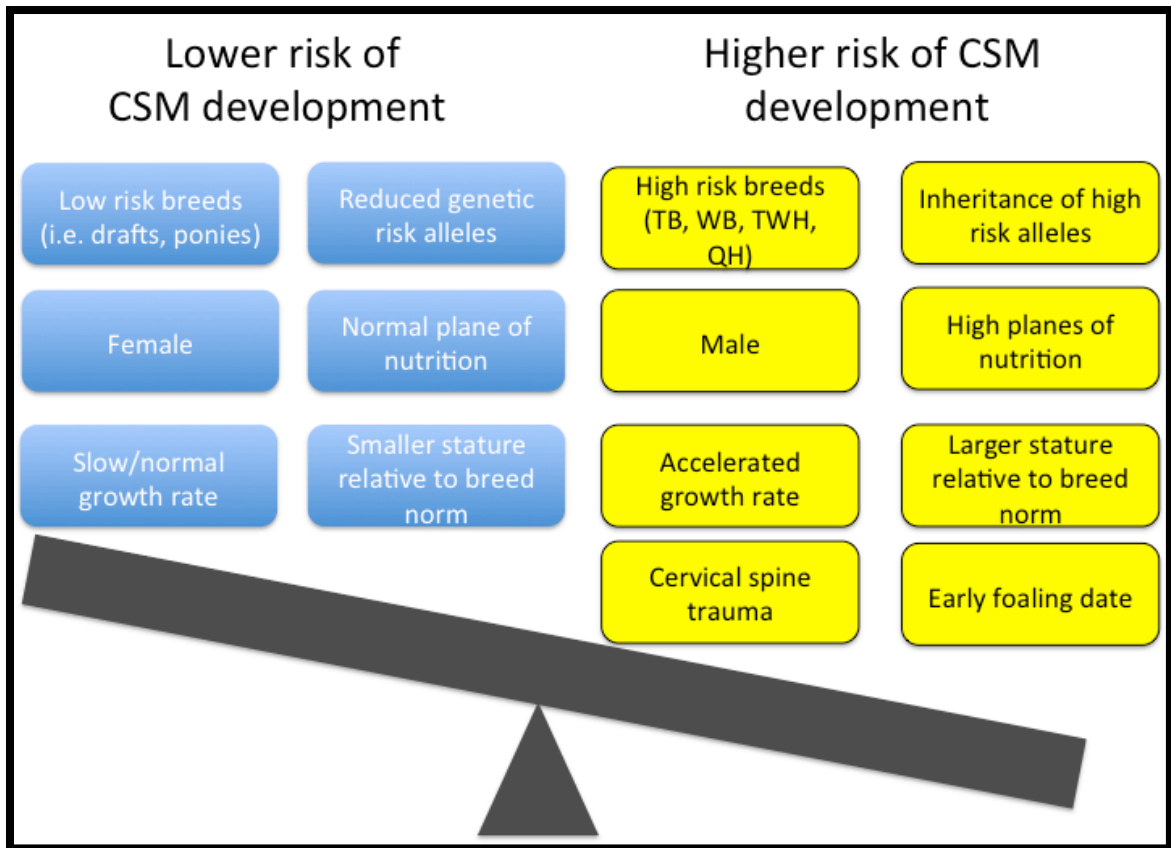


Figure 5.1: Risk factors for cervical stenotic myelopathy (CSM). A variety of factors are known or believed to contribute to clinical development of CSM. Factors listed on the left side are associated with a decrease risk of disease, while factors on the right in a combinatorial manner increase disease incidence.

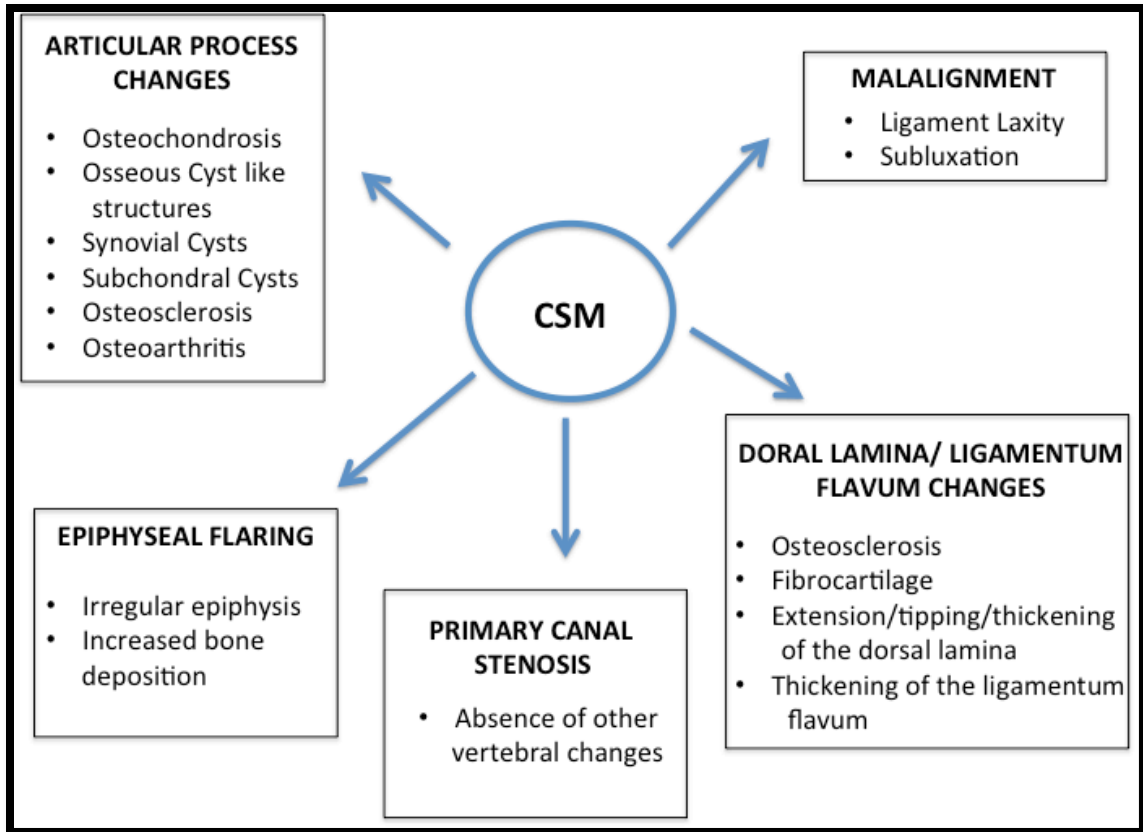


Figure 5.2: Vertebral gross and histopathologic changes associated with CSM. Each box represents a particular anatomical structure with listed gross and/or histopathologic lesions that have been identified with this disease. It is important to note that while these changes can be seen individually, it is also common to see combinations of lesions.

It is much more challenging to develop a working model of CSM etiology and pathogenesis. There are multiple ways to achieve spinal canal stenosis; some paths are straightforward while others are likely complex. A simple path to canal stenosis and cord compression would be a horse experiencing a traumatic event that results in a cervical vertebral subluxation. Another relatively straightforward example might be a horse developing epiphysitis and flaring of the vertebral growth plates. Other pathways, however, will clearly be more complex.

Given the strong evidence that development, growth, and maturation of cervical vertebrae are important variables, consideration of a timeline should be helpful (Figure 5.3). The figure illustrates important events and time periods in comparison to age of CSM diagnosis for 252 Thoroughbred cases. Genotype of an individual is defined at conception. Skeletal ossification in the equine fetus begins around gestational day 37 (Jenner et al., 2014). By 2 years of age, Thoroughbreds have attained approximately 95% of their final height and 90% of their final body weight (Kocher and Staniar, 2013). Closure of the vertebral growth plates occurs between 4-6 years of age (Whitwell and Dyson, 1994, Stephen Reed - personal communication). Osteochondrosis (OC) is generally reported to develop between birth and 5 months of age (Carlson et al., 1995; Dik et al., 1999; van Weeren, 2006), but recent work is also considering cartilage biology *in utero* (Olstad et al., 2011). Environmental variables are relevant throughout these periods.

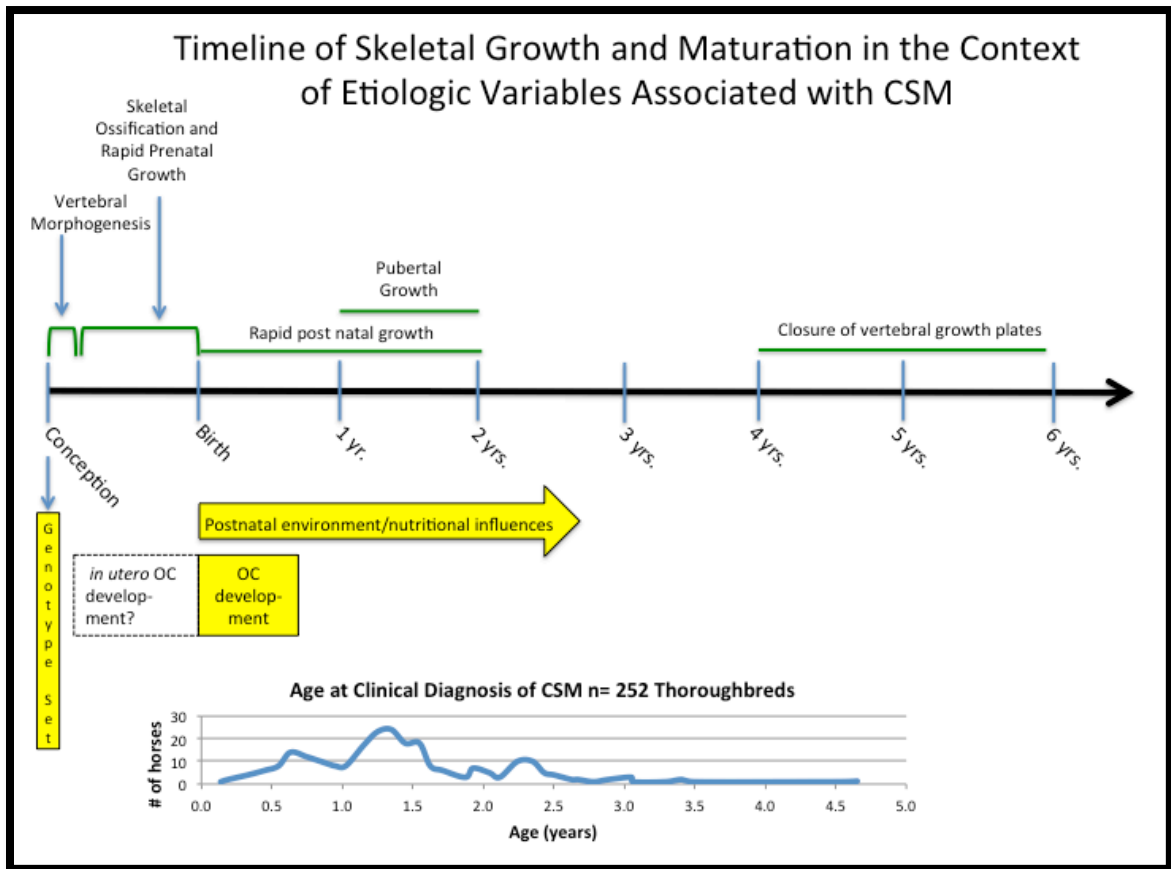


Figure 5.3: Skeletal growth and maturation timeline in the context of variables and pathology associated with CSM. The timeline is presented from conception to 6 years of age. Above the timeline, pertinent points related to general skeletal and vertebral growth are indicated. Below the timeline, the influence of proposed etiology factors are depicted. A survey of the age at CSM clinical diagnosis for Thoroughbreds scaled to match the timeline is at the bottom.

CSM remains an important neurologic and musculoskeletal disease of the horse and therefore warrants continued research for further understanding of disease mechanisms. With discovery science, the investigation of relevant questions often results in generating more questions. This dissertation thesis is no different.

Rapid advances in genomics, diagnostic imaging, and molecular technologies allow for continued investigation and hopefully relevant contributions to the understanding of CSM.

REFERENCES

- Anastasiou, A., Skioldebrand, E., Ekman, S. and Hall, L. (2003) Ex vivo magnetic resonance imaging of the distal row of equine carpal bones: assessment of bone sclerosis and cartilage damage. *Veterinary Radiology & Ultrasound* **44**, 501-512.
- Bland JH, B.D. (1987) *Disorder of the cervical spine: Diagnosis and medical management*, 2nd edn., Saunders, Philadelphia.
- Carlson, C., Cullins, L. and Meuten, D. (1995) Osteochondrosis of the articular-epiphyseal cartilage complex in young horses: evidence for a defect in cartilage canal blood supply. *Veterinary Pathology Online* **32**, 641-647.
- Carlson, C., and Weisbrode, S. Bones, Joints, Tendons, and Ligaments. *Pathologic Basis of Veterinary Disease*. 5th edn., Elsevier., St. Louis.
- Chen, J.-H., Liu, C., You, L. and Simmons, C.A. (2010) Boning up on Wolff's Law: mechanical regulation of the cells that make and maintain bone. *Journal of Biomechanics* **43**, 108-118.
- Chigira, M., Maehara, S., Arita, S. and Udagawa, E. (1983) The aetiology and treatment of simple bone cysts. *Journal of Bone & Joint Surgery, British Volume* **65**, 633-637.
- Claridge, H., Piercy, R., Parry, A. and Weller, R. (2010) The 3D anatomy of the cervical articular process joints in the horse and their topographical relationship to the spinal cord. *Equine Veterinary Journal* **42**, 726-731.
- Corbin, L.J., Blott, S.C., Swinburne, J.E., Sibbons, C., Fox-Clipsham, L.Y., Helwegen, M., Parkin, T.D., Newton, J.R., Bramlage, L.R. and McIlwraith, C.W. (2012) A genome-wide association study of osteochondritis dissecans in the Thoroughbred. *Mammalian Genome* **23**, 294-303.
- da Costa, R.C., Parent, J., Dobson, H., Holmberg, D. and Partlow, G. (2006) Comparison of magnetic resonance imaging and myelography in 18 Doberman pinscher dogs with cervical spondylomyelopathy. *Vet Radiol Ultrasound* **47**, 523-531.
- da Costa, R.C., Parent, J.M., Partlow, G., Dobson, H., Holmberg, D.L. and Lamarre, J. (2006) Morphologic and morphometric magnetic resonance imaging features of Doberman Pinschers with and without clinical signs of cervical spondylomyelopathy. *Am J Vet Res* **67**, 1601-1612.
- de Lahunta, A. (1983) *Veterinary Neuroanatomy and Clinical Neurology*, 2nd edn., W.B. Saunders Co., Philadelphia.
- Dierks, C., Komm, K., Lampe, V. and Distl, O. (2010) Fine mapping of a quantitative trait locus for osteochondrosis on horse chromosome 2. *Animal genetics* **41**, 87-90.

- Dik, K., Enzerink, E. and Weeren, P. (1999) Radiographic development of osteochondral abnormalities, in the hock and stifle of Dutch Warmblood foals, from age 1 to 11 months. *Equine Veterinary Journal* **31**, 9-15.
- Dimock, W.W. (1950) "Wobbles" an hereditary disease in horses. *J Hered* **41**, 319-323.
- Dimock, W.W., Errington B.J. (1939) Incoordination of Equidae: Wobblers. *Journal of the American Veterinary Medical Association* **XCIV**, 261-267.
- Distl, O. (2013) The genetics of equine osteochondrosis. *The Veterinary Journal* **197**, 13-18.
- Doan, R., Cohen, N., Harrington, J., Veazy, K., Juras, R., Cothran, G., McCue, M.E., Skow, L. and Dindot, S.V. (2012) Identification of copy number variants in horses. *Genome Research* **22**, 899-907.
- Donawick, W., Mayhew, I., Galligan, D., Osborne, J., Green, S. and Stanley, E. (1989) Early diagnosis of cervical vertebral malformation in young Thoroughbred horses and successful treatment with restricted, paced diet and confinement. In: *Proceedings of the annual convention of the American Association of Equine Practitioners (USA)*.
- Donawick, W.J. (1993) Results of a low-protein, low-energy diet and confinement on young horses with wobbles. In: *Proceedings of the annual convention of the American Association of Equine Practitioners (USA)*.
- Falco, M.J., Whitwell, K. and Palmer, A.C. (1976) An investigation into the genetics of 'wobbler disease' in thoroughbred horses in Britain. *Equine Vet J* **8**, 165-169.
- Felicetti, M., Lampe, V., Ehrhardt, S., Cappelli, K. and Verini, A. (2009) Mapping of a quantitative trait locus on equine chromosome 21 responsible for osteochondrosis in hock joints of Hanoverian warmblood horses. *Tierärztliche Hochschule Hannover*, 103.
- Fisher, L., Bowman, K. and MacHarg, M. (1981) Spinal ataxia in a horse caused by a synovial cyst. *Veterinary Pathology Online* **18**, 407-410.
- Gabriel, S.B., Schaffner, S.F., Nguyen, H., Moore, J.M., Roy, J., Blumenstiel, B., Higgins, J., DeFelice, M., Lochner, A. and Faggart, M. (2002) The structure of haplotype blocks in the human genome. *Science* **296**, 2225-2229.
- Hahn, C.N., Handel, I., Green, S.L., Bronsvoort, M.B. and Mayhew, I.G. (2008) Assessment of the utility of using intra- and intervertebral minimum sagittal diameter ratios in the diagnosis of cervical vertebral malformation in horses. *Vet Radiol Ultrasound* **49**, 1-6.

Hudson, N. and Mayhew, I. (2005) Radiographic and myelographic assessment of the equine cervical vertebral column and spinal cord. *Equine Veterinary Education* **17**, 34-38.

Jenner, F., Närväinen, J., Ruijter - Villani, M., Stout, T., Weeren, P. and Brama, P. (2014) Magnetic resonance microscopy atlas of equine embryonic development. *Equine veterinary journal* **46**, 210-215.

Jirtle, R.L. and Skinner, M.K. (2007) Environmental epigenomics and disease susceptibility. *Nature Reviews Genetics* **8**, 253-262.

Jones, T.C., Doll, E.R. and Brown, R.G. (1954) The pathology of equine incoordination (Ataxia or "Wobbles" of foals). Proc. Am. Vet. Med. Ass. 91st Ann. Meeting, 139-149.

Judex, S., Gupta, S., and Rubin, C. (2009) Regulation of mechanical signals in bone. *Orthodontics and Craniofacial Research* **12**, 94-104.

Khurana, J.S., McCarthy, E.F. and Zhang, P.J. (2010) *Essentials in Bone and Soft-Tissue Pathology*, Springer.

Kocher, A. and Burton Staniar, W. (2013) The pattern of thoroughbred growth is affected by a foal's birthdate. *Livestock Science* **154**, 204-214

Kronfeld, D., Meacham, T. and Donoghue, S. (1990) Dietary aspects of developmental orthopedic disease in young horses. *The Veterinary Clinics of North America: Equine Practice* **6**, 451-465.

Lampe, V., Dierks, C. and Distl, O. (2009) Refinement of a quantitative trait locus on equine chromosome 5 responsible for fetlock osteochondrosis in Hanoverian warmblood horses. *Animal Genetics* **40**, 553-555.

Lepeule, J., Bareille, N., Robert, C., Ezanno, P., Valette, J., Jacquet, S., Blanchard, G., Denoix, J. and Seegers, H. (2009) Association of growth, feeding practices and exercise conditions with the prevalence of Developmental Orthopaedic Disease in limbs of French foals at weaning. *Preventive Veterinary Medicine* **89**, 167-177.

Levine, J.M., Adam, E., MacKay, R.J., Walker, M.A., Frederick, J.D. and Cohen, N.D. (2007) Confirmed and presumptive cervical vertebral compressive myelopathy in older horses: a retrospective study (1992-2004). *Journal of Veterinary Internal Medicine* **21**, 812-819.

Levine, J.M., Ngheim, P.P., Levine, G.J. and Cohen, N.D. (2008) Associations of sex, breed, and age with cervical vertebral compressive myelopathy in horses: 811 cases (1974-2007). *J Am Vet Med Assoc* **233**, 1453-1458.

Levine, J.M., Scrivani, P.V., Divers, T.J., Furr, M., Mayhew, I.J., Reed, S., Levine, G.J., Foreman, J.H., Boudreau, C., Credille, B.C., Tennent-Brown, B. and Cohen, N.D. (2010) Multicenter case-control study of signalment, diagnostic features, and outcome

associated with cervical vertebral malformation-malarticulation in horses. *J Am Vet Med Assoc* **237**, 812-822.

Maniatis, T., Fritsch, E.F. and Sambrook, J. (2012) *Molecular Cloning: A Laboratory Manual*, 4th ed., Cold Spring Harbor Laboratory Cold Spring Harbor, NY.

Marklund, L., Moller, M.J., Sandberg, K. and Andersson, L. (1996) A missense mutation in the gene for melanocyte-stimulating hormone receptor (MC1R) is associated with the chestnut coat color in horses. *Mammalian Genome* **7**, 895-899.

MATLAB 7.1, The MathWorks, Inc., Natick, Massachusetts, United States.

Mayhew, I.G., deLahunta, A., Whitlock, R.H., Krook, L. and Tasker, J.B. (1978) Spinal cord disease in the horse. *Cornell Vet* **68 Suppl 6**, 1-207.

Mayhew, I.G., Donawick, W.J., Green, S.L., Galligan, D.T., Stanley, E.K. and Osborne, J. (1993) Diagnosis and prediction of cervical vertebral malformation in thoroughbred foals based on semi-quantitative radiographic indicators. *Equine Vet J* **25**, 435-440.

Mayhew, I. (1999) The diseased spinal cord. In: *Proc. Am. Ass. equine Practnrs.* pp 67-84.

McCarthy, M.I., Abecasis, G.R., Cardon, L.R., Goldstein, D.B., Little, J., Ioannidis, J.P. and Hirschhorn, J.N. (2008) Genome-wide association studies for complex traits: consensus, uncertainty and challenges. *Nature Reviews Genetics* **9**, 356-369.

McCoy, A. and McCue, M. (2014) Validation of imputation between equine genotyping arrays. *Animal Genetics* **45**, 153-153.

McCue, M.E., Bannasch, D.L., Petersen, J.L., Gurr, J., Bailey, E., Binns, M.M., Distl, O., Guérin, G., Hasegawa, T. and Hill, E.W. (2012) A high density SNP array for the domestic horse and extant *Perissodactyla*: utility for association mapping, genetic diversity, and phylogeny studies. *PLoS Genetics* **8**, e1002451.

Mitchell, C.W., Nykamp, S.G., Foster, R., Cruz, R. and Montieth, G. (2012) The use of magnetic resonance imaging in evaluating horses with spinal ataxia. *Vet Radiol Ultrasound* **53**, 613-620.

Moore, B.R., Holbrook, T.C., Stefanacci, J.D., Reed, S.M., Tate, L.P. and Menard, M.C. (1992) Contrast-enhanced computed tomography and myelography in six horses with cervical stenotic myelopathy. *Equine Vet J* **24**, 197-202.

Moore, B., Reed, S. and Robertson, J. (1993) Surgical treatment of cervical stenotic myelopathy in horses: 73 cases (1983-1992). *Journal of the American Veterinary Medical Association* **203**, 108-112.

Moore, B.R., Reed, S.M., Biller, D.S., Kohn, C.W. and Weisbrode, S.E. (1994) Assessment of vertebral canal diameter and bony malformations of the cervical part of the spine in horses with cervical stenotic myelopathy. *Am J Vet Res* **55**, 5-13.

- Murray, R.C. (2010) *Equine MRI*, 1st edn., John Wiley & Sons.
- Neuwirth, L. (1992) Equine myelography. *The Compendium on Continuing Education for the Practicing Veterinarian*.
- Nixon AJ, S.T., Ingram J (1982) Diagnosis of cervical vertebral malformation in the horse. *Proceedings of the American Association of Equine Practitioners* **28**, 253-266.
- Nout, Y. and Reed, S. (2003) Cervical vertebral stenotic myelopathy. *Equine Veterinary Education* **15**, 212-223.
- Nyland, T., Blythe, L., Pool, R., Helphrey, M. and O'Brien, T. (1980) Metrizamide myelography in the horse: clinical, radiographic, and pathologic changes. *American Journal of Veterinary Research* **41**, 204-211.
- Olstad, K., Ytrehus, B., Ekman, S., Carlson, C. and Dolvik, N. (2011) Early lesions of articular osteochondrosis in the distal femur of foals. *Veterinary Pathology Online* **48**, 1165-1175.
- Oswald, J., Love, S., Parkin, T. and Hughes, K. (2010) Prevalence of cervical vertebral stenotic myelopathy in a population of thoroughbred horses. *Veterinary Record* **166**, 82-83.
- Papageorges, M., Gavin, P.R., Sande, R.D., Barbee, D.D. and Grant, B.D. (1987) Radiographic and myelographic examination of the cervical vertebral column in 306 ataxic horses. *Veterinary Radiology* **28**, 53-59.
- Parfitt, A.M. (1977) The cellular basis of bone turnover and bone loss: a rebuttal of the osteocytic resorption-bone flow theory. *Clinical Orthopaedics and Related Research* **127**, 236-247.
- Powell, S. (2011) The fetlock region. *Equine MRI*, 1st edn., 315-359.
- Powers, B., Stashak, T., Nixon, A., Yovich, J. and Norrdin, R. (1986) Pathology of the vertebral column of horses with cervical static stenosis. *Veterinary Pathology* **23**, 392-399.
- Rantanen, N., Gavin, P., Barbee, D. and Sande, R. (1981) Ataxia and paresis in horses. Part II. Radiographic and myelographic examination of the cervical vertebral column. *Compend Contin Educ Pract Vet* **3**, S161-S171.
- Rasband, W.S., ImageJ, U. S. National Institutes of Health, Bethesda, Maryland, USA, <http://imagej.nih.gov/ij/>, 1997-2014.
- Rooney, J.R. (1969) Biomechanics of lameness in horses. *Biomechanics of lameness in horses*.

- Rosset, A., Spadola, L. and Ratib, O. (2004) OsiriX: An Open-Source Software for Navigating in Multidimensional DICOM Images. *Journal of Digital Imaging* **17**, 205-216.
- SAS Institute Inc., (2000-2004) SAS 9.1.3 Help and Documentation, Cary, NC: SAS Institute Inc.
- Schultz, L. Cl., Schebitz, H., Pohlenz, J. and Mechlenberg, G. (1965). On the spondylarthrotic pathogenesis of the spinal ataxia of horses. *Dt. Tierarztl. Wschr.* **72**, 502-506.
- Segura, V., Vilhjálmsson, B.J., Platt, A., Korte, A., Seren, Ü., Long, Q. and Nordborg, M. (2012) An efficient multi-locus mixed-model approach for genome-wide association studies in structured populations. *Nature Genetics* **44**, 825-830.
- Schafer, A.J. and Hawkins, J.R. (1998) DNA variation and the future of human genetics. *Nature biotechnology* **16**, 33-39.
- Shoukri MM, E.V. (1996) *Statistical Methods for Health Sciences*, CRC Press, Boca Raton.
- Smith, M., Dyson, S. and Murray, R. (2012) Reliability of high - and low - field magnetic resonance imaging systems for detection of cartilage and bone lesions in the equine cadaver fetlock. *Equine Veterinary Journal* **44**, 684-691.
- Steel, J.D., Whittem, J.H. and Hutchins, D.R. (1959). Equine sensory ataxia ("wobbles"). *Aust. Vet. Journal.* **35**, 442-449.
- Stewart, R.H., Reed, S.M. and Weisbrode, S.E. (1991) Frequency and severity of osteochondrosis in horses with cervical stenotic myelopathy. *Am J Vet Res* **52**, 873-879.
- Summers BA, C.J., de Lahunta A. (1995) *Veterinary Neuropathology*, Mosby, St. Louis, MO.
- Trostle, S., Dubielzig, R. and Beck, K. (1993) Examination of frozen cross sections of cervical spinal intersegments in nine horses with cervical vertebral malformation: lesions associated with spinal cord compression. *Journal of Veterinary Diagnostic Investigation* **5**, 423-431.
- Tsianos, E.V., Katsanos, K.H. and Tsianos, V.E. (2012) Role of genetics in the diagnosis and prognosis of Crohn's disease. *World Journal of Gastroenterology: WJG* **18**, 105.
- van Biervliet, J., Scrivani, P.V., Divers, T.J., Erb, H.N., de Lahunta, A. and Nixon, A. (2004) Evaluation of decision criteria for detection of spinal cord compression based on cervical myelography in horses: 38 cases (1981-2001). *Equine Vet J* **36**, 14-20.

Van Weeren, P. (2006) Osteochondrosis. *Equine Surgery*, 3rd edition., 1166-1178.

Voor, M.J., Yang, S., Burden, R.L. and Waddell, S.W. (2008) In vivo micro-CT scanning of a rabbit distal femur: Repeatability and reproducibility. *Journal of Biomechanics* **41**, 186-193.

Wade, C., Giulotto, E., Sigurdsson, S., Zoli, M., Gnerre, S., Imsland, F., Lear, T., Adelson, D., Bailey, E., Bellone, R., Blocker, H., Distl, O., Edgar, R.C., Garber, M., Leeb, T., Mauceli, E., Macleod, J. N., Penedo, M.C.T., Raison, J.M., Sharpe, T., Vogel, J., Andersson, L., Antczak, D.F., Biagi, T., Binns, M.M., Chowdhary, B.P., Coleman, S.J., Della Valle, G., Frye, S., Guerin, G., Hasegawa, T., Hill, E.W., Jurka, J., Kiialainen, A., Lindgren, G., Liu, J., Magnani, E., Mickelson, J.R., Murray, J., Nergadze, S.G., Onofrio, R., Pedroni, S., Piras, M.F., Raudsepp, T., Rocchi, M., Roed, K.H., Ryder, O.A., Searle, S., Skow, L., Swinburne, J.E., Syvanen, A.C., Tozaki, T., Valberg, S.J., Vaudin, M., White, J.R., Zody, M.C., (2009) Genome sequence, comparative analysis, and population genetics of the domestic horse. *Science* **326**, 865-867.

Wagner, P., Grant, B., Watrous, B., Appell, L. and Blythe, L. (1985) A study of the heritability of cervical vertebral malformation in horses. In: *Proceedings of the annual convention of the American Association of Equine Practitioners (USA)*.

Waterland, R.A. and Jirtle, R.L. (2003) Transposable elements: targets for early nutritional effects on epigenetic gene regulation. *Molecular and Cellular Biology* **23**, 5293-5300.

Weisher, F. von. (1944). Genetically conditioned hind quarter paralysis in the young horse. *Berliner Munchener tierarztl. Wschr.* **39/40**, 317.

Weisher, F. von. (1946). Cited by Schebitz, H. and Schultz, L. Cl. (1965). On the pathogenesis of spinal ataxia in horses-spondylarthrosis, clinical findings. *Dt. tierarztl. Wschr.* **72**, 496-501.

Whitewell, K.E. and Dyson, S. (1987) Interpreting radiographs 8: Equine cervical vertebrae. *Equine Veterinary Journal* **19**, 8-14.

Williams, N. (2003) Equine Neurologic Disease. *Equine Disease Quarterly* **12**,6.

Wittwer, C., Löhring, K., Drögemüller, C., Hamann, H., Rosenberger, E. and Distl, O. (2007) Mapping quantitative trait loci for osteochondrosis in fetlock and hock joints and palmar/plantar osseous fragments in fetlock joints of South German Coldblood horses. *Animal Genetics* **38**, 350-357.

Wolff, J., Maquet, P. and Furlong, R. (1986) *The law of bone remodelling*, Springer Berlin.

Wolff, G.L., Kodell, R.L., Moore, S.R. and Cooney, C.A. (1998) Maternal epigenetics and methyl supplements affect agouti gene expression in Avy/a mice. *The FASEB Journal* **12**, 949-957.

Wright, F., Rest, J.R. and Palmer, A. (1973) Ataxia of the Great Dane caused by stenosis of the cervical vertebral canal: comparison with similar conditions in the Basset Hound, Doberman Pinscher, Ridgeback and the Thoroughbred horse. *Veterinary Record* **92**, 1-6.

Ytrehus, B., Carlson, C. and Ekman, S. (2007) Etiology and pathogenesis of osteochondrosis. *Veterinary Pathology* **44**, 429-448.

VITA

Jennifer G. Janes

Place of Birth: Nashville, Tennessee

Education

University of Kentucky 2007-present

Lexington, KY, USA

Doctor of Philosophy in Veterinary Science

College of Agriculture, Food, and Environment, Department of Veterinary Science

Maxwell H. Gluck Equine Research Center

University of Kentucky 2007-2011

Lexington, KY, USA

Anatomic Pathology Residency

College of Agriculture, Food, and Environment, Department of Veterinary Science

University of Kentucky Veterinary Diagnostic Laboratory

University of Tennessee 2002-2006

Knoxville, Tennessee, USA

Doctorate of Veterinary Medicine

College of Veterinary Medicine

Vanderbilt University 1998-2002

Nashville, Tennessee, USA

Bachelors of Music—*cum laude*

Blair School of Music

Professional Positions

Graduate Research Assistant, University of Kentucky – July 2007 to Present

Anatomic Pathology Resident, University of Kentucky – July 2007 to July 2011

Veterinary Intern, Wisconsin Equine Clinic and Hospital – June 2006 to June 2007

Awards and Honors

Morris Animal Foundation Fellowship Training Award, September 2009- September 2011

American Association of Equine Practitioners Past Presidents' Research Fellow Award, December 2009

Publications

Accepted Publications

JG Janes, KS Garrett, KM McQuerry, AP Pease, NM Williams, SM Reed, JN MacLeod. (2013) Comparison of magnetic resonance imaging to standing cervical radiographs for evaluation of vertebral canal stenosis in equine cervical stenotic myelopathy. Equine Veterinary Journal. (In press; DOI: 10.1111/evj.12221)

AM Shank, UK Bryant, CB Jackson, NM Williams, **JG Janes**. (2008) Anomalous origin of the left coronary artery from the pulmonary artery (ALCAPA) in four calves. Veterinary Pathology 45 (5):634-639.

Publications in Preparation

JG Janes, KS Garrett, NM Williams, MJ Voor, SM Reed, JN MacLeod. Skeletal pathology of vertebral articular processes in equine cervical stenotic myelopathy. (In preparation)

JG Janes, DW Fardo, EF Bailey, CM McQueen, SV Dindot, SM Reed, JN MacLeod. The role of inherited genetic determinants in equine cervical stenotic myelopathy. (In preparation)

Abstracts

JG Janes, DW Fardo, EF Bailey, CM McQueen, SV Dindot, SM Reed, JN MacLeod. (2014) Genomic Analyses of Equine Cervical Stenotic Myelopathy. Plant and Animal Genome Conference XXII. (poster)

JG Janes, EF Bailey, SR Reed, JN MacLeod. (2012) Investigating Genetic Determinants in Equine Cervical Stenotic Myelopathy. Plant and Animal Genome Conference XX. (poster)

Oral Presentations

Genomic Analyses of Equine Cervical Stenotic Myelopathy. Plant and Animal Genome Conference XXII. San Diego, CA. January 2014.

Wobbler Syndrome: What we know and remaining questions. University of Kentucky Equine Showcase. Lexington, Kentucky. January 2013.

Diagnostic Approach to Equine Neurologic Cases. Ninth International Conference on Equine Infectious Diseases. Lexington, Kentucky. October, 2012.

Investigating the Role of Genetic Determinants in Equine Cervical Stenotic Myelopathy (Wobbler Syndrome). University of Kentucky Departmental Seminar. Lexington, Kentucky. May, 2012.

Wobbler Syndrome. Advances in Equine Neurologic Disease Symposium. Lexington, Kentucky. December, 2011.

Comparison of cervical radiographs and MRI to assess vertebral canal stenosis in Wobbler Syndrome. American Association of Equine Practitioners Annual Convention. San Antonio, Texas. November, 2011.

Wobbler Syndrome: What do we know and where do we go from here. Equine Research Diagnostic Seminar. Lexington, Kentucky. October, 2009. (Joint seminar with Dr. Stephen Reed, Rood and Riddle Equine Hospital)

Hepatoblastoma in an Equine Fetus. Midwest Association of Veterinary Pathology Conference. Marshall, Indiana. August, 2009.

Halicephalobus gingivalis in an Adult Equine. Southeastern Veterinary Pathology Conference. Tifton, Georgia. May, 2009.

Hepatocellular Carcinoma in a Sheep. Midwest Association of Veterinary Pathology Conference. College Corners, Ohio. August, 2008.